CCI

BIOMASS

PRODUCT VALIDATION & INTERCOMPARISON REPORT

VERSION 6.0

DOCUMENT REF:	CCI_BIOMASS_PVIR_V6
DELIVERABLE REF:	D4.1_PVIR
VERSION:	6.0
CREATION DATE:	2025-05-23
LAST MODIFIED	2025-06-04

Document Authorship

	NAME	FUNCTION	ORGANISATION	SIGNATURE	DATE
PREPARED					
PREPARED	A. Araza	WP2	WUR/GFZ		
PREPARED	M. Herold	WP2 Co-lead	GFZ		
PREPARED					
PREPARED					
PREPARED					
PREPARED					
PREPARED					

VERIFIED	H. Friendship-Kay	Project Coordinator	Aberystwyth University		
VERIFIED	R. Lucas	Project Manager	Aberystwyth University		
VERIFIED	S. Quegan	Science Leader	Sheffield University		
APPROVED					

Document Distribution

ORGANISATION	NAME	QUANTITY
ESA	Frank Seifert	

Document History

VERSION	DATE	DESCRIPTION	APPROVED
0.1	2025-06-04	First draft version	
1.0	2025-06-28	Second draft version	

Document Change Record (from Year 1 to Year 2)

VERSION	DATE	DESCRIPTION	APPROVED

TABLE OF CONTENTS

LIST OF TABLES

LIST OF FIGURES

SYMBOLS AND ACRONYMS

AGB	Aboveground biomass
AGB_{map}	Aboveground biomass according to the map
AGB_{ref}	Aboveground biomass from plot, corrected for plot inventory date and if plot size < 1 ha, corrected for partial forest fraction at pixel level
CCI	Climate Change Initiative
CoFor	Congo basin Forests AGB dataset (Ploton et al., 2020)
GNSS	Global Navigation Satellite System
IPCC	Intergovernmental Panel on Clmate Change
I_{Var}	Indicator variable: 1 if the SE_{CCI} is consistent with (Plt), MD and MSD, and 0 otherwise. The latter indicates that the SE_{CCI} layer is overly pessimistic regarding AGB map precision.
LiDAR	LIght Detection And Ranging
MD	Mean difference between AGB_{map} and AGB_{ref}
MSD	Mean square difference (between AGB_{map} and AGB_{ref})
NEON	National Ecological Observatory Network, USA
NFI	National Forest Inventory
PUG	Product User Guide (Santoro, 2020)
PVIR	Product Validation and Inter-comparison Report
PVP	CCI Biomass Product Validation Plan
RMSD	Root mean square difference (between AGB_{map} and AGB_{ref})
SE_{CCI}	Error layer (standard deviation) provided with the CCI Biomass product; if squared denoted as $\mathrm{SE}_{\mathrm{CCI}}^2$.
SLB	Sustainable Landscape Brazil
SRTM	Shuttle Radar Topography Mission
TERN	Terrestrial Ecosystem Research Network, Australia
Var(Plt)	Estimated variance of the plot measurement error
Var(S(x))	Estimated variance of the within-pixel sampling error (owing to smaller plot footprint)

1.Introduction

Validation is critical for increasing acceptance of satellite-derived products by user communities (e.g., carbon cycle science, climate modelling). To assess the accuracy of the aboveground biomass density (AGB; Mg/ha) estimates for the 2007, 2010 and 2015 - 2021 epochs of the refined CCI Biomass global products (Santoro, 2024), AGB predictions from the map have been compared with independent AGB data from plots and LiDAR campaigns, which were used as reference values. The main aim of this report is to provide an independent assessment of the quality of the CCI Biomass (Version 6) products generated in Year 5 of the project, with this primarily providing (climate) users with uncertainty information (including both precision and bias) when using the map, including for global and regional climate modelling and assessment purposes. A second purpose is to provide feedback to map producers to establish where the maps can be improved.

The reference AGB data are not error-free. *In situ* estimates of AGB are computed based on stem diameter (typically cm), tree height (m), wood density (g cm^3) and allometric models, while geolocation is determined using Global Navigation Satellite System (GNSS) measurements that have variable and often limited accuracy. GNSS accuracy is degraded if the paths between the satellites and the GNSS receiver are partly blocked by vegetation cover, which is not uncommon in forests. An additional cause of discrepancies between plots and pixel-based AGB estimates is the difference in support (shape and size) between map pixels and plots. The latter are often much smaller than the areas of the pixels they are being compared with, which may introduce two types of error. The first is a sampling error, since an estimate of the AGB in only part of the pixel area (the plot) is being compared with that of the full pixel area. Secondly, and more subtly, a representation error can occur if plots are selected with particular properties, such as only being from mature forest despite being in a mixed age forest which results in them not being representative of the forest population. This type of representation error is often termed selection bias. Both types of error can occur even if the pixel's footprint is fully covered by forest, largely because of AGB heterogeneity inside the pixel. There may also be a representation error if, for example, a forest plot is used to represent a pixel that is only partially forested. Additionally, the plot inventory date often differs from the biomass map epoch, which gives a temporal mismatch between the compared AGB values.

LiDAR-based AGB estimates used as reference data can completely cover map pixels or even larger pixel blocks, which minimizes the sampling errors referred to above. However, as with *in situ* estimates of AGB, LiDAR-based AGB values are themselves predictions, so are subject to prediction errors that must be considered.

Each of the above-mentioned factors can introduce errors with a random or a systematic nature. The systematic error is of particular concern since it cannot be reduced by aggregating individual tree measurements over large plots or by averaging small plot data over many plots. Systematic errors in reference data have to be reduced as much as possible by adhering to a standardized measurement protocol (CEOS, 2021).

The five versions of the CCI Biomass Product Validation Plan (PVP; de Bruin et al., 2019a, 2020, 2021, 2022) presented approaches for addressing the temporal mismatch between plot and pixel data and partial forest fractions within map pixels. The reports also proposed methods for assessing the variance of the other error sources. In this fifth PVIR, the temporal mismatch between plot and pixel data and partial forest fractions within map pixel are handled similarly to the first four PVIRs. The proposed approaches for accounting for other error sources are partly implemented, up to the point supported by available data.

An extensive dataset of forest plot data across the world was acquired for the purpose of the validation (see Appendix A,

Figure 1 and Table 1). As before, the plots underwent a series of quality checks (see Section 2.1). Forest plot data and LiDAR were not used to calibrate the CCI Biomass map in order to guarantee full independence from the production process. The contributions of AGB measurement error and spatial representation error are known to be largest for small plots, such as those typical of National Forest Inventories (NFIs), while detailed measurements of all trees within large plots are expected to deliver the highest quality AGB data (Réjou-Méchain et al., 2019; Réjou-Méchain et al., 2014). To take into account expected differences in the accuracy of plot data, a tiered approach was chosen which comprised:

- Tier 1 - small plots (≤ 0.6 ha), including NFI data,
- Tier 2 - larger plots (0.9-3 ha; Tier 2), and
- Tier 3- high-quality large super-plots (≥ 6 ha; mainly from Labrière et al. (2018)).

The Tiers were analysed separately in the plot-pixel comparisons. AGB map comparisons with data derived from LiDAR and aggregated plot data (see Section 2.2) were also analysed separately.

The map inter-comparison presented in this document concerns consistency of map-reference deviations amongst the CCI Biomass AGB products and comparisons with Version 5 of the CCI Biomass products of the same epochs (Santoro, 2021). Results from two external map inter-comparisons, as examples of user-led independent validation, are also included. Lastly, the CCI maps are inter-compared with other AGB map products.

2.Materials and methods

2.1. Forest plot data

For CCI Biomass, new forest inventory and plot data from research networks were added to the previously established GlobBiomass reference database (Rozendaal et al., 2017). Additional reference data were collected during the span of the CCI Biomass project focusing on potentially under-represented areas (i.e., forests in boreal and mountainous regions). Reference data were only included if quality criteria, as described in the PVP, were met. Specifically, the plots needed:

- A citable reference source and metadata to assess the procedures and quality of biomass estimation.
- Precise coordinates (4-6 decimals for coordinates in decimal degrees of plot centroids).
- A census date within ten years of the reference year of the AGB map to avoid temporal inconsistency with the assessed maps.
- Inclusion of measurements of all trees of diameter at breast high ≥ 10 cm (or less).
- To have experienced no deforestation between the year of the inventory and the reference year of the CCI Biomass map (i.e., 2010; and 2017-2020). This was assessed based on the forest loss layer of the Hansen dataset (Hansen et al., 2013).

Table 1. Number of plots used in each Tier for the different AGB map reference years.

Map ref. year	Tier1	Tier2	Tier3	Total
2007	150890	795	130	153822
2010	149844	879	130	152863
2015	108773	816	249	111853
2016	97812	752	249	100829
2017	82544	601	249	85411
2018	73118	512	247	75895
2019	68376	490	230	71115
2020	63919	466	228	66633
2021	59150	440	228	61839
2022	52747	251	211	55231

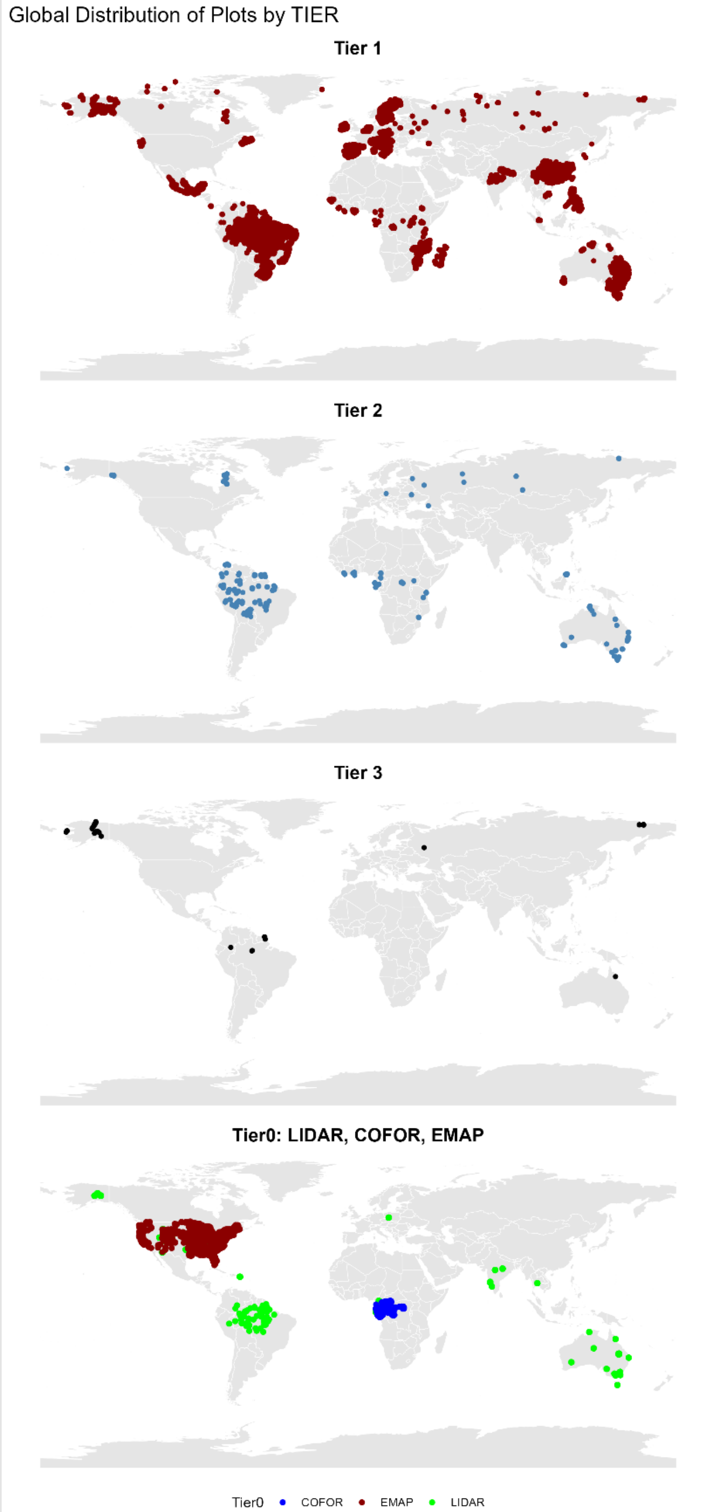

Figure 1. Geographical locations of plots and footprints of the reference datasets used to assess the 2010 biomass map (CoFor = Congo basin Forests, LiDAR and EMAP = Environmental Monitoring and Assessment Program).

2.2. AGB estimates from LiDAR, Congo basin management inventories, and US Forest Service plots

In addition to the plot data, we used LiDAR-based AGB data at 100 m resolution from the Sustainable Landscape Brazil project (SLB), the National Ecological Observatory Network, USA (NEON) and the Terrestrial Ecosystem Research Network, Australia (TERN), which were processed by Labrière and Chave (2020a, b, c); a dataset from the Piñon-Juniper woodlands in the USA; the Rodda *et al*. (2022) dataset from Africa and Asia ALS missions. The 1-km pixel forest management inventory data used in this report originated from the Congo basin Forests AGB (CoFor) dataset (Ploton et al., 2020). For the CoFor dataset, only pixels having at least five *in situ* forest management inventoried plots were used. Lastly, we used the Environmental Monitoring and Assessment Program (EMAP) AGB aggregates of 27-km hexagons estimated from the Forest Inventory and Analysis Program of the US Forest Service (Menlove and Healey, 2020), which was useful for the 2015-2022 comparative analysis.

Table 2. Number of LiDAR, CoFor and EMAP footprints used for the different AGB map reference years.

Map ref. year	CoFor	LiDAR	EMAP	Total
2007	33792	149412	2874	188085
2010	33792	381562	3874	421238
2015	24474	655122	3874	685485
2016	24268	655122	3874	685280
2017	18712	655122	3874	679725
2018	17554	655122	3874	678568
2019	15136	655122	3874	676151
2020	13162	655122	3874	674178
2021	8292	648636	3874	662823
2022	2206	619122	3874	627224

As described in the PVPs, we rely on opportunistic AGB plot data that were not specifically produced for validation purposes but were rather collected within the context of country NFIs and research efforts at local to regional scales.

2.3. Increase of reference data from version 5 to version 6

The reference data used to assess CCI Biomass Version 6 has increased compared to the previous reference data used for the Version 5 maps. The validation team focused on acquiring new reference data in potentially under-represented regions (Labriere et al. 2022, Araza et al. Under review). The additions include NFI data from Brazil, Ireland, Italy; permanent plots in the Boreal region; and airborne LiDAR-based maps in Brazil, Africa and Asia. Unlike the previous additions acquired under data-use agreements, new additions now are mostly open-source data; see Appendix A for further information.

2.4. Preparation of validation datasets

2.4.1. Temporal harmonization

Differences between the inventory date of AGB plots and the reference year of the AGB map were harmonized using updated IPCC growth rates (IPCC, 2019; Requena Suarez et al., 2019) following the approach described in Version 1 of the PVP. For plots in tropical and subtropical ecological zones, age-category-dependent growth rates are available (IPCC, 2019; Requena Suarez et al., 2019). In these cases, plot AGB values in the range 0-99 Mg/ha were assumed to represent young secondary forest, AGB values in the range 100-128 Mg/ha were treated as old secondary forest (Van Breugel et al., 2007), and AGB above 129 Mg/ha was assumed to correspond to old-growth stands (Brown et al., 1989; Clark & Clark, 2000; Mello et al., 2016). Given the absence of data on plot forest age, mature forests of low biomass could not be distinguished from young stands with similarly low biomass, with potential implications for the growth rates applied. For temperate oceanic forests in Europe and boreal coniferous forests and tundra woodlands, no differentiation of growth rates over age categories was used. The temporal adjustments by growth rates were applied up to a difference of ten years between the inventory date and the map reference year. Plots having a longer temporal difference were discarded in the analyses. Some of the LiDAR dataset (NEON and SLB) were exempted from temporal adjustment because it contained repeated measurements between 2011 and 2018.

2.4.2. Correction for forest fraction

As described in the PVP, correction for inclusion of non-forested areas within map pixels was undertaken by multiplying the temporally adjusted plot AGB by the forest fraction at the pixel level of 100 m. The forest fraction was computed by setting a 10 % threshold on the 2010 tree cover product (Hansen et al., 2013), which had a resolution of 1 arc-second per pixel, or approximately 30 meters per pixel at the equator. Moreover, tree cover datasets corresponding to 2015-2021 were produced for this purpose, removing associated deforestation pixels from annual tree cover data using the annual forest loss product of Hansen et al. (2013). In the rare case of more than one AGB plot within a hectare/CCI map pixel, the average of the adjusted AGB per plot was used. The correction for forest fraction was only applied to plots with area below 1 ha.

2.4.3. Comparisons at 0.1° cell resolution

To reduce the effect of short-range AGB spatial variations in the map and their potential interaction with plot-map geolocation mismatches and to assess the CCI Biomass map at a resolution commonly used by climate modellers, AGB_{map} - AGB_{ref} comparisons from Tier 1 data were also made over multi-pixel blocks at 0.1° cell resolution. In this case, correction for partial forest fraction (see above) was undertaken at the level of the coarse resolution cells. The mean AGB_{ref} at 0.1° cell level was computed by multiplying the forest fraction at the 0.1° cell level by the mean temporally adjusted AGB of at least five plots in that cell. The procedure is illustrated in Figure 5 of the PVP (de Bruin et al., 2019a). The choice to use a minimum number of plots inside grid cells was motivated by previous and recent studies e.g., , Fazakas et al. (1999); Baccini et al., 2012, Baccini et al., 2017; Xu et al. (2021); and Araza et al. (2022a). The AGB reference values thus obtained were compared with the average map AGB spatially aggregated over the 0.1° cells. In the case of the EMAP dataset comparison, the map AGB was averaged to 0.25°.

The correction for forest fraction was not applied to the LiDAR dataset since the LiDAR footprints were assumed to representatively sample forest/non-forest fractions within the 0.1° cells, i.e., forested areas were not preferentially sampled.

2.4.4. Ecoregions / biomes

AGB_{map} - AGB_{ref} comparisons at 0.1° cell resolution were also stratified according to ecoregions derived from a recent global ecoregion map (Dinerstein et al., 2017), which was downloaded from https://ecoregions2017.appspot.com/. The original vector maps were rasterized to 0.1° resolution. Resulting raster cells were assigned to the category covering the largest portion of the cell area. Comparisons were stratified from Tier 3 data at 0.1° cell resolution per biome.

2.5. Comparing AGB map pixels with reference data

2.5.1. Assumptions

After adjustments for temporal discrepancies and partial forest fraction and having at least ten plots within a reference AGB range, the unweighted means computed from reference data in Tiers 1 and 2 were assumed to be unbiased given that plot data were used where AGB was estimated using the most appropriate allometries by the data providers (Araza et al. 2022a) The AGB ranges used are listed in the first column of Table 2. For Tier 3 data, the requirement of ten plots per AGB range was relaxed because these data were recorded over large plots (≥ 6 ha) and followed a strict measurement protocol. Under the unbiasedness assumption, mean differences between harmonized plot data and map values aggregated over bins covering ranges of reference AGB values are interpreted as map bias. To empirically verify the assumption of unbiased plot data, the analysis was conducted for each of the three tiers and assessed consistency of results between these, whenever this was allowed by the data volumes.

When reporting mean differences (MD) and (root) mean square difference ((R)MSD) over ecoregions, plot-map comparisons within ecoregions were assumed to be representative of those regions.

2.5.2. Measures

Besides reporting mean differences between reference and map AGB per biomass range, which are interpreted as map bias (see above), RSMD between map values and plots are reported. At this stage, the MSD was not interpreted as error of the map since we will elaborate on the assessment of the variance of individual error components in later stages of the project. However, we did assess whether the mean variance of map error ($\mathrm{mean}(\mathrm{SE}_{\mathrm{CCI}}^2)$)—where $\mathrm{SE}_{\mathrm{CCI}}$ is the standard error layer provided with the CCI Biomass AGB map—is consistent with MSD, MD and the mean variance of plot measurement error $\mathrm{mean}(\mathrm{Var}(\mathrm{Plt}))$. The $\mathrm{SE}_{\mathrm{CCI}}$ layer only represents the random part of AGB errors and the aggregated $\mathrm{SE}_{\mathrm{CCI}}$ layer at 0.1° already accounts for spatially correlated map errors identified using LiDAR datasets (Santoro, 2023b). Leaving out three random error components listed in the PVP (positional error, within-pixel representation error and the data harmonization error) and under the assumptions given above, we checked whether $\mathrm{mean}(\mathrm{SE}_{\mathrm{CCI}}^2) \leq \mathrm{MSD} - \mathrm{MD}^2 - \mathrm{mean}(\mathrm{Var}(\mathrm{Plt}))$.

For this purpose, we defined an indicator variable $\mathrm{I}_{\mathrm{Var}}$, as follows:

$$\mathrm{I}_{\mathrm{Var}} = \begin{cases} 1 \ \text{if } \mathrm{mean}(\mathrm{SE}_{\mathrm{CCI}}^2) \leq \mathrm{MSD} - \mathrm{MD}^2 - \mathrm{mean}(\mathrm{Var}(\mathrm{Plt})) \\ 0 \quad \text{otherwise} \end{cases}$$

If $\mathrm{I}_{\mathrm{Var}}$ has value zero, $\mathrm{mean}(\mathrm{SE}_{\mathrm{CCI}}^2)$ would be too large. In other words, the $\mathrm{SE}_{\mathrm{CCI}}$ layer provided with the AGB product would be pessimistic about map precision, unless the variance of plot measurement error is greatly underestimated.

For plots having tree-level data, $Var(Plt)$ was computed using the Réjou-Méchain et al. (2017) biomass R-package. For other plots lacking such data, $Var(Plt)$ was predicted by a random forest model trained on the plots having tree-level data, using plot biomass, plot size, general and specific eco-zones and continent as explanatory variables.

2.6. Spatial correlation of AGB

Experimental semi-variograms were computed and variogram models were fitted using gstat (Pebesma, 2004) based on LiDAR-AGB data acquired over two forest sites in Remningstorp, Sweden, and Lope, Gabon (i.e., a boreal and a tropical forest site). These ALS datasets were acquired in the framework of the airborne ESA BIOSAR (Ulander et al., 2011) and AfriSAR (Hajnsek et al., 2017) campaigns to provide detailed information on forest vertical structure and to produce high-resolution AGB maps. The AGB data have a spatial resolution of 10 m (Remningstorp) and 20 m (Lope) and were also used in Version 2 of the Product User Guide (PUG; Santoro, 2024). Non-forest areas (such as savanna in the Lope study area) were masked out after manually digitizing forested areas using high resolution Google Earth imagery. Accordingly, the variogram models represent spatial correlation of AGB within forested areas at the study sites.

2.7. Effect of spatial support on sampling error and suggested map bias

The variogram models described above were used to assess the effects of the within-pixel sampling error (see Introduction) for the forest sites in Remningstorp and Lope. This was undertaken by two means:

- By computing the variance of the difference between sub-pixel plots and plot configurations (i.e., for plots smaller than pixels) and AGB map pixels at locations x as:

$$\mathrm{Var}(\mathrm{S}(\mathrm{x})) = \mathrm{Var}\left(\mathrm{AGB_{ref}}(\mathrm{x}) - \mathrm{AGB_{map}}(\mathrm{x})\right) = \mathrm{Var}(\mathrm{AGB_{ref}}) + \mathrm{Var}(\mathrm{AGB_{map}}) - 2 * \mathrm{Cov}(\mathrm{AGB_{ref}}, \mathrm{AGB_{map}}),$$

  where $\mathrm{Var}(\mathrm{AGB_{ref}})$ is the sill of the variogram at the spatial support of the plots, $\mathrm{Var}(\mathrm{AGB_{map}})$ is the within-pixel covariance, and $\mathrm{Cov}(\mathrm{AGB_{ref}},\ \mathrm{AGB_{map}})$ is the plot to pixel covariance. Note that for brevity, reference to the location x is omitted in the right-hand side of the above equation. The latter two terms are computed using the geostatistical framework for change of support (Kyriakidis, 2010).
- By simulating possible plot AGB, conditional on given AGB values at the pixel level, using the $\mathrm{Var}(\mathrm{AGB_{ref}} -\ \mathrm{AGB_{map}})$ computed in the above step. The aim of this simulation is to provide a proof of concept on the effect of within-pixel sampling error in the plot-map comparisons.

3. Validation results for the global maps

3.1. Global assessments per Tier of plot data

3.1.1. Tier 1 non-aggregated

An overall feature of the comparisons is the large scatter (see Figure 2); this is expected, given that small reference plots are being compared to larger pixels without considering scaling effects. The plots for binned ranges (Fig. 2) show over-prediction for the low reference biomass and under-prediction of higher reference AGB values, while relative accuracy is within 25 % in the middle range. On average, under-prediction by the map starts at a reference AGB of approximately 90 Mg/ha but the interquartile range of plot data still covers the 1:1 line between $\mathrm{AGB_{ref}}$ and $\mathrm{AGB_{map}}$ up to approximately 180 Mg/ha. All maps show under-prediction starting at 90 Mg/ha. The 2007 and 2010 results show that maps tend to overestimate more the lower biomass regions than the rest of the epochs probably due to more older plots being used. Moreover, the $\mathrm{AGB_{ref}}$ values originate from small plots, some with exceptionally high AGB that is unlikely to cover extensive areas and is unlikely to be captured by the AGB retrieval algorithm. These plot data are also dominated by data from several countries from subtropical and temperate regions (Figure 1). The banding observed in the left column of Figure 2 especially for the 2010 map seems to be caused by a maximum AGB level set for particular regions in the retrieval algorithm. A first impression is that the accuracy of the current map versions has been affected by the maximum AGB and has improved in several regions compared to the previous edition reported in de Bruin *et al*. (2022b: Table 1 and Figure 4 therein). This is further analyzed in Section 3.7.

For AGB bins > 200 Mg/ha in Table 4 and > 250 Mg/ha in Tables 5-10, the indicator variable $\mathrm{I_{Var}}$ = 1, suggesting the $\mathrm{SE_{CCI}}$ layer provided with the AGB product is optimistic about the precision of the CCI Biomass maps. The considerable mean variance of plot measurement error, $\mathrm{mean(Var(Plt))}$, of the smallest plot size category, definitely contributes to this observation. Only for the highest reference AGB value does $\mathrm{I_{Var}}$ attain the value 1. Further analyses of the random error components are needed to assess whether the reported $\mathrm{SE_{CCI}}$ for $\mathrm{AGB_{ref}} > 400$ Mg/ha is indeed reasonable.

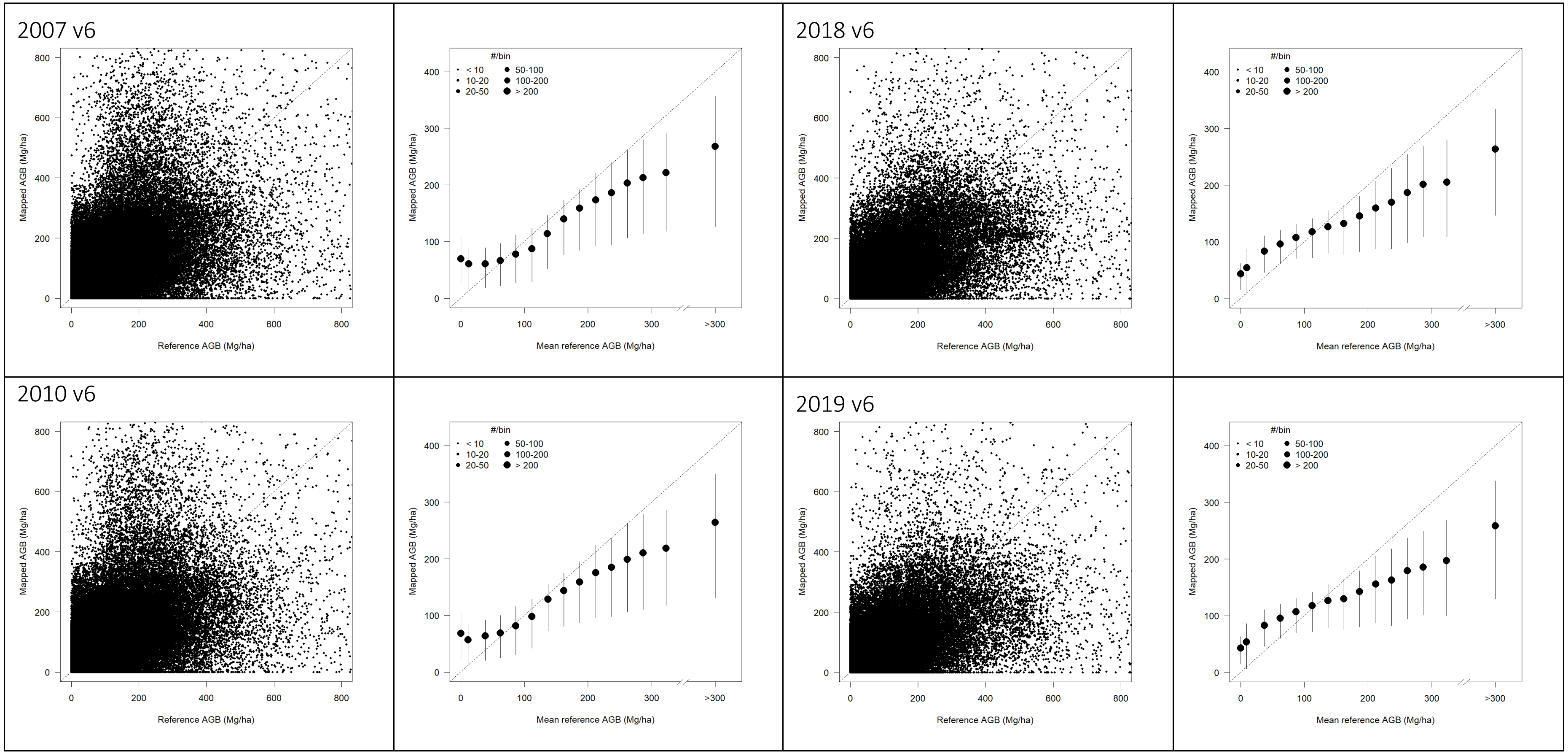

2007 v6
2018 v6
2010 v6
2019 v6
Mapped AGB (Mg/ha)
Reference AGB (Mg/ha)
Mean reference AGB (Mg/ha)
#/bin
< 10
10-20
20-50
50-100
100-200
> 200

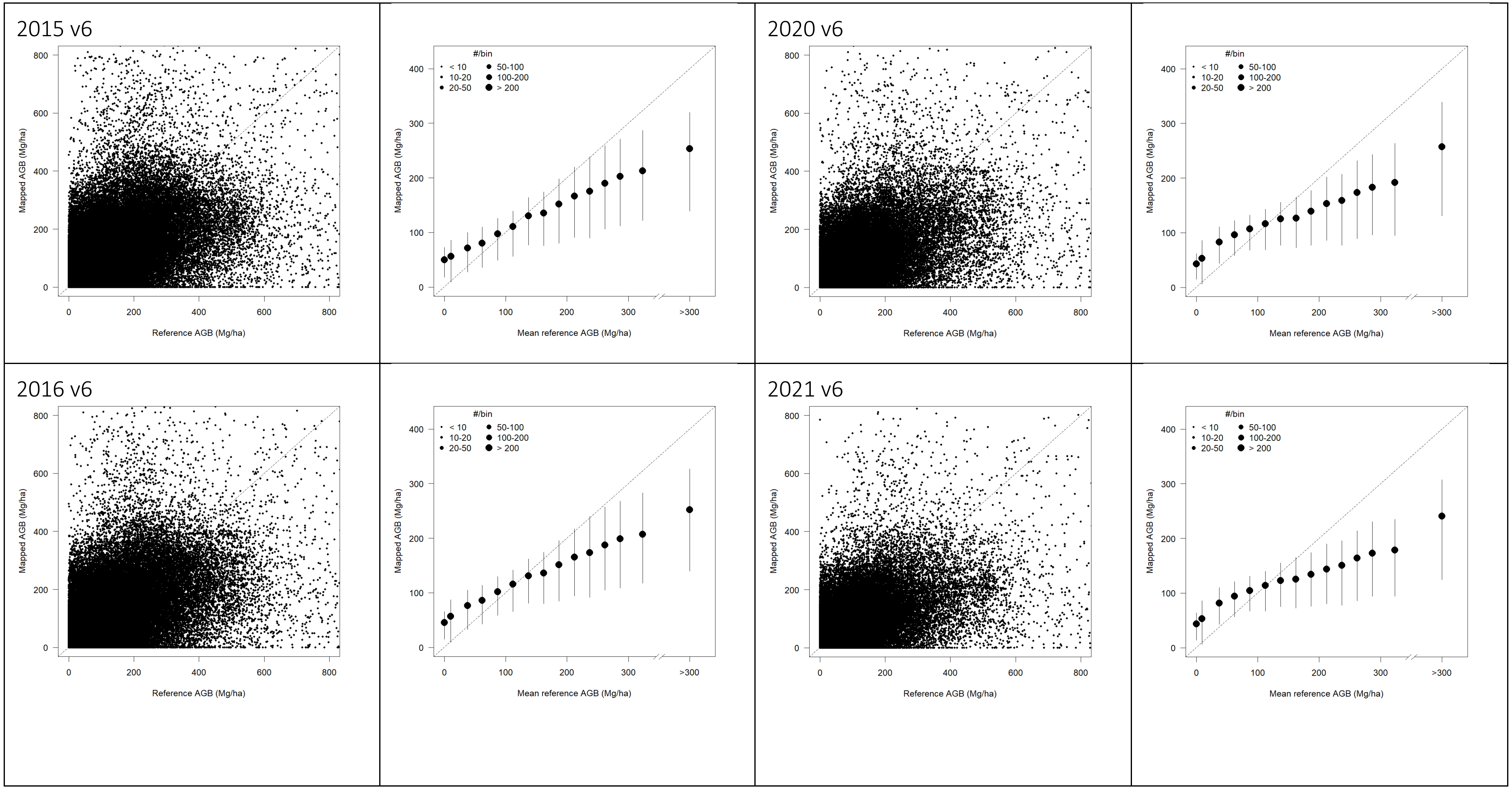

2015 v6
2020 v6
2016 v6
2021 v6
Mapped AGB (Mg/ha)
Reference AGB (Mg/ha)
Mean reference AGB (Mg/ha)
#/bin
< 10
10-20
20-50
50-100
100-200
> 200
>300

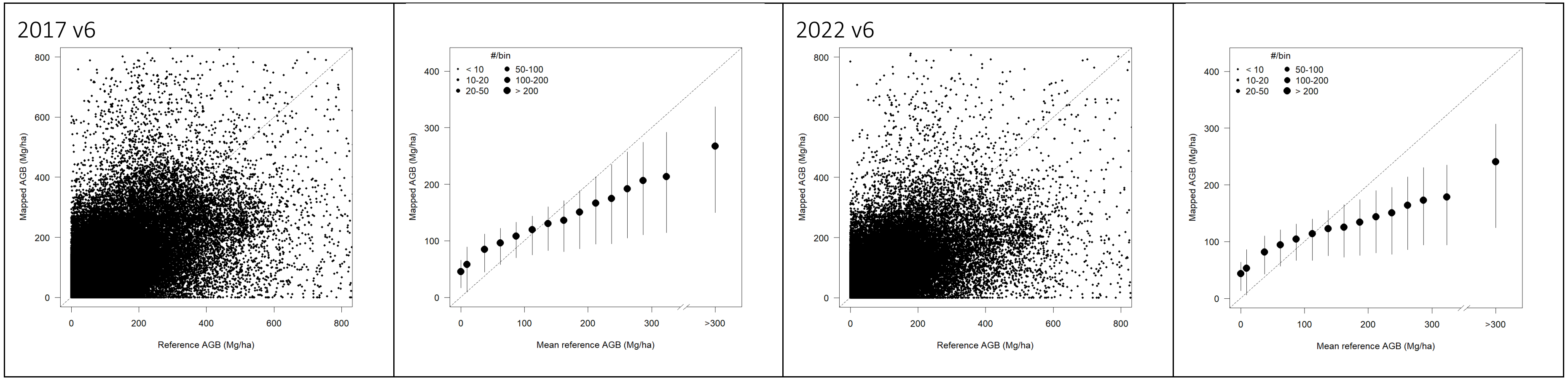

Figure 2. Plot-map comparisons for Tier 1 data at original resolution (i.e., without spatial aggregation) for the five AGB maps; left column: scatterplots; right column: binned over 25 Mg/ha wide biomass ranges with whiskers representing the interquartile range of mapped biomass values. AGB_{ref} > 350 Mg/ha data are grouped into a single bin. Note the different scales on the left and right graphs.

Table 3. Validation results per biomass range for Tier 1 data at original resolution for the 2007 map.

AGB_{ref} bin [Mg/ha]	# plots count	AGB_{ref}	AGB_{map}	MD	RMSD	Var(Plt) [a] [Mg/ha]²	SE^2_{CCI} [a]	I_{Var}
		[Mg/ha]						
0-50	39383	27	61	34	68	10402	223	0
50-100	50954	73	71	-2	62	6868	211	0
100-150	28385	121	97	-24	89	8931	401	0
150-200	10318	173	148	-25	117	14900	886	0
200-250	6160	223	179	-44	141	13836	1243	1
250-300	3727	273	207	-66	159	15478	1525	1
300-400	3743	342	226	-116	194	31026	1835	1
>400	3031	718	284	-434	736	44839	3016	1
total	145701	109	95	-13	137	10719	476	1

[a] simplified notation; referring to means over biomass ranges

Table 4. Validation results per biomass range for Tier 1 data at original resolution for the 2010 map.

AGB_{ref} bin [Mg/ha]	# plots count	AGB_{ref}	AGB_{map}	MD	RMSD	Var(Plt) [a] [Mg/ha]²	SE^2_{CCI} [a]	I_{Var}
		[Mg/ha]						
0-50	43602	25	61	35	68	9426	217	0
50-100	47841	72	74	2	63	7167	227	0
100-150	23749	121	109	-12	88	10173	468	0
150-200	10131	173	150	-23	119	14887	901	0
200-250	6157	223	180	-43	141	13951	1255	1
250-300	3779	273	204	-69	157	15262	1509	1
300-400	3797	342	224	-118	192	17845	1846	1
>400	3070	716	279	-437	734	40329	3002	1
total	142126	106	98	-8	139	10424	494	1

[a] simplified notation; referring to means over biomass ranges

Table 5. Validation results per biomass range for Tier 1 data at original resolution for the 2015 map.

AGB_{ref} bin [Mg/ha]	# plots count	AGB_{ref}	AGB_{map}	MD	RMSD	Var(Plt)[a]	SE^2_{CCI} [a]	I_{Var}
		---------------------[Mg/ha]			---------------------	[Mg/ha] ²		
0-50	36147	22	63	41	71	11307	208	0
50-100	25897	72	87	15	69	12245	294	0
100-150	15917	123	119	-4	85	14147	520	0
150-200	9338	174	143	-30	107	15663	741	0
200-250	6012	223	170	-53	130	14209	995	1
250-300	3825	273	196	-77	147	15147	1261	1
300-400	4086	343	217	-126	183	17942	1475	1
>400	3510	685	268	-417	691	39396	2269	1
total	104732	119	109	-10	155	13866	527	1

[a] simplified notation; referring to means over biomass ranges

Table 6. Validation results per biomass range for Tier 1 data at original resolution for the 2016 map.

AGB_{ref} bin [Mg/ha]	# plots count	AGB_{ref}	AGB_{map}	MD	RMSD	Var(Plt)[a]	SE^2_{CCI} [a]	I_{Var}
		---------------------[Mg/ha]			---------------------	[Mg/ha] ²		
0-50	33023	21	64	43	30	1454	120	0
50-100	21348	73	93	20	30	2161	220	0
100-150	13921	123	123	-1	77	2206	699	1
150-200	8699	174	143	-31	117	1319	1725	1
200-250	5702	223	169	-54	106	1270	1722	1
250-300	3681	273	193	-81	109	1103	2432	1
300-400	3963	343	213	-130	137	2086	3070	1
>400	3464	687	266	-422	447	6542	4738	1
total	93801	122	112	-11	65	1829	416	1

[a] simplified notation; referring to means over biomass ranges

Table 7. Validation results per biomass range for Tier 1 data at original resolution for the 2017 map.

AGB_{ref} bin	# plots	AGB_{ref}	AGB_{map}	MD	RMSD	Var(Plt)[a]	SE^2_{CCI}[a]	I_{Var}
[Mg/ha]	count	---------------------[Mg/ha]		---------------------		[Mg/ha]^2		
0-50	28310	19	67	48	75	12129	205	0
50-100	16740	74	102	28	73	15776	333	0
100-150	12098	123	124	1	82	15254	477	0
150-200	7683	174	143	-31	105	15130	669	0
200-250	4850	223	170	-53	129	12431	942	1
250-300	2998	273	198	-75	147	11961	1264	1
300-400	3195	343	222	-121	182	13576	1514	1
>400	3043	714	280	-434	731	38457	2307	1
total	78917	124	116	-7	170	14760	539	1

[a] simplified notation; referring to means over biomass ranges

Table 8. Validation results per biomass range for Tier 1 data at original resolution for the 2018 map.

AGB_{ref} bin	# plots	AGB_{ref}	AGB_{map}	MD	RMSD	Var(Plt)[a]	SE^2_{CCI}[a]	I_{Var}
[Mg/ha]	count	---------------------[Mg/ha]		---------------------		[Mg/ha]^2		
0-50	25410	18	64	45	69	11328	175	0
50-100	14230	74	101	28	69	15726	314	0
100-150	10615	123	122	-2	80	14800	447	0
150-200	6774	174	138	-36	103	14644	623	0
200-250	4279	223	164	-59	130	12266	870	1
250-300	2639	273	193	-80	150	12237	1200	1
300-400	2851	344	215	-128	184	14113	1444	1
>400	2919	723	277	-446	745	39359	2272	1
total	69717	126	114	-12	177	14456	510	1

[a] simplified notation; referring to means over biomass ranges

Table 9. Validation results per biomass range for Tier 1 data at original resolution for the 2019 map.

AGB_{ref} bin [Mg/ha]	# plots count	AGB_{ref}	AGB_{map}	MD	RMSD	$Var(Plt)^a$ [Mg/ha]^2	$SE^2_{CCI}{}^a$	I_{Var}
		---------------------[Mg/ha] ---------------------						
0-50	24251	18	63	45	70	10358	166	0
50-100	13266	74	101	27	68	14698	306	0
100-150	9849	123	122	-2	82	13877	436	0
150-200	6280	174	136	-38	102	14066	595	0
200-250	3951	223	159	-64	129	12120	811	1
250-300	2324	273	182	-91	154	12650	1114	1
300-400	2452	343	207	-137	193	15291	1348	1
>400	2708	739	272	-467	766	41307	2317	1
Total	65081	124	111	-13	180	13795	484	1

[a] simplified notation; referring to means over biomass ranges

Table 10. Validation results per biomass range for Tier 1 data at original resolution for the 2020 map.

AGB_{ref} bin [Mg/ha]	# plots count	AGB_{ref}	AGB_{map}	MD	RMSD	$Var(Plt)^a$ [Mg/ha]^2	$SE^2_{CCI}{}^a$	I_{Var}
		---------------------[Mg/ha] ---------------------						
0-50	22962	18	62	45	70	9180	158	0
50-100	12254	74	101	27	71	13478	295	0
100-150	9077	123	120	-3	81	12746	418	0
150-200	5825	174	133	-41	101	13219	557	0
200-250	3664	223	156	-67	130	11847	763	1
250-300	2115	273	178	-95	157	12936	1053	1
300-400	2240	343	203	-141	194	15694	1292	1
>400	2488	730	271	-459	757	40686	2262	1
total	60625	122	109	-13	178	12797	459	1

[a] simplified notation; referring to means over biomass ranges

Table 11. Validation results per biomass range for Tier 1 data at original resolution for the 2021 map.

AGB_{ref} bin	# plots	AGB_{ref}	AGB_{map}	MD	RMSD	Var(Plt)[a]	SE^2_{CCI} [a]	I_{Var}
[Mg/ha]	count	---------------------[Mg/ha]	---------------------			[Mg/ha]^2		
0-50	21794	17	61	44	68	8153	154	0
50-100	11276	74	99	25	67	11919	286	0
100-150	8352	123	118	-6	77	11360	403	0
150-200	5413	174	130	-45	99	12202	510	0
200-250	3403	223	147	-76	127	11421	661	1
250-300	1920	273	168	-105	156	12652	918	1
300-400	1943	343	188	-155	200	16259	1071	1
>400	2055	721	255	-467	764	39612	1961	1
total	56156	118	104	-14	171	11560	406	1

[a] simplified notation; referring to means over biomass ranges

Table 12. Validation results per biomass range for Tier 1 data at original resolution for the 2022 map.

AGB_{ref} bin	# plots	AGB_{ref}	AGB_{map}	MD	RMSD	Var(Plt)[a]	SE^2_{CCI} [a]	I_{Var}
[Mg/ha]	count	---------------------[Mg/ha]	---------------------			[Mg/ha]^2		
0-50	19434	17	61	44	69	6997	157	0
50-100	9863	74	99	26	68	10021	271	0
100-150	7451	124	118	-5	77	9823	390	0
150-200	4908	174	130	-44	99	10985	495	0
200-250	3075	222	146	-77	125	10452	621	1
250-300	1684	273	164	-109	157	11891	859	1
300-400	1737	343	184	-159	199	15562	963	1
>400	1775	720	252	-468	757	40223	1819	1
total	49927	117	104	-14	168	10265	387	1

[a] simplified notation; referring to means over biomass ranges

3.1.2. Tier 2 non-aggregated

Here, a better agreement between plot and map estimates is observed compared to the Tier 1 results, which can be attributed to the decreasing spatial mismatch between plots and map pixels. The binned ranges (right-hand plots for each year in Figure 3) show most biomass bins overlapping the 1:1 line except for the 2007, 2010, 2015 and 2016 maps until 200 Mg/ha, while the rest of the years show better agreement throughout all of the bins.

The results for 2018-2022 are very similar due to minimal changes in the biomass estimates from reference data used and maps. Note that the 2018-2022 comparisons also used less reference data than the rest of the comparisons (see Table 2). Most Tier 2 plots are located in the tropics (

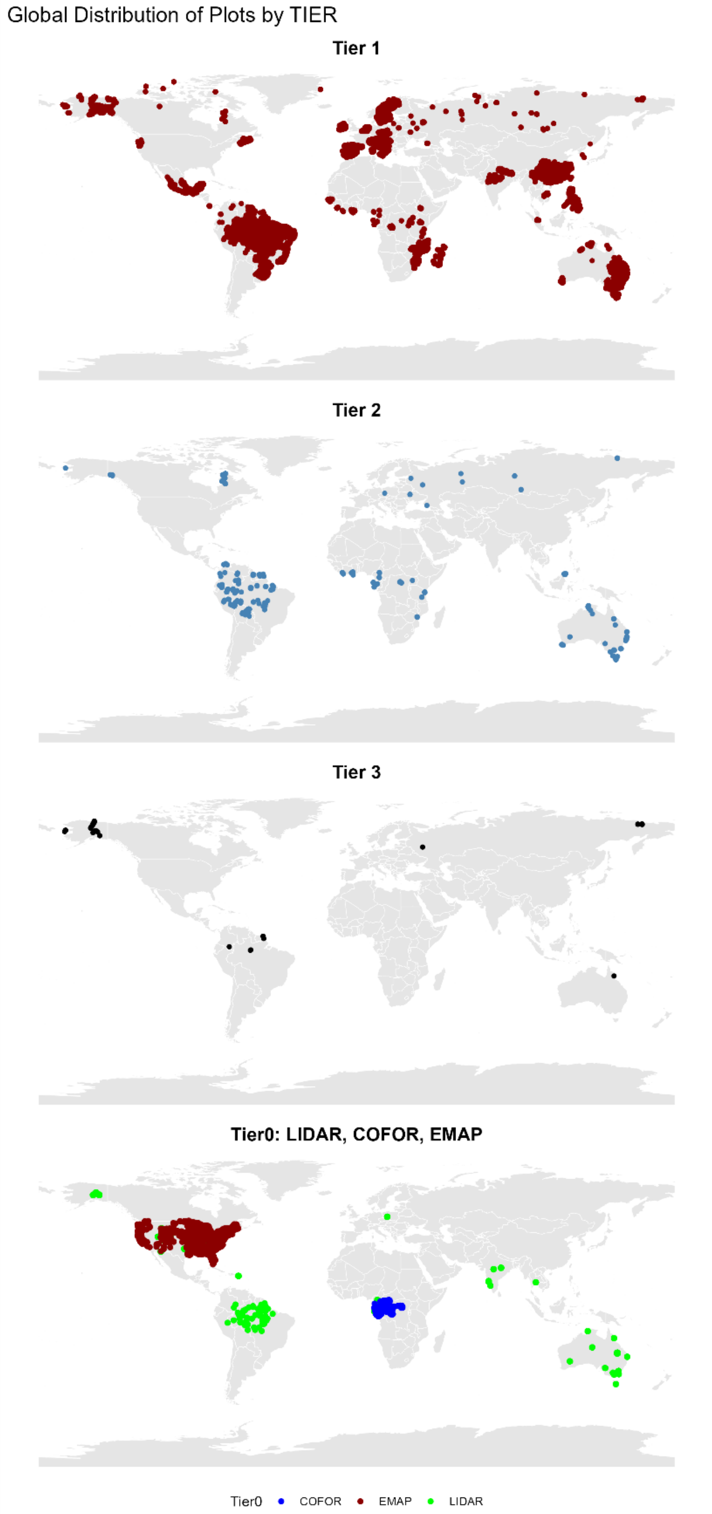
Global Distribution of Plots by TIER
Tier 1
Tier 2
Tier 3
Tier0: LIDAR, COFOR, EMAP
Tier0
COFOR
EMAP
LIDAR

Figure 1).

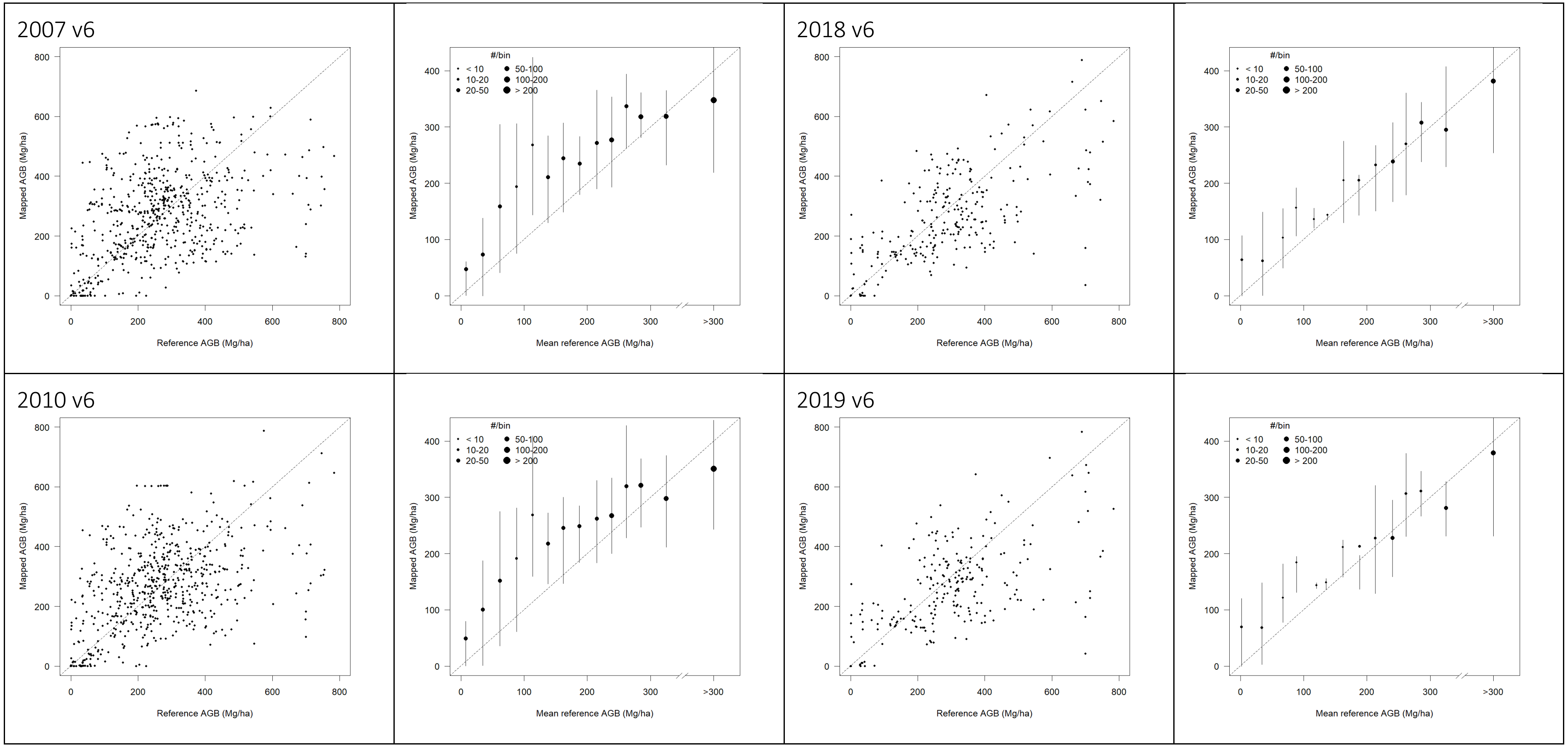

2007 v6
2018 v6
2010 v6
2019 v6
Mapped AGB (Mg/ha)
Reference AGB (Mg/ha)
Mean reference AGB (Mg/ha)
#/bin
< 10
10-20
20-50
50-100
100-200
> 200

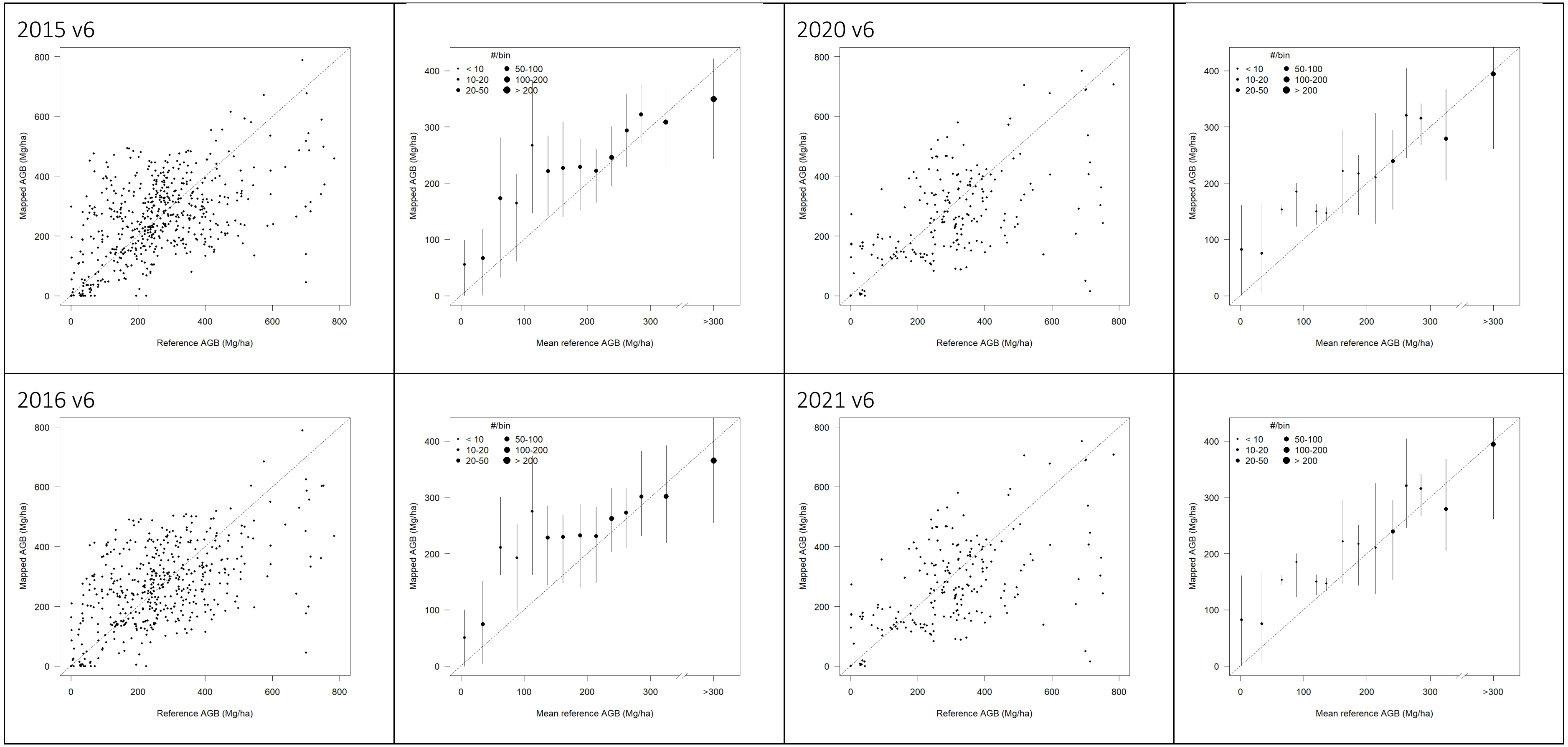

2015 v6
2020 v6
2016 v6
2021 v6
Mapped AGB (Mg/ha)
Reference AGB (Mg/ha)
Mean reference AGB (Mg/ha)
#/bin
< 10
10-20
20-50
50-100
100-200
> 200

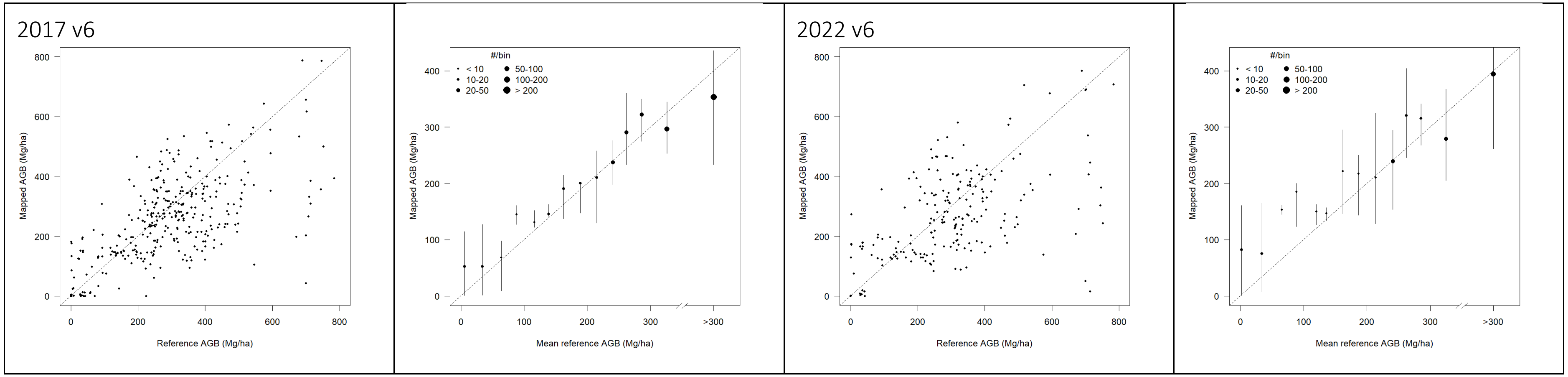

Figure 3. Plot-map comparisons for Tier 2 data at original resolution (i.e., without spatial aggregation); left column: scatterplots; rights column: binned over 25 Mg/ha wide AGB ranges with whiskers representing the interquartile range of mapped AGB values and symbol size representing the number of plots per AGB range. AGB_{ref} > 350 Mg/ha data are grouped into a single bin. Note the different scales on the left and right graphs.

Table 13. Validation results per biomass range for Tier 2 data at original resolution for the 2007 map.

AGB_{ref} bin	# plots	AGB_{ref}	AGB_{map}	MD	RMSD	Var(Plt)[a]	SE^2_{CCI}[a]	I_{Var}
[Mg/ha]	count	---------------------[Mg/ha] ---------------------				$[Mg/ha]^2$		
0-50	55	22	61	39	96	2187	980	1
50-100	43	73	173	101	168	270	1982	1
100-150	50	128	233	104	164	366	3589	1
150-200	63	175	240	65	139	1512	2441	1
200-250	103	229	275	46	126	2116	2654	1
250-300	97	274	327	52	127	746	2980	1
300-400	121	347	308	-39	142	692	3184	1
>400	123	593	371	-222	329	7590	5016	1
total	655	285	276	-10	188	2371	3110	1

[a] simplified notation; referring to means over biomass ranges

Table 14. Validation results per biomass range for Tier 2 data at original resolution for the 2010 map.

AGB_{ref} bin	# plots	AGB_{ref}	AGB_{map}	MD	RMSD	Var(Plt)[a]	SE^2_{CCI}[a]	I_{Var}
[Mg/ha]	count	---------------------[Mg/ha] ---------------------				$[Mg/ha]^2$		
0-50	56	21	75	53	116	2099	969	1
50-100	43	73	168	96	161	146	1838	1
100-150	50	128	237	109	164	306	3309	1
150-200	64	175	248	72	142	1474	2324	1
200-250	103	229	265	36	123	2079	2614	1
250-300	96	275	321	46	126	697	2957	1
300-400	121	347	299	-49	113	632	3186	1
>400	123	593	374	-219	327	7558	5011	1
total	656	285	273	-12	184	2318	3052	1

[a] simplified notation; referring to means over biomass ranges

Table 15. Validation results per biomass range for Tier 2 data at original resolution for the 2015 map.

AGB_{ref} bin [Mg/ha]	# plots count	AGB_{ref}	AGB_{map}	MD	RMSD	$Var(Plt)^a$ [Mg/ha]^2	SE^2_{CCI} [a]	I_{Var}
		[Mg/ha]						
0-50	46	23	63	39	97	608	1107	1
50-100	42	73	170	96	164	494	1682	1
100-150	46	128	240	112	163	428	3240	1
150-200	53	174	228	54	129	610	2457	1
200-250	95	229	237	8	96	2272	2717	1
250-300	84	274	308	35	86	833	3049	1
300-400	103	347	297	-50	110	749	3290	1
>400	105	614	378	-236	339	8719	4581	1
total	574	286	265	-22	180	2403	3023	1

[a] simplified notation; referring to means over biomass ranges

Table 16. Validation results per biomass range for Tier 2 data at original resolution for the 2016 map.

AGB_{ref} bin [Mg/ha]	# plots count	AGB_{ref}	AGB_{map}	MD	RMSD	$Var(Plt)^a$ [Mg/ha]^2	SE^2_{CCI} [a]	I_{Var}
		[Mg/ha]						
0-50	43	23	65	42	93	802	1154	1
50-100	32	75	202	127	175	715	2075	1
100-150	44	128	247	119	163	496	3174	1
150-200	47	175	231	57	128	618	2576	1
200-250	79	230	251	21	105	2601	2913	1
250-300	68	273	286	14	89	868	3292	1
300-400	97	347	302	-45	113	814	3301	1
>400	100	618	393	-225	340	9116	4560	1
total	510	293	272	-21	185	2673	3151	1

[a] simplified notation; referring to means over biomass ranges

Table 17. Validation results per biomass range for Tier 2 data at original resolution for the 2017 map.

AGB_{ref} bin [Mg/ha]	# plots count	AGB_{ref}	AGB_{map}	MD	RMSD	Var(Plt)[a] [Mg/ha]^2	SE^2_{CCI}[a]	I_{Var}
		[Mg/ha]						
0-50	36	20	53	33	77	1098	865	1
50-100	14	80	117	38	88	993	419	1
100-150	14	133	141	9	43	644	195	1
150-200	24	178	196	18	90	764	800	1
200-250	51	231	228	-3	83	3692	1386	1
250-300	56	273	306	33	95	1001	2514	1
300-400	89	348	290	-57	114	923	2997	1
>400	93	625	383	-242	362	9749	4206	1
total	377	329	267	-63	198	3485	2462	1

[a] simplified notation; referring to means over biomass ranges

Table 18. Validation results per biomass range for Tier 2 data at original resolution for the 2018 map.

AGB_{ref} bin [Mg/ha]	# plots count	AGB_{ref}	AGB_{map}	MD	RMSD	Var(Plt)[a] [Mg/ha]^2	SE^2_{CCI}[a]	I_{Var}
		[Mg/ha]						
0-50	28	20	63	43	92	1457	1088	1
50-100	12	83	143	60	111	1361	472	1
100-150	12	131	141	11	28	674	144	0
150-200	18	179	205	26	104	752	836	1
200-250	41	231	237	6	99	4408	1243	1
250-300	38	274	290	16	91	1122	2092	1
300-400	70	346	298	-47	108	1023	2869	1
>400	69	683	416	-268	391	12733	4032	1
total	288	339	275	-64	210	4348	2300	1

[a] simplified notation; referring to means over biomass ranges

Table 19. Validation results per biomass range for Tier 2 data at original resolution for the 2019 map

AGB_{ref} bin [Mg/ha]	# plots count	AGB_{ref} [Mg/ha]	AGB_{map} [Mg/ha]	MD [Mg/ha]	RMSD [Mg/ha]	Var(Plt)[a] [Mg/ha]^2	SE^2_{CCI}[a]	I_{Var}
0-50	24	19	69	50	99	1928	1260	1
50-100	10	82	165	83	128	1836	430	1
100-150	10	131	148	16	22	753	153	0
150-200	15	180	212	33	117	854	865	1
200-250	35	233	228	-5	114	3453	1424	1
250-300	36	273	309	35	90	1299	2132	1
300-400	69	345	290	-55	109	1180	2885	1
>400	67	691	411	-280	398	13151	4179	1
total	266	351	281	-71	219	4568	2461	1

[a] simplified notation; referring to means over biomass ranges

Table 20. Validation results per biomass range for Tier 2 data at original resolution for the 2020 map.

AGB_{ref} bin [Mg/ha]	# plots count	AGB_{ref} [Mg/ha]	AGB_{map} [Mg/ha]	MD [Mg/ha]	RMSD [Mg/ha]	Var(Plt)[a] [Mg/ha]^2	SE^2_{CCI}[a]	I_{Var}
0-50	22	20	78	59	106	2425	1368	1
50-100	9	83	178	95	118	2115	472	1
100-150	9	131	148	17	31	845	159	0
150-200	13	177	219	42	113	952	959	1
200-250	30	234	232	-2	110	4010	1306	1
250-300	33	275	318	43	108	1516	2104	1
300-400	65	345	296	-49	112	1377	2958	1
>400	61	708	427	-282	400	14370	4443	1
total	242	357	290	-67	222	5078	2563	1

[a] simplified notation; referring to means over biomass ranges

Table 21. Validation results per biomass range for Tier 2 data at original resolution for the 2021 map.

AGB_{ref} bin [Mg/ha]	# plots count	AGB_{ref}	AGB_{map}	MD	RMSD	Var(Plt)[a]	SE^2_{CCI} [a]	I_{Var}
		[Mg/ha]				[Mg/ha]^2		
0-50	22	20	86	67	123	2864	1365	1
50-100	9	83	168	84	115	2222	460	1
100-150	8	131	141	11	39	1005	159	1
150-200	12	177	212	35	117	1047	864	1
200-250	12	233	235	1	130	1494	1575	1
250-300	31	275	328	53	102	1746	2081	1
300-400	62	344	286	-59	105	1586	2988	1
>400	60	712	432	-280	416	14647	4535	1
total	216	369	295	-74	238	5337	2716	1

[a] simplified notation; referring to means over biomass ranges

Table 22. Validation results per biomass range for Tier 2 data at original resolution for the 2022 map.

AGB_{ref} bin [Mg/ha]	# plots count	AGB_{ref}	AGB_{map}	MD	RMSD	Var(Plt)[a]	SE^2_{CCI} [a]	I_{var}
		[Mg/ha]				[Mg/ha]^2		
0-50	19	19	80	62	106	3540	1546	1
50-100	7	87	172	86	119	1879	306	1
100-150	3	132	146	14	48	1995	192	1
150-200	6	181	233	51	126	1284	1307	1
200-250	11	232	215	-17	124	1666	1574	1
250-300	24	274	292	18	82	2058	2244	1
300-400	37	342	316	-27	126	2081	3714	1
>400	40	725	440	-285	405	15378	4549	1
total	147	362	294	-68	232	5809	2928	1

[a] simplified notation; referring to means over biomass ranges

In most cases, the indicator variable I_{Var} = 1, indicating the CCI Biomass maps are optimistic about map precision.

3.1.3. Tier 3 non-aggregated

The non-aggregated results (i.e., at original plot level) of global plot-map comparisons using Tier 3 data (plot size ≥ 6 ha) are shown in Figure 4 and Tables 23-32. Similar to Tier 2, spatial aggregation to 0.1° cells was omitted because of the small number of available Tier 3 plots.

It is important to note that most Tier 3 plots are in the tropics and cover an AGB range of between 150 and 450 Mg/ha (i.e., the AGB range where the maximum AGB parameter of the AGB retrieval algorithm needs revision), and so lack low AGB densities. The small number of plots and the large scatter hardly allow conclusions to be drawn based on these data, except for the general trend of the map to under-predict AGB in the higher part of the assessed AGB range, which was also observed with the Tier 1 & 2 data. Note that 2015-2021 comparisons used fewer reference data.

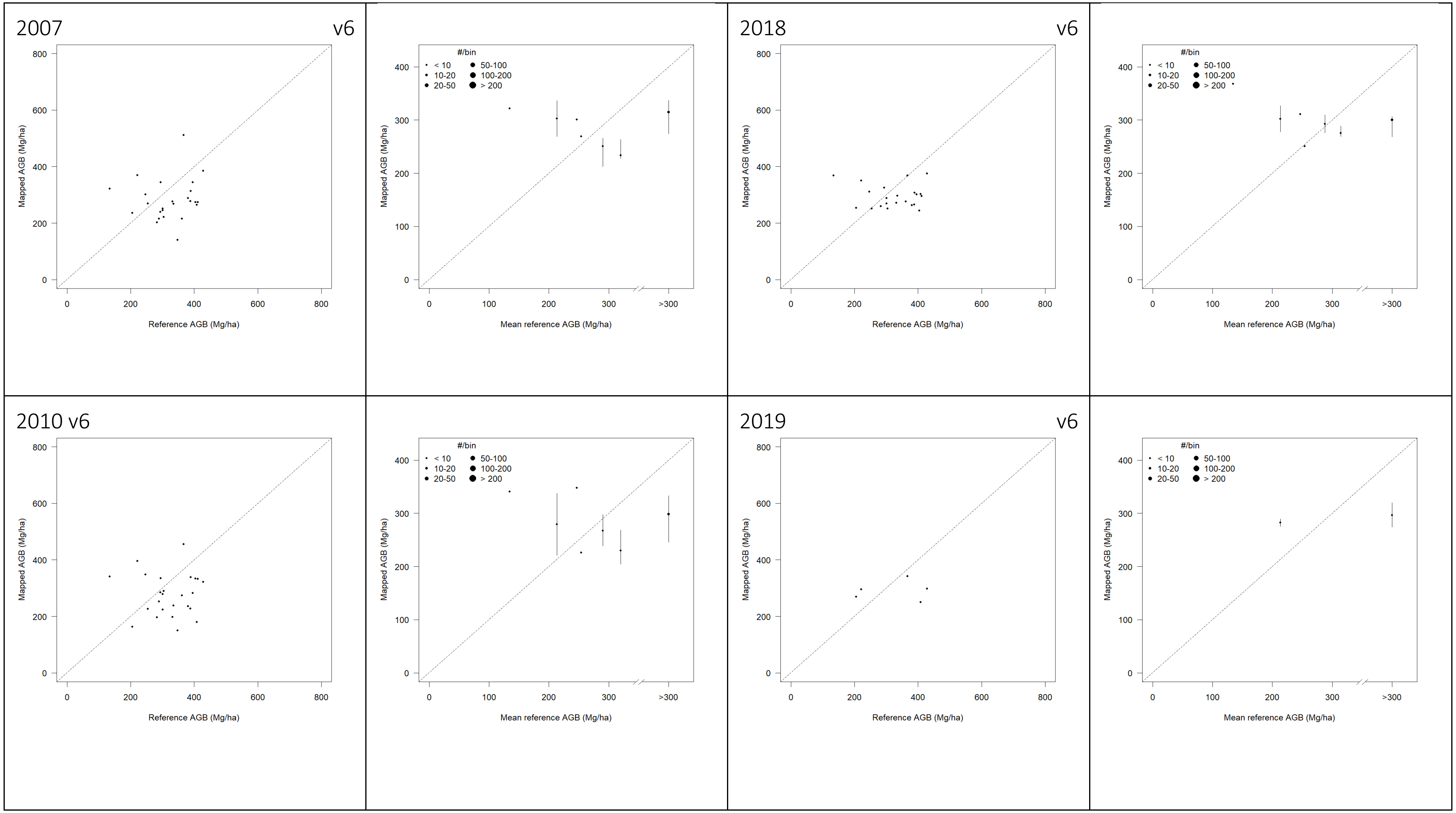

2007
v6
2018
v6
2010 v6
2019
v6
Mapped AGB (Mg/ha)
Reference AGB (Mg/ha)
Mean reference AGB (Mg/ha)
#/bin
< 10
10-20
20-50
50-100
100-200
> 200

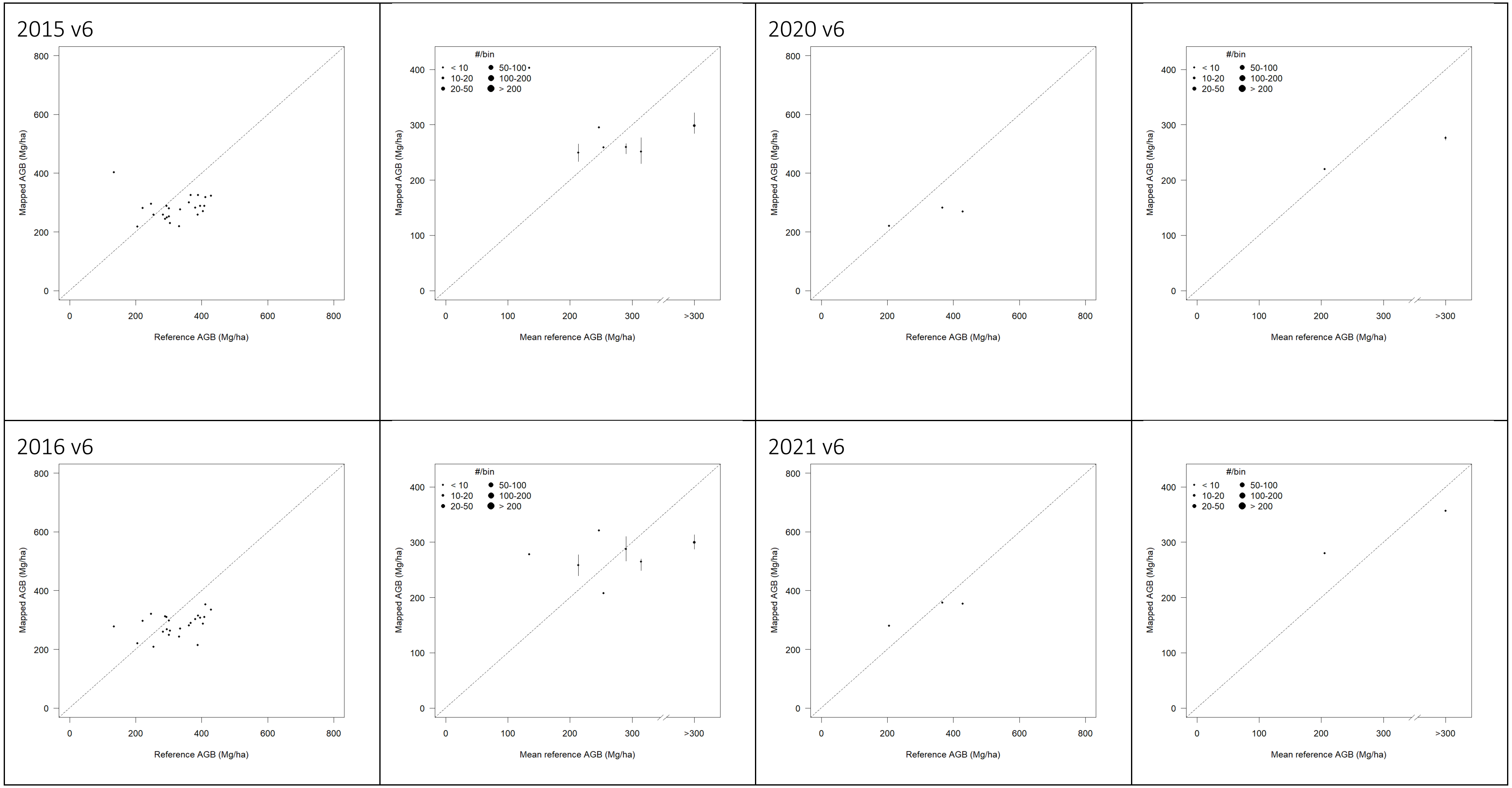

2015 v6
2020 v6
2016 v6
2021 v6
#/bin
< 10
10-20
20-50
50-100
100-200
> 200
Mapped AGB (Mg/ha)
Reference AGB (Mg/ha)
Mean reference AGB (Mg/ha)

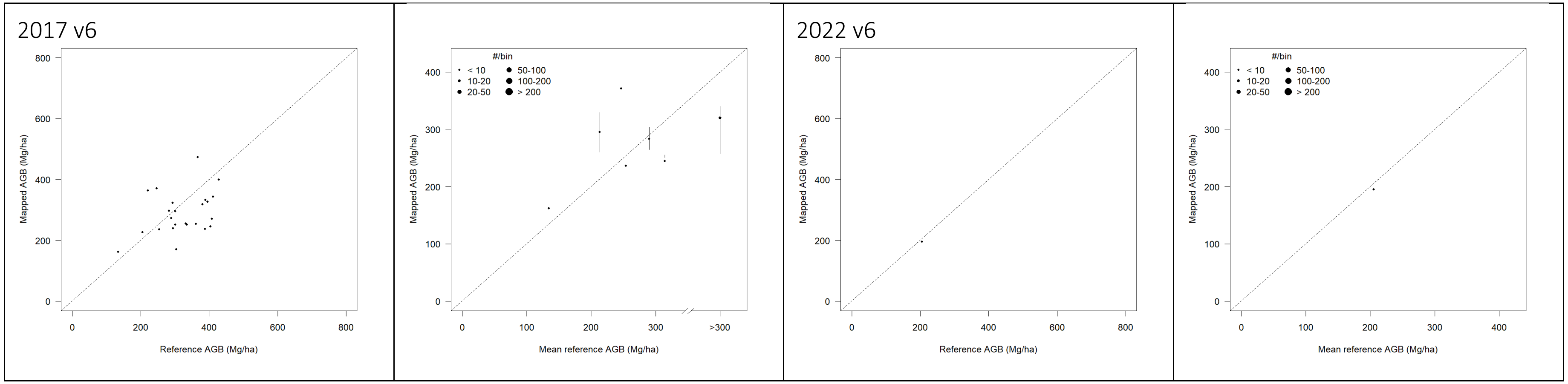

Figure 4. Plot-map comparisons for Tier 3 data at original resolution (i.e., without spatial aggregation); left column: scatterplots; right column: binned over 25 Mg/ha wide AGB ranges with whiskers representing the interquartile range of mapped AGB

Table 23. Validation results per biomass range for Tier 3 data at the original resolution for the 2007 map.

AGB_{ref} bin	# plots	AGB_{ref}	AGB_{map}	MD	RMSD	Var(Plt)[a]	SE^2_{CCI}[a]	I_{Var}
[Mg/ha]	count	---------------------[Mg/ha]		---------------------		[Mg/ha]^2		
0-50	-	-	-	-	-	-	-	-
50-100								
100-150	1	134	322	188	188	134	1609	1
150-200	-	-	-	-	-	-	-	-
200-250	3	225	302	78	93	690	1422	1
250-300	5	283	254	-28	59	438	2452	1
300-400	12	350	280	-70	105	314	2986	1
>400	4	413	300	-113	120	302	3541	1
total	25	323	282	-41	104	375	2725	1

[a] simplified notation; referring to means over the biomass ranges

Table 24. Validation results per biomass range for Tier 3 data at the original resolution for the 2010 map.

AGB_{ref} bin	# plots	AGB_{ref}	AGB_{map}	MD	RMSD	Var(Plt)[a]	SE^2_{CCI}[a]	I_{Var}
[Mg/ha]	count	---------------------[Mg/ha]		---------------------		[Mg/ha]^2		
0-50	-	-	-	-	-	-	-	-
50-100								
100-150	1	134	341	207	207	123	1623	1
150-200	-	-	-	-	-	-	-	-
200-250	3	225	302	78	119	666	1503	1
250-300	5	283	259	-23	47	402	2418	0
300-400	12	350	266	-84	112	278	2961	1
>400	4	413	292	-121	136	266	3561	1
total	25	323	276	-47	113	341	2713	1

[a] simplified notation; referring to means over the biomass ranges

Table 25. Validation results per biomass range for Tier 3 data at the original resolution for the 2015 map.

AGB_{ref} bin [Mg/ha]	# plots count	AGB_{ref}	AGB_{map}	MD	RMSD	Var(Plt)[a] [Mg/ha]^2	SE^2_{CCI} [a]	I_{Var}
		---------------------[Mg/ha]	---------------------					
0-50	-	-	-	-	-	-	-	-
50-100	-	-	-	-	-	-	-	-
100-150	-	-	-	-	-	-	-	-
150-200	1	150	426	276	276	76035	213	1
200-250	2	220	252	32	37	1401	985	0
250-300	3	268	214	-54	54	2950	231	1
300-400	12	344	265	-79	94	8913	381	1
>400	5	416	296	-120	123	15027	294	1
total	23	331	271	-60	108	11730	388	1

[a] simplified notation; referring to means over the biomass ranges

Table 26. . Validation results per biomass range for Tier 3 data at the original resolution for the 2016 map.

AGB_{ref} bin [Mg/ha]	# plots count	AGB_{ref}	AGB_{map}	MD	RMSD	Var(Plt)[a] [Mg/ha]^2	SE^2_{CCI} [a]	I_{Var}
		---------------------[Mg/ha]	---------------------					
0-50	-	-	-	-	-	-	-	-
50-100	-	-	-	-	-	-	-	-
100-150	1	134	278	144	144	166	1456	1
150-200	-	-	-	-	-	-	-	-
200-250	3	225	279	55	62	762	1377	1
250-300	5	283	272	-11	29	546	2185	0
300-400	11	350	276	-74	84	367	2741	1
>400	4	413	321	-91	94	410	3270	1
total	24	322	283	-39	79	453	2490	1

[a] simplified notation; referring to means over the biomass ranges

Table 27. Validation results per biomass range for Tier 3 data at the original resolution for the 2017 map.

AGB_{ref} bin [Mg/ha]	# plots count	AGB_{ref}	AGB_{map}	MD	RMSD	Var(Plt)[a]	SE^2_{CCI} [a]	I_{Var}
		---------[Mg/ha]	---------			[Mg/ha]^2		
0-50	-	-	-	-	-	-	-	-
50-100	-	-	-	-	-	-	-	-
100-150	1	134	162	28	28	182	1498	0
150-200	-	-	-	-	-	-	-	-
200-250	3	225	320	96	110	796	1431	1
250-300	5	283	274	-9	31	598	2320	0
300-400	11	350	288	-62	91	419	2963	1
>400	4	413	314	-98	111	462	3453	1
total	24	322	288	-34	87	501	2658	1

[a] simplified notation; referring to means over the biomass ranges

Table 28. Validation results per biomass range for Tier 3 data at the original resolution for the 2018 map.

AGB_{ref} bin [Mg/ha]	# plots count	AGB_{ref}	AGB_{map}	MD	RMSD	Var(Plt)[a]	SE^2_{CCI} [a]	I_{Var}
		---------[Mg/ha]	---------			[Mg/ha]^2		
0-50	-	-	-	-	-	-	-	-
50-100	-	-	-	-	-	-	-	-
100-150	1	134	368	234	234	200	1419	1
150-200	-	-	-	-	-	-	-	-
200-250	3	225	305	81	88	836	1462	1
250-300	3	277	279	2	23	459	2517	0
300-400	11	350	287	-63	74	479	2812	1
>400	4	413	304	-108	115	522	3329	1
total	22	324	295	-29	93	520	2618	1

[a] simplified notation; referring to means over the biomass ranges

Table 29. Validation results per biomass range for Tier 3 data at the original resolution for the 2019 map.

AGB_{ref} bin	# plots	AGB_{ref}	AGB_{map}	MD	RMSD	Var(Plt)[a]	SE^2_{CCI}[a]	I_{Var}
[Mg/ha]	count	---------------------[Mg/ha] ---------------------				[Mg/ha]^2		
0-50	-	-	-	-	-	-	-	-
50-100	-	-	-	-	-	-	-	-
100-150	-	-	-	-	-	-	-	-
150-200	-	-	-	-	-	-	-	-
200-250	2	213	282	69	69	1058	1146	1
250-300	-	-	-	-	-	-	-	-
300-400	1	366	342	-24	24	562	5766	0
>400	2	418	274	-144	144	601	4154	1
total	5	326	291	-35	102	776	3273	1

[a] simplified notation; referring to means over the biomass ranges

Table 30. Validation results per biomass range for Tier 3 data at the original resolution for the 2020 map.

AGB_{ref} bin	# plots	AGB_{ref}	AGB_{map}	MD	RMSD	Var(Plt)[a]	SE^2_{CCI}[a]	I_{Var}
[Mg/ha]	count	---------------------[Mg/ha] ---------------------				[Mg/ha]^2		
0-50	-	-	-	-	-	-	-	-
50-100	-	-	-	-	-	-	-	-
100-150	-	-	-	-	-	-	-	-
150-200	-	-	-	-	-	-	-	-
200-250	1	206	220	14	14	1113	202	0
250-300	-	-	-	-	-	-	-	-
300-400	1	366	283	-83	83	638	5766	1
>400	1	428	269	-159	159	686	5766	1
total	21	333	257	-76	104	812	3911	1

[a] simplified notation; referring to means over the biomass ranges

Table 31. Validation results per biomass range for Tier 3 data at the original resolution for the 2021 map.

AGB_{ref} bin [Mg/ha]	# plots count	AGB_{ref}	AGB_{map}	MD	RMSD	Var(Plt)[a]	SE^2_{CCI}[a]	I_{Var}
		[Mg/ha]						
0-50	-	-	-	-	-	-	-	-
50-100	-	-	-	-	-	-	-	-
100-150	-	-	-	-	-	-	-	-
150-200	-	-	-	-	-	-	-	-
200-250	1	206	280	74	74	1113	171	1
250-300	-	-	-	-	-	-	-	-
300-400	1	366	359	-7	7	720	5764	0
>400	1	428	355	-73	73	770	5764	0
total	3	333	331	-2	60	868	3900	1

[a] simplified notation; referring to means over the biomass ranges

Table 32. Validation results per biomass range for Tier 3 data at the original resolution for the 2022 map.

AGB_{ref} bin [Mg/ha]	# plots count	AGB_{ref}	AGB_{map}	MD	RMSD	Var(Plt)[a]	SE^2_{CCI}[a]	I_{Var}
		[Mg/ha]						
0-50	-	-	-	-	-	-	-	-
50-100	-	-	-	-	-	-	-	-
100-150	-	-	-	-	-	-	-	-
150-200	-	-	-	-	-	-	-	-
200-250	1	206	195	-11	11	1113	181	0
250-300	-	-	-	-	-	-	-	-
300-400	-	-	-	-	-	-	-	-
>400	-	-	-	-	-	-	-	-
total	3	333	331	-2	60	868	181	1

[a] simplified notation; referring to means over the biomass ranges

3.2. Tier 1 plot data spatially aggregated to 0.1° cells

The results of global AGM_{map} - AGB_{ref} comparisons using Tier 1 data (plot size ≤ 0.6 ha) spatially aggregated to 0.1° cells are shown in Figure 5 and Tables 33-42. The rightmost variance columns shown in the non-aggregated results are omitted here because spatial correlation of errors within 0.1° cells may be non-negligible, but we lack data to assess such correlation for most biomes at the current stage of the project.

Spatial aggregation to 0.1° cells improved the fit between AGB_{ref} and AGB_{map} with absolute mean differences within 30 Mg/ha below 200 Mg/ha. Beyond 200 Mg ha^{-1}, AGB values are still under-predicted and the 0.1° cells producing the most under-prediction are located in southeast Australia. These cells show lower estimates than the previous version of CCI

Biomass products (not shown here). The results of the six years for Version 6 of the CCI maps show less consistency than their previous versions, particularly 2010 compared to the rest of the map epochs (see Section 3.7 for further analysis of consistency). In particular, the 2007, 2010, 2015-2017 maps show overestimation until 180 Mg/ha similar to the Tier 2 results observation. This could be an effect of using a different number of reference data (as many as 2500+ more than the reference data used for the 2018-2022 maps, see Table 2).

Spatial aggregation reduced the effect of localized AGB fluctuations in the map and their potential interaction with plot-map geolocation mismatches. These results (Figure 5, Tables 33-42) suggest the CCI Biomass predictions at 0.1° cell size are more precise than at the original pixel resolution. Note that at 0.1°, averages from both plots and maps correspond to the same forest definition (Section 2.4). Most 0.1° cells meeting the criterion of at least five plots per cell happen to be located in the temperate region (Section 3.5). The spatial aggregation also resulted in minimizing inconsistency between the 2010 and the 2015-2021 comparisons except for the 300 Mg ha^{-1} bin. The latter years are nearly identical, including the number of 0.1° grid cells used.

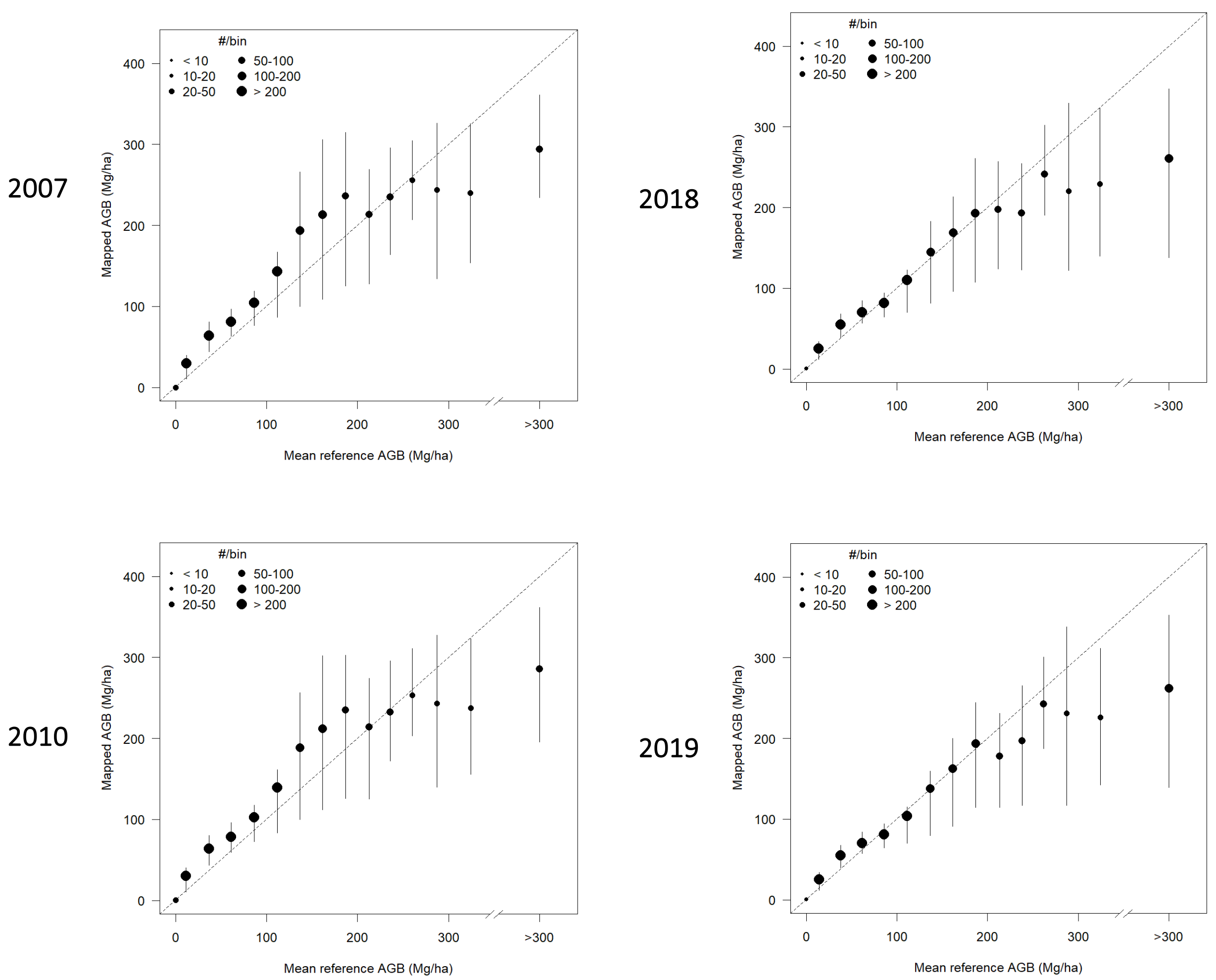

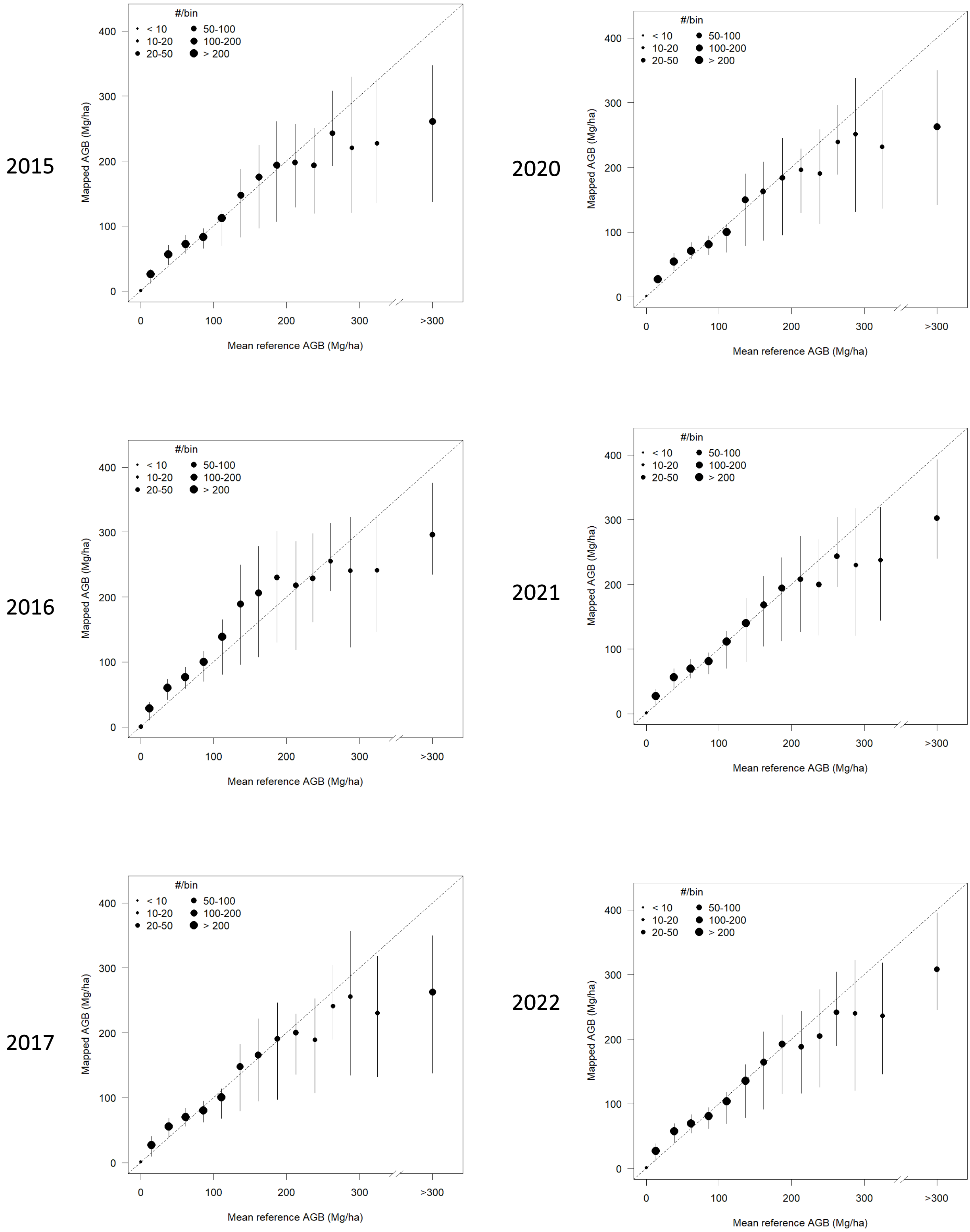

Figure 5. AGBref - AGBmap comparisons for Tier 1 data spatially aggregated to 0.1° and binned over 25 Mg/ha wide biomass ranges with whiskers representing the interquartile range of mapped AGB values and symbol size representing

the number of 0.1° cells per AGB range. AGBref > 350 Mg/ha data are grouped into a single bin.

Table 33. Validation results per biomass range for Tier 1 data spatially aggregated to 0.1° cells for the 2007 map.

AGB_{ref} bin [Mg/ha]	# cells count	AGB_{ref}	AGB_{map}	MD	RMSD
		[Mg/ha]			
0-50	5802	23	45	22	34
50-100	2008	69	88	19	41
100-150	478	121	162	41	110
150-200	236	172	223	51	146
200-250	124	224	224	0	121
250-300	65	272	251	-22	105
300-400	66	343	243	-100	144
>400	62	658	312	-346	425

Table 34. Validation results per biomass range for Tier 1 data spatially aggregated to 0.1° cells for the 2010 map.

AGB_{ref} bin [Mg/ha]	# cells count	AGB_{ref}	AGB_{map}	MD	RMSD
		[Mg/ha]			
0-50	5781	23	45	22	34
50-100	2103	69	87	17	42
100-150	510	121	158	37	109
150-200	242	172	222	50	144
200-250	130	224	223	-1	117
250-300	66	272	249	-23	104
300-400	72	345	235	-110	152
>400	63	654	311	-343	420

Table 35. Validation results per biomass range for Tier 1 data spatially aggregated to 0.1° cells for the 2015 map.

AGB_{ref} bin [Mg/ha]	# cells count	AGB_{ref}	AGB_{map}	MD	RMSD
		[Mg/ha]			
0-50	3023	29	44	16	26
50-100	2107	69	75	6	28
100-150	538	120	125	4	82
150-200	230	173	184	11	120
200-250	142	223	196	-28	110
250-300	86	273	234	-38	109
300-400	76	342	238	-103	148
>400	66	635	210	-425	514
total	6267	79	76	-3	66

Table 36. Validation results per biomass range for Tier 1 data spatially aggregated to 0.1° cells for the 2016 map.

AGB_{ref} bin	# cells	AGB_{ref}	AGB_{map}	MD	RMSD
[Mg/ha]	count	---------------------[Mg/ha]			---------------------
0-50	2628	29	47	17	30
50-100	2296	70	74	5	30
100-150	570	120	117	-3	77
150-200	234	173	183	10	117
200-250	133	225	197	-28	106
250-300	89	272	244	-28	109
300-400	68	341	248	-93	137
>400	53	688	322	-367	447

Table 37. Validation results per biomass range for Tier 1 data spatially aggregated to 0.1° cells for the 2017 map.

AGB_{ref} bin	# cells	AGB_{ref}	AGB_{map}	MD	RMSD
[Mg/ha]	count	---------------------[Mg/ha]			---------------------
0-50	2628	29	47	17	30
50-100	2296	70	74	5	30
100-150	570	120	117	-3	77
150-200	234	173	183	10	117
200-250	133	225	197	-28	106
250-300	89	272	244	-28	109
300-400	68	341	248	-93	137
>400	53	688	322	-367	447

Table 38. Validation results per biomass range for Tier 1 data spatially aggregated to 0.1° cells for the 2018 map.

AGB_{ref} bin	# cells	AGB_{ref}	AGB_{map}	MD	RMSD
[Mg/ha]	count	---------------------[Mg/ha]			---------------------
0-50	2628	29	47	17	30
50-100	2296	70	74	5	30
100-150	570	120	117	-3	77
150-200	234	173	183	10	117
200-250	133	225	197	-28	106
250-300	89	272	244	-28	109
300-400	68	341	248	-93	137
>400	53	688	322	-367	447

Table 39. Validation results per biomass range for Tier 1 data spatially aggregated to 0.1° cells for the 2019 map.

AGB_{ref} bin	# cells	AGB_{ref}	AGB_{map}	MD	RMSD
[Mg/ha]	count	---------------------[Mg/ha]			---------------------
0-50	2554	30	44	15	25
50-100	2144	70	74	4	28
100-150	540	120	116	-4	74
150-200	222	173	177	4	116
200-250	131	225	187	-38	106
250-300	92	272	238	-34	113
300-400	76	343	238	-106	149
>400	89	721	264	-457	579

Table 40. Validation results per biomass range for Tier 1 data spatially aggregated to 0.1° cells for the 2020 map

AGB_{ref} bin	# cells	AGB_{ref}	AGB_{map}	MD	RMSD
[Mg/ha]	count	---------------------[Mg/ha]			---------------------
0-50	1914	32	47	15	25
50-100	1999	70	74	4	27
100-150	415	118	115	-4	75
150-200	185	173	172	-1	114
200-250	92	225	193	-32	112
250-300	72	273	244	-29	108
300-400	69	343	249	-94	142
>400	93	724	259	-465	618

Table 41. Validation results per biomass range for Tier 1 data spatially aggregated to 0.1° cells for the 2021 map

AGB_{ref} bin	# cells	AGB_{ref}	AGB_{map}	MD	RMSD
[Mg/ha]	count	---------------------[Mg/ha]			---------------------
0-50	3101	28	45	17	29
50-100	2255	69	73	4	30
100-150	572	120	121	1	76
150-200	244	172	180	7	108
200-250	140	223	204	-19	108
250-300	81	272	238	-34	107
300-400	70	340	247	-94	141
>400	53	692	320	-372	452

Table 42. Validation results per biomass range for Tier 1 data spatially aggregated to 0.1° cells for the 2022 map

AGB_{ref} bin [Mg/ha]	# cells count	AGB_{ref}	AGB_{map}	MD	RMSD
		---[Mg/ha]---			
0-50	2628	29	46	17	30
50-100	2296	70	73	4	30
100-150	570	120	115	-5	74
150-200	234	173	177	4	112
200-250	133	225	195	-29	103
250-300	89	272	241	-31	109
300-400	68	341	248	-92	138
>400	53	688	321	-367	448

3.3. Comparisons with LiDAR-based, 1-km pixel Congo basin Forests AGB and EMAP 25-km aggregates

The results of the global AGM_{map} - AGB_{ref} comparisons at 0.1° resolution using LiDAR-based and CoFor AGB as reference data are shown in Figure 6 and Tables 43-52. The key observation is map overestimation in almost all the AGB bins for the 2007 and 2010 maps and consistently good agreement between reference data and map estimates for 2015-2022. This can be a result of key modifications of the AGB retrieval algorithm in the wet tropics in the current CCI maps. Previous assessments did not have LiDAR data in temperate woodlands (USA) unlike this current assessment. The 2010 results may also be influenced by the CoFor data having a dense plot network in the forest management areas of the Congo Basin. Since the original plot data inside the 1-km aggregates of the CoFor dataset are not available, we were unable to account for partly deforested areas. Such areas are likely to exist given the active forestry activities in the area. On the other hand, similar results were observed using the plot data (Tier 2 plots in particular), which builds confidence in using LiDAR and CoFor data for accuracy assessments.

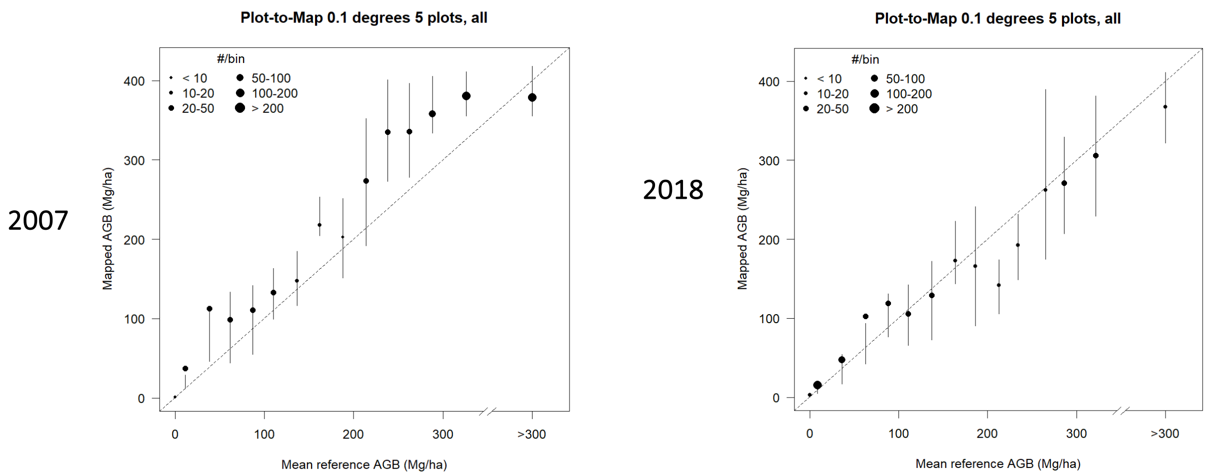

2010

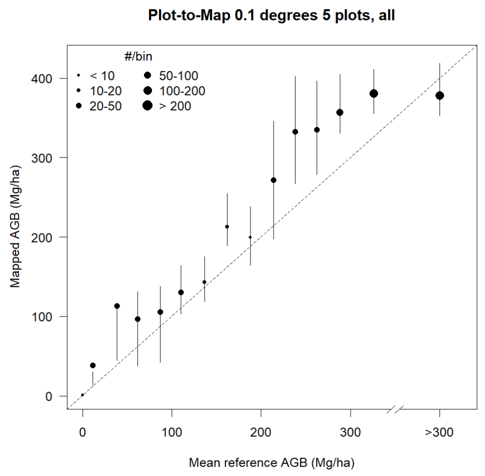

2019

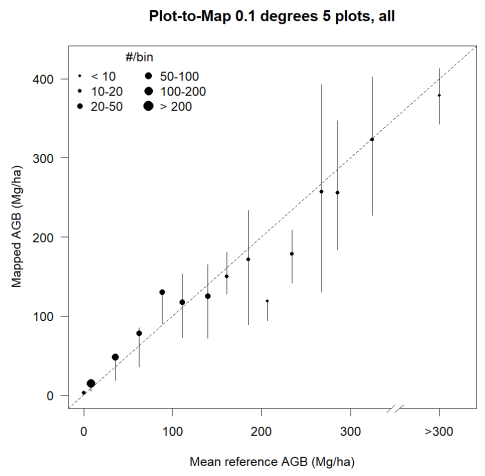

2015

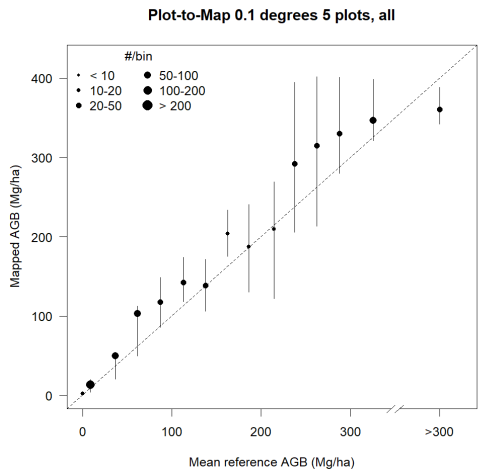

2020

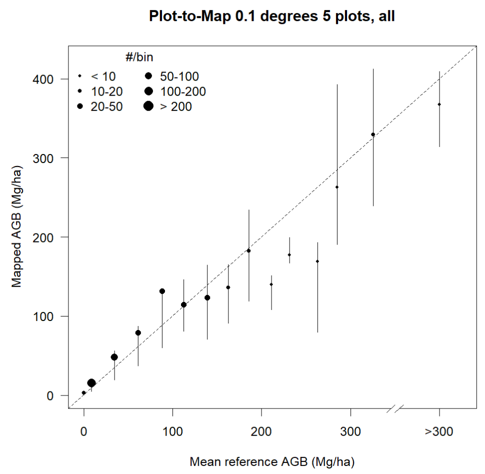

2016

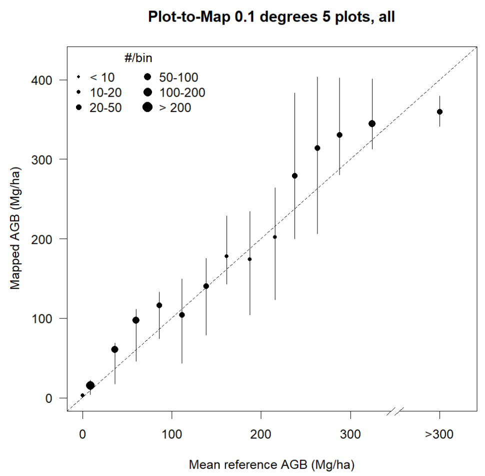

2021

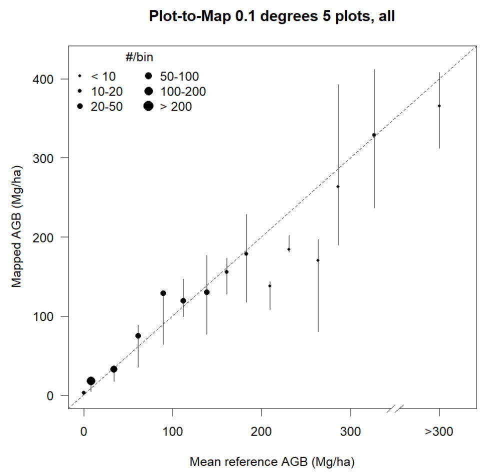

2017

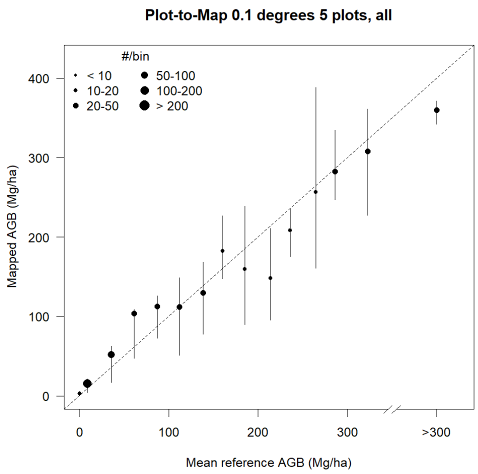

2022

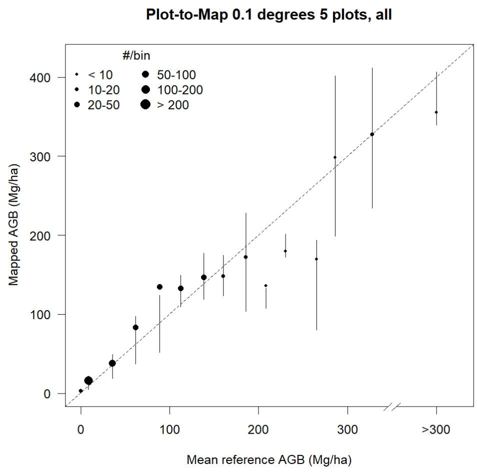

Figure 6. AGBref - AGBmap comparisons for LiDAR-based and CoFor AGB data spatially aggregated to 0.1° and binned over 25 Mg/ha wide AGB ranges with whiskers representing the interquartile range of mapped AGB values and symbol size representing the number of 0.1° cells per AGB range. AGBref > 350 Mg/ha data are grouped into a single bin.

Table 43. Validation results per biomass range using LiDAR-based and CoFor AGB data spatially aggregated to 0.1° cells for the 2007 map.

AGB_{ref} bin [Mg/ha]	# cells count	AGB_{ref}	AGB_{map}	MD	RMSD
		---------------------[Mg/ha]	---------------------		
0-50	79	19	59	40	104
50-100	45	74	104	31	74
100-150	35	121	139	18	60
150-200	20	173	212	39	74
200-250	51	229	311	82	123
250-300	100	277	348	71	109
300-400	210	345	379	34	72
>400	30	429	389	-39	78
total	570	241	281	41	89

Table 44. Validation results per biomass range using LiDAR-based and CoFor AGB data spatially aggregated to 0.1° cells for the 2010 map.

AGB_{ref} bin [Mg/ha]	# cells count	AGB_{ref}	AGB_{map}	MD	RMSD
		---------------------[Mg/ha]	---------------------		
0-50	79	19	60	40	103
50-100	45	74	101	27	73
100-150	35	121	135	15	56
150-200	20	173	207	35	70
200-250	51	229	309	80	121
250-300	100	277	347	70	108
300-400	210	345	378	33	72
>400	30	429	389	-39	78
total	570	241	280	39	88

Table 45. Validation results per biomass range using LiDAR-based and CoFor AGB data spatially aggregated to 0.1° cells for the 2015 map.

AGB_{ref} bin [Mg/ha]	# cells count	AGB_{ref}	AGB_{map}	MD	RMSD
		---------------------[Mg/ha]	---------------------		
0-50	254	15	22	7	35
50-100	91	72	109	37	88
100-150	46	126	141	15	61
150-200	25	177	194	17	68
200-250	41	230	264	35	109
250-300	76	274	322	48	113
300-400	75	335	350	15	68
>400	9	437	356	-81	109
total	617	130	149	19	72

Table 46. Validation results per biomass range using LiDAR-based and CoFor AGB data spatially aggregated to 0.1° cells for the 2016 map

AGB_{ref} bin [Mg/ha]	# cells count	AGB_{ref}	AGB_{map}	MD	RMSD
		---------------------[Mg/ha]	---------------------		
0-50	79	19	59	40	104
50-100	45	74	96	22	65
100-150	35	121	133	12	54
150-200	20	173	204	31	68
200-250	51	229	303	74	119
250-300	100	277	344	68	107
300-400	210	345	376	31	72
>400	30	429	389	-40	77
total	570	241	278	37	88

Table 47. Validation results per biomass range using LiDAR-based and CoFor AGB data spatially aggregated to 0.1° cells for the 2017 map

AGB_{ref} bin [Mg/ha]	# cells count	AGB_{ref}	AGB_{map}	MD	RMSD
		---------------------[Mg/ha]	---------------------		
0-50	247	14	23	8	31
50-100	89	73	108	35	97
100-150	46	124	120	-4	59
150-200	26	172	172	0	70
200-250	26	227	183	-44	82
250-300	39	276	270	-6	108
300-400	51	340	328	-12	69
>400	9	440	362	-78	108
total	533	109	114	4	66

Table 48. Validation results per biomass range using LiDAR-based and CoFor AGB data spatially aggregated to 0.1° cells for the 2018 map

AGB_{ref} bin [Mg/ha]	# cells count	AGB_{ref}	AGB_{map}	MD	RMSD
		---------------------[Mg/ha]	---------------------		
0-50	250	15	23	8	31
50-100	74	76	111	35	105
100-150	57	122	115	-7	56
150-200	26	173	170	-3	66
200-250	26	226	173	-53	77
250-300	38	276	267	-9	109
300-400	34	332	318	-14	83
>400	3	460	395	-65	143
total	508	98	102	3	67

Table 49. Validation results per biomass range using LiDAR-based and CoFor AGB data spatially aggregated to 0.1° cells for the 2019 map

AGB_{ref} bin [Mg/ha]	# cells count	AGB_{ref}	AGB_{map}	MD	RMSD
		---------------------[Mg/ha]			---------------------
0-50	246	15	23	8	31
50-100	79	76	106	30	103
100-150	53	123	121	-2	56
150-200	26	171	159	-12	68
200-250	15	225	159	-66	82
250-300	29	276	257	-19	126
300-400	23	337	335	-2	89
>400	3	461	400	-61	147
total	474	87	91	5	68

Table 50. Validation results per biomass range using LiDAR-based and CoFor AGB data spatially aggregated to 0.1° cells for the 2020 map

AGB_{ref} bin [Mg/ha]	# cells count	AGB_{ref}	AGB_{map}	MD	RMSD
		---------------------[Mg/ha]			---------------------
0-50	246	14	23	8	26
50-100	74	76	108	32	111
100-150	54	123	118	-4	53
150-200	28	171	153	-18	65
200-250	13	224	163	-61	73
250-300	12	278	232	-46	146
300-400	15	342	338	-3	92
>400	2	461	396	-65	177
total	444	74	79	5	65

Table 51. Validation results per biomass range using LiDAR-based and CoFor AGB data spatially aggregated to 0.1° cells for the 2021 map

AGB_{ref} bin [Mg/ha]	# cells count	AGB_{ref}	AGB_{map}	MD	RMSD
		---------------------[Mg/ha]			---------------------
0-50	79	19	61	41	111
50-100	45	74	97	23	69
100-150	35	121	130	9	53
150-200	20	173	197	25	67
200-250	51	229	299	70	118
250-300	100	277	343	66	107
300-400	210	345	376	31	73
>400	30	429	389	-40	76
total	570	241	277	36	89

Table 52. Validation results per biomass range using LiDAR-based and CoFor AGB data spatially aggregated to 0.1° cells for the 2022 map

AGB_{ref} bin [Mg/ha]	# cells count	AGB_{ref}	AGB_{map}	MD	RMSD
		---------------------[Mg/ha]	---------------------		
0-50	237	15	20	6	18
50-100	75	77	112	35	121
100-150	57	124	139	16	52
150-200	23	171	159	-12	64
200-250	13	222	163	-59	72
250-300	11	278	251	-27	128
300-400	15	344	337	-7	93
>400	-	-	-	-	-
total	431	73	81	8	65

The 0.25° results using the 2017 EMAP dataset as reference data are shown in Figure **7** and Table 53. The rest of the epochs were opted out due to result similarities. All maps show underestimation starting from AGB_{ref} ≈ 300 Mg/ha as indicated by six 0.1° grid cells. Note that fewer reference data are available as AGB increases.

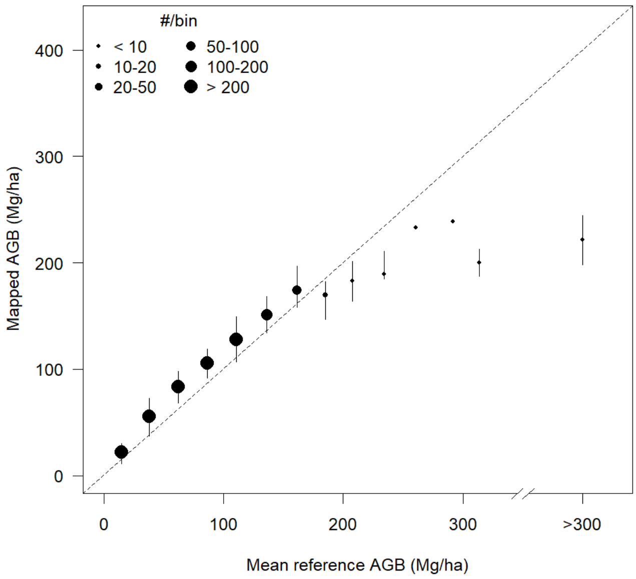

Figure 7. AGBref - AGBmap comparisons for EMAP AGB data spatially aggregated to 0.25° and binned over 25 Mg/ha wide AGB ranges with whiskers representing the interquartile range of mapped AGB values and symbol size representing the number of 0.25° cells per AGB range. AGBref > 350 Mg/ha data are grouped into a single bin.

Table 53. Validation results per biomass range using EMAP AGB data spatially aggregated to 0.25° cells for the 2017 map.

AGB_{ref} bin [Mg/ha]	# cells count	AGB_{ref}	AGB_{map}	MD	RMSD
		---------------------[Mg/ha]	---------------------		
0-50	1617	28	41	13	24
50-100	1691	73	93	20	30
100-150	481	119	135	17	33
150-200	67	167	173	6	37
200-250	12	225	187	-38	57
250-300	2	276	236	-40	42
300-400	4	339	211	-128	132
total	3874	62	79	16	29

To facilitate interpretation, the bias and RMSD estimates per map for different AGB_{ref} bins differentiated by Tier are shown in Table 54 and Table 55, respectively.

Figure 8. Legend for colour schemes used in summary tables of bias and RMSD.

Figure 8 provides the legend for the colour schemes used in these tables.

Table 54 and Table 55 shows that for the mid-range of AGB_{ref}, bias is within 20% of AGB_{ref} for Tier 1 data (which is consistent with GCOS requirements (GCOS, 2015)) but not for Tier 2 or 3 data. For the range between 250 and 400 Mg/ha the bias is usually less than 30% of $AGB_{ref.}$ At the lower and upper ends of the AGB range considered, bias always exceeds 20%. The RMSD exceeds 20% in all cases except for Tier 3 in 2015-2021 when AGB_{ref} exceeds 250-300 Mg/ha (Table 55). This means map error is dominated by the random component rather than the bias.

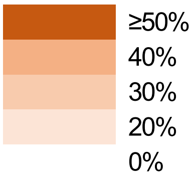

Figure 8. Legend for colour schemes used in summary tables of bias and RMSD.

Table 54. AGB bias [Mg/ha] differentiated per Tier and per AGB bin. Colour shading is based on relative bias; legend in Figure 8.

AGB_{ref}	Tier 1 non-aggregated										Tier 2 non-aggregated										Tier 3 non-aggregated										T1 aggregated									
[Mg/ha]	2007	2010	2015	2016	2017	2018	2019	2020	2021	2022	2007	2010	2015	2016	2017	2018	2019	2020	2021	2022	2007	2010	2015	2016	2017	2018	2019	2020	2021	2022	2007	2010	2015	2016	2017	2018	2019	2020	2021	2022
0-50	34	35	41	43	48	45	45	45	44	44	39	53	39	42	33	43	50	59	67	62											22	22	16	19	16	15	15	15	19	17
50-100	-2	2	15	20	28	28	27	27	25	26	101	96	96	127	38	60	83	95	84	86											19	17	6	15	4	5	4	4	14	4
100-150	-24	-12	-4	-1	1	-2	-2	-3	-6	-5	104	109	112	119	9	11	16	17	11	14	188	207	269	144	28	234					41	37	4	37	-3	2	-4	-4	32	-5
150-200	-25	-23	-30	-31	-31	-36	-38	-41	-45	-44	65	72	54	57	18	26	33	42	35	51											51	50	11	44	4	7	4	-1	36	4
200-250	-44	-43	-53	-54	-53	-59	-64	-67	-76	-77	46	36	8	21	-3	6	-5	-2	1	-17	78	78	40	55	96	81	69	14	74	11	0	-1	-28	0	-30	-28	-38	-32	-5	-29
250-300	-66	-69	-77	-81	-75	-80	-91	-95	-105	-109	52	46	35	14	33	16	35	43	53	18	-28	-23	-23	-11	-9	2					-22	-23	-38	-23	-26	-39	-34	-29	-24	-31
300-400	-116	-118	-126	-130	-121	-128	-137	-141	-155	-159	-39	-49	-50	-45	-57	-47	-55	-49	-59	-27	-70	-84	-74	-74	-62	-63	-24	-83	-7		-100	-110	-103	-100	-95	-102	-106	-94	-100	-92
>400	-434	-437	-417	-422	-434	-446	-467	-459	-467	-468	-222	-219	-236	-225	-242	-268	-280	-282	-280	-285	-113	-121	-113	-91	-98	-108	-144	-159	-73		-346	-343	-453	-342	-465	-453	-457	-465	-342	-367
Total	-13	-8	-10	-11	-7	-12	-13	-13	-14	-14	-10	-12	-22	-21	-63	-64	-71	-67	-74	-68	-41	-47	-41	-39	-34	-29	-35	-76	-2	-11	19	18	1	16	-3	0	-2	-4	15	3

Table 55. Root mean square difference (RMSD) is differentiated per Tier and per AGB bin. Column headings are exactly the same as table above (Table 48)

AGB_{ref}	Tier 1 non-aggregated										Tier 2 non-aggregated										Tier 3 non-aggregated										T1 aggregated									
[Mg/ha]	2007	2010	2015	2016	2017	2018	2019	2020	2021	2022	2007	2010	2015	2016	2017	2018	2019	2020	2021	2022	2007	2010	2015	2016	2017	2018	2019	2020	2021	2022	2007	2010	2015	2016	2017	2018	2019	2020	2021	2022
0-50	68	68	71	72	75	69	70	70	68	69	96	116	97	93	77	92	99	106	123	106											34	34	26	31	27	25	25	25	31	30
50-100	62	63	69	70	73	69	68	71	67	68	168	161	164	175	88	111	128	118	115	119											41	42	28	40	28	28	28	27	40	30
100-150	89	88	85	84	82	80	82	81	77	77	164	164	163	163	43	28	22	31	39	48	188	207	269	144	28	234					110	109	82	110	75	79	74	75	104	74
150-200	117	119	107	105	105	103	102	101	99	99	139	142	129	128	90	104	117	113	117	126											146	144	120	141	115	117	116	114	130	112
200-250	141	141	130	128	129	130	129	130	127	125	126	123	96	105	83	99	114	110	130	124	93	119	45	62	110	88	69	14	74	11	121	117	110	123	113	111	106	112	121	103
250-300	159	157	147	145	147	150	154	157	156	157	127	126	86	89	95	91	90	108	102	82	59	47	31	29	31	23					105	104	109	106	111	108	113	108	106	109
300-400	194	192	183	183	182	184	193	194	200	199	142	113	110	113	114	108	109	112	105	126	105	112	80	84	91	74	24	83	7		144	152	148	147	142	148	149	142	147	138
>400	736	734	691	700	731	745	766	757	764	757	329	327	339	340	362	391	398	400	416	405	120	136	114	94	111	115	144	159	73		425	420	600	423	618	600	579	618	423	448
Total	137	139	155	162	170	177	180	178	171	168	188	184	180	185	198	210	219	222	238	232	104	113	93	79	87	93	102	104	60	11	64	64	87	62	97	87	86	98	61	64

3.4. Assessments by ecoregion

To allow assessments of validation results over different ecoregions, spatially aggregated comparisons of AGB_{ref} and AGB_{map} were stratified by biomes (Dinerstein et al., 2017). The 2010 and 2021 results are presented in Figure 9 and Figure 10, while the 2015-2020 results are omitted due to their similarity with the 2021 results. Several strata had limited data or no data at all (e.g., deserts, flooded grassland, etc.). These cases are not included here.

For the boreal forests, mangroves, temperate grassland savannas and shrublands and tundra biomes, reasonable fits with minor over-predictions are found in the lower AGB ranges. A few plots in the boreal and tundra (arctic zones) exhibit high biomass while the map is depicting very low biomass. A reason for this is the new arctic dataset which with a few plots having high biomass estimates. Map over- and under-prediction are mostly present in tropical and subtropical dry broadleaf forest and and temperate broadleaf and mixed forest. Note that data in the dry tropical regions are limited, which hampers drawing solid conclusions. Spikes of map under-prediction are also found in tropical and subtropical grasslands, which is the opposite of the previous version where over-prediction was observed in these biomes. Under-prediction was also observed in Mediterranean forests, woodland and scrub around the 120 Mg/ha bin. The AGB_{ref} density at which under-prediction starts differs by biome. For boreal forests, saturation of AGB_{map} occurs at approximately 110 Mg/ha, for example. The strong similarity of results for the temperate broadleaf and mixed forests biome (Figures 9-10) with those of the spatially aggregated results obtained with the Tier 1 data (Figure 5) was already mentioned above. Such similarity is also present between results from tropical and subtropical moist broadleaf forest and results from Tier 2 and LiDAR/CoFor.

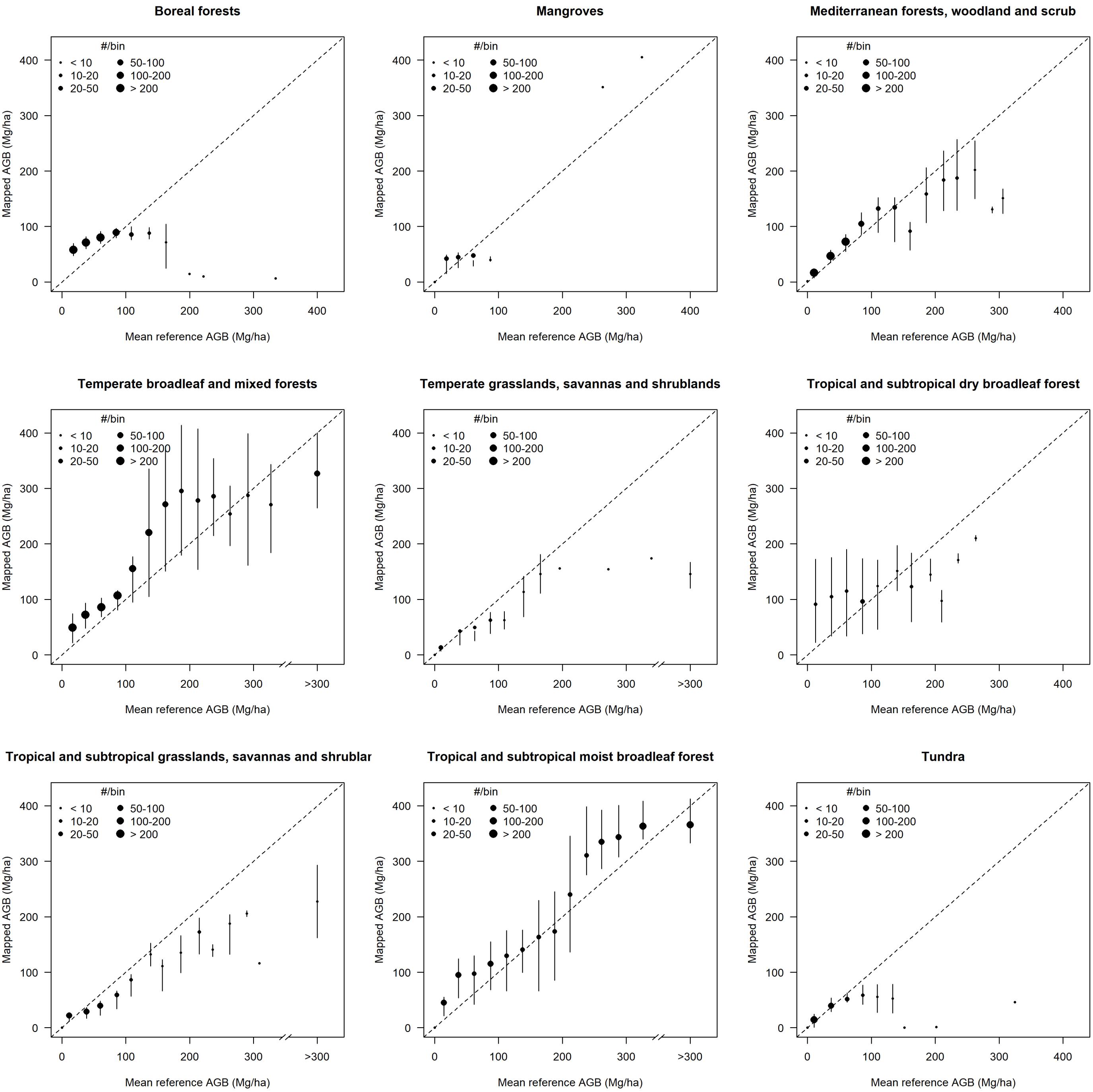

Figure 9. Comparisons between AGB_{ref} and the 2010 AGB map per biome (Dinerstein et al., 2017) using all available data binned over 25 Mg/ha wide biomass ranges with whiskers representing the interquartile range of mapped biomass values and symbol size representing the number of 0.1° cells per biomass range.

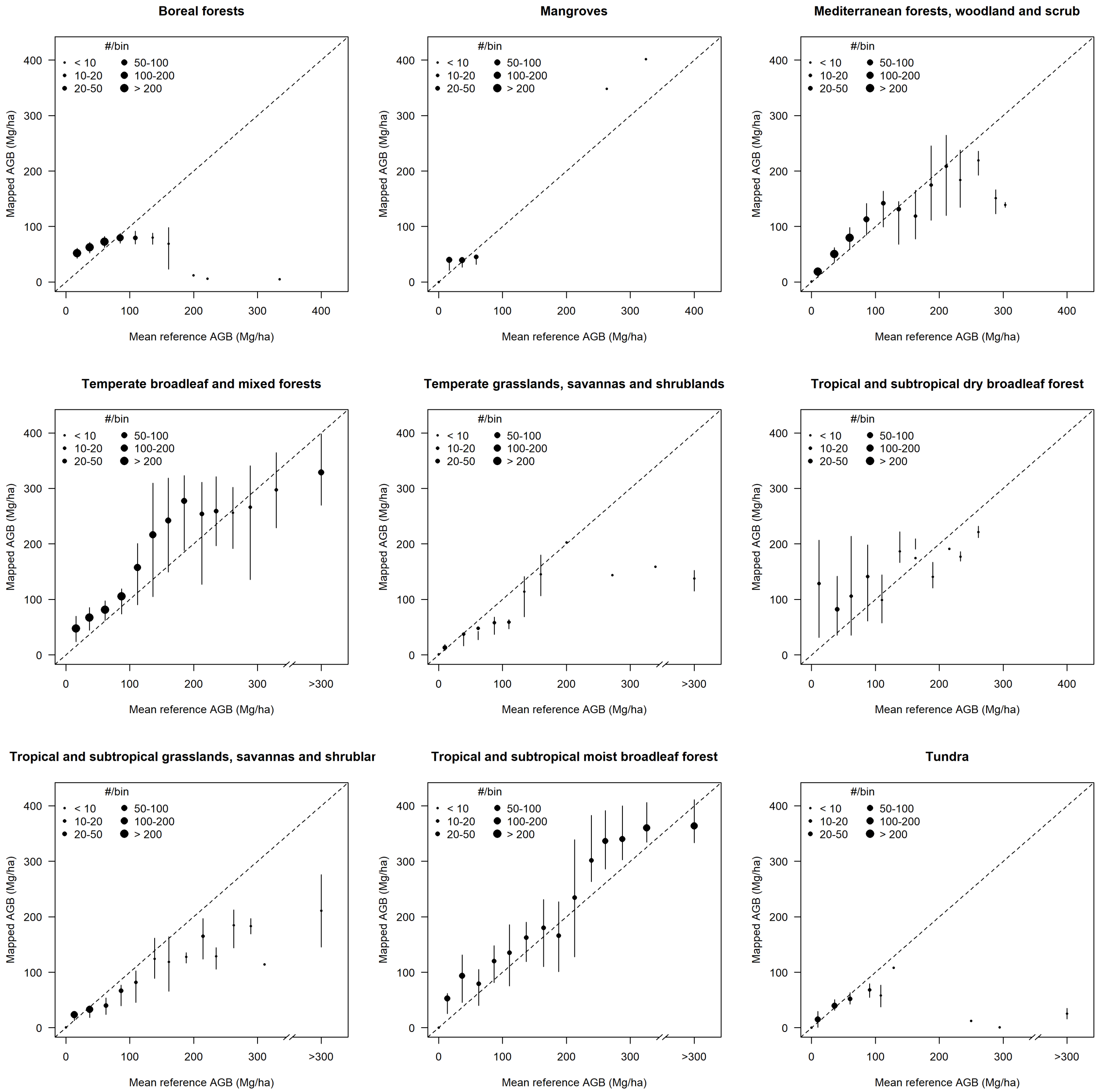

Figure 10. Comparisons between AGB_{ref} and the 2021 AGB map per biome (Dinerstein et al., 2017) using all available data binned over 25 Mg/ha wide AGB ranges with whiskers representing the interquartile range of mapped AGB values and symbol size representing the number of 0.1° cells per AGB range.

3.5. User-led validation

Two recent user-led independent map validations using own country data are reported here.

3.5.1. Forest Enterprise, near Moscow, Russia

The Schelkovo Forest Enterprise lies northeast of Moscow (37.7°-38.5° E, 55.8°-56.2° N). A stand-wise forest management inventory was completed in 2020. Forest inventory professionals compared the previous inventory's forest map (2004) to recent very high-resolution imagery, updating polygons where canopy changes were detected. During the field campaign, every polygon (whether changed or stable) was visited to record updated forest descriptions, including species composition and growing stock volume, with a target error of ≤ 15%.

Aboveground biomass (AGB) for each forest stand (polygon) was calculated from growing stock volume, species, site index and stand age. These stand level polygons were then rasterised to 10 m pixels and aggregated to a 100 m grid, retaining only pixels entirely covered by ground-truth data. This process yielded approximately 28,000 CCI Biomass pixels.

Notably, a series of bark beetle outbreaks in the area caused significant tree mortality followed by partial recovery, complicating mapping efforts. There is some temporal mismatch between forest loss recorded with CCI AGB and very high-resolution imagery.

Table 56. Validation results using the Schelkovo reference dataset: comparison of CCI Biomass v5 and v6.

Inventory AGB		CCI-AGB_v5		CCI-AGB_v6		# pixels
range	Average	AGB	RMSD	AGB	RMSD	
1-25	16	82	85	86	89	1604
26-50	38	108	90	112	94	2487
51-75	64	135	91	139	96	3312
76-100	89	148	81	155	88	4409
101-125	113	151	64	160	72	5303
126-150	138	155	54	162	60	5449
151-175	162	166	47	174	54	3995
176-200	184	175	44	187	49	1281
Total	107	145	99	152	107	28033

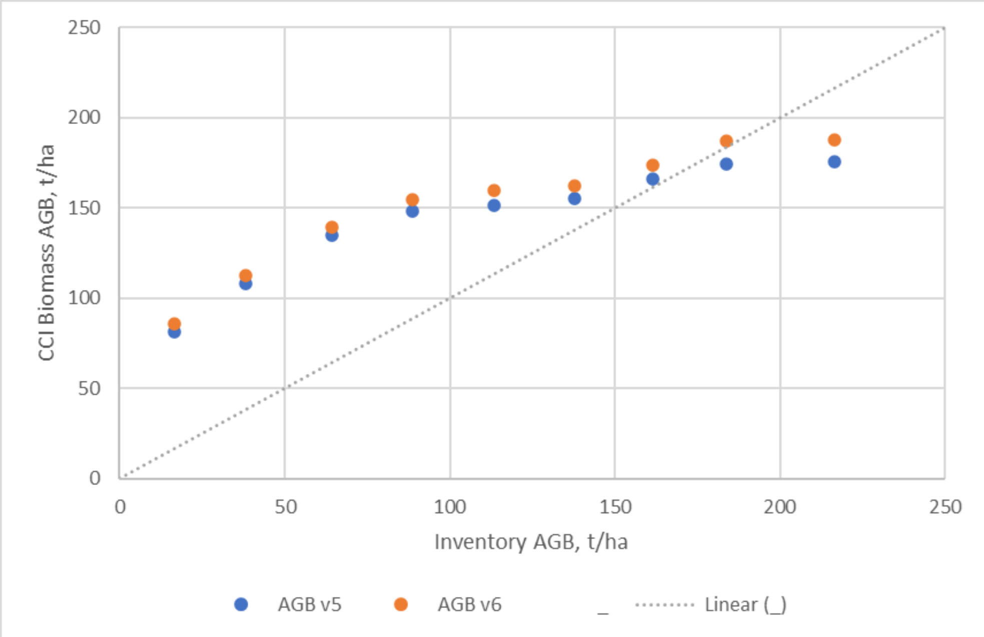

Figure 11. Binned scatterplots of the comparisons between Schelkovo reference dataset and the two CCI Biomass versions.

Both AGB estimations overstate biomass across most of the range, except at the highest values. This overestimation is slightly greater in v6, although v6 more accurately captures high-biomass stands.

3.5.2. GEO-TREES plots in Russia

The GEO-TREES network (https://data.geo-trees.org/) provides open access to large (> 0.25 ha) research plots with accurate geolocation. In Russia, 184 plots are available. Validation results (Table 57) show that CCI-Biomass underestimates AGB above 200 t/ha, although this bias is reduced in v6 compared to v5.

Table 57. Agreement between GEO-TREES research plots and CCI Biomass AGB data

Inventory AGB		CCI-AGB_v5		CCI-AGB_v6		# pixels
Range	Average	AGB	RMSD	AGB	RMSD	
1-50	25	26	22	28	21	16
51-100	77	84	63	86	62	20
101-150	132	166	68	170	70	38
151-200	175	183	49	206	52	44
201-250	221	172	75	200	60	41
251-300	268	198	84	221	64	20
301-380	341	218	127	233	112	5
Total	167	155	95	171	86	184

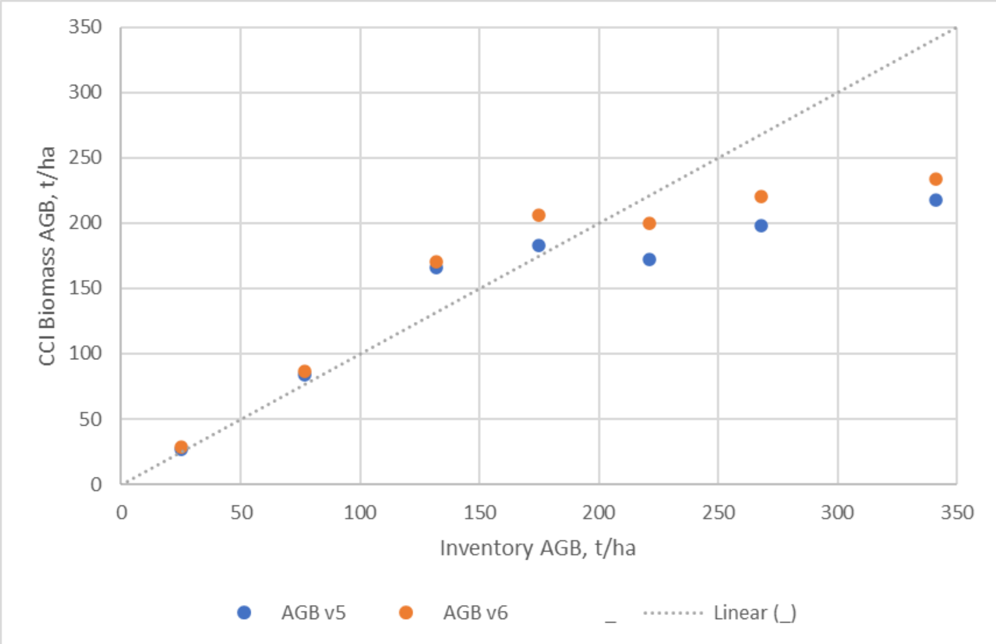

Figure 12. Binned scatterplots of the comparing the GEO-Trees reference dataset with CCI Biomass versions 5 and 6.

CCI-Biomass version 6 provides higher Above Ground Biomass estimates and a smaller RMSD than Version 5. However, it still overestimates in low biomass forests and underestimates in high biomass forests.

3.5.3. Comparison with the Brazil National Forest Inventory

Data and methods

The Brazilian National Forest Inventory (Inventário Florestal Nacional – IFN) is an ongoing, nationwide survey coordinated by the Serviço Florestal Brasileiro. It is based on a systematic sampling design using a 20 × 20 km grid that spans all Brazilian biomes, comprising more than 10,000 sampling points. As of December 2024, the IFN has surveyed approximately 513 million hectares of both natural and planted forests across Brazil. This effort includes measurements of over 900,000 individual trees, the identification of around 8,400 species—including 13 newly described ones—and socio-environmental interviews with more than 38,000 community members. Biome-level coverage currently includes 100% of the Pampa, 78% of the Cerrado, 71% of the Caatinga, 58% of the Atlantic Forest (Mata Atlântica), and 44% of the Amazon, with the Pantanal scheduled for complete coverage next (Serviço Florestal Brasileiro, n.d.)

Each standard plot consists of four subplots, positioned 50 meters from the plot center in cardinal directions. Within each subplot, ten sampling parcels are established, each measuring 10 × 10 meters (0.01 hectares). This results in a sampling area of 0.1 hectares per subplot, and consequently 0.4 hectares per plot under the standard design (Figure 13). In the Amazon biome, the sampling intensity is increased to account for the presence of larger trees. An additional ten parcels per subplot are established specifically to sample trees with a diameter at breast height (DBH) greater than 40 cm. This expansion doubles the sampling area to 0.2 hectares per subplot, resulting in a total of 0.8 hectares per plot. The total plot area (including both sampled and unsampled ground) is 200 × 200 meters (4 hectares) under the standard configuration, and 300 × 300 meters (9 hectares) in the Amazon biome, where larger plots accommodate the increased sampling effort (Serviço Florestal Brasileiro, 2021).

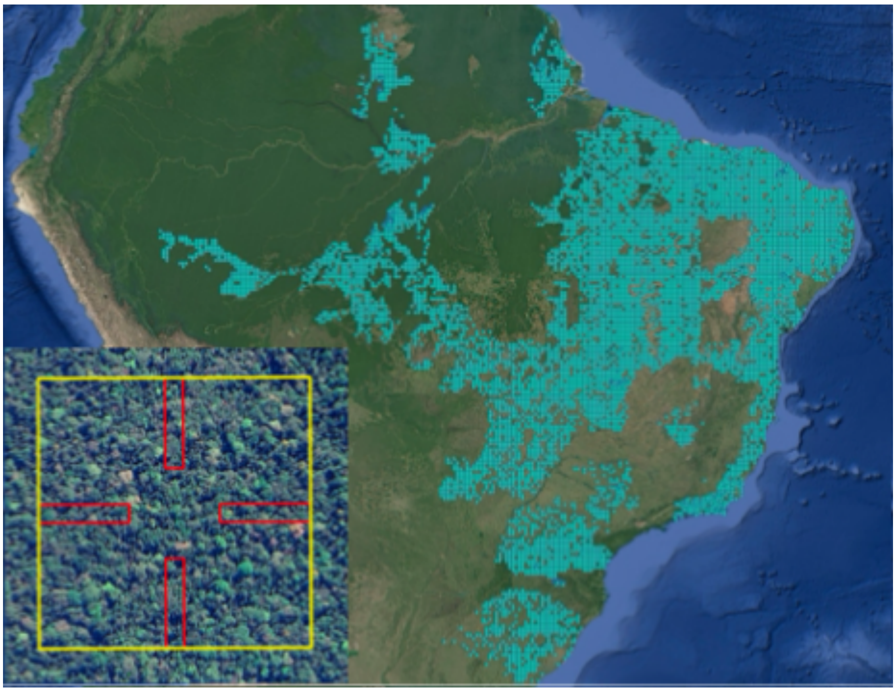

Figure 13. Plot design and spatial distribution of currently available NFI plots. The yellow area represents the total plot extent (4 ha), while the red rectangles indicate subplots covering 20 × 50 m each.

In this exercise, we used tree-level data available through the web-portal of the Serviço Florestal Brasileiro. Using tree measurements (DBH and tree height) we estimated the aboveground biomass of individual trees based on Chave *et al*. (2014) pan-tropical allometric equation:

agb = 0.0673 * (wd * DBH^2 *height)^0.976

For wood density (wd), we applied a mean value of 0.632 g/cm^3, representative for South American Tropical forests of Chave et al. (2009). Total biomass was then calculated by summing the estimated tree-level AGB within each subplot or plot and normalized to a per-hectare basis.

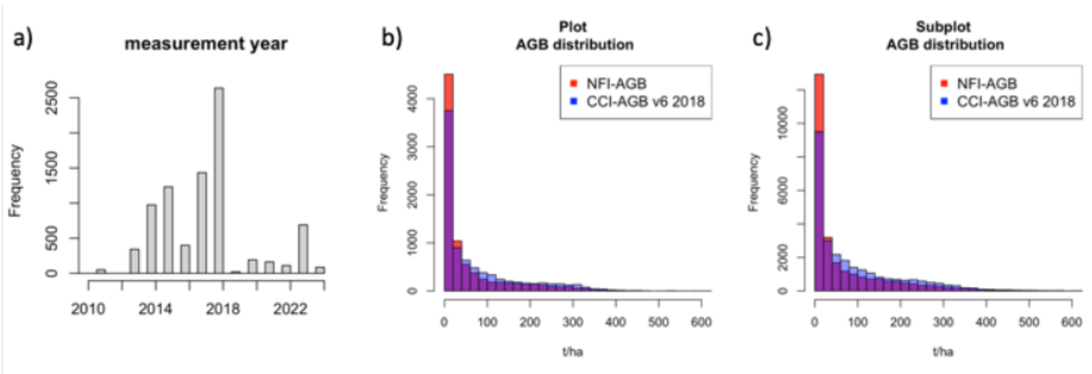

Figure 14. plots (a); AGB distribution from the NFI at the plot (b) and at the subplot levels (c) with corresponding estimates from the CCI Biomass v6 2018 product.

Since the majority of NFI plots were sampled in 2018 (Figure 14a), we used the CCI Biomass Version 6 product from the same year for comparison.

The pixel size of CCI Biomass product (100x100 m) does not match the dimensions of a plot or subplot, therefore, we extracted the mean value of the CCI biomass map over each corresponding (sub)plot area.

Results

Agreement between the NFI data and the ESA CCI product improves from the subplot- to plot-level estimates. Aggregating subplot data to the plot-level reduces the variability associated with smaller sampling units and helps to mitigate the impact of outliers (

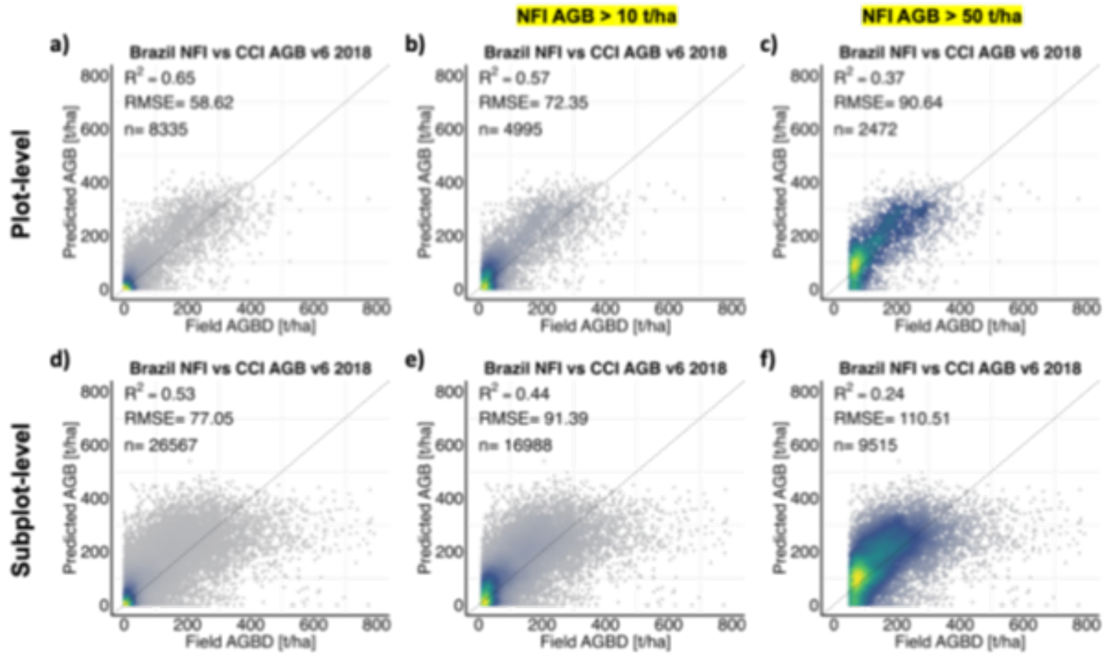

Figure 15). As many NFIs plots possess low AGB values (<10 t/ha), we truncated the data to NFI AGB > 10 t/ha (

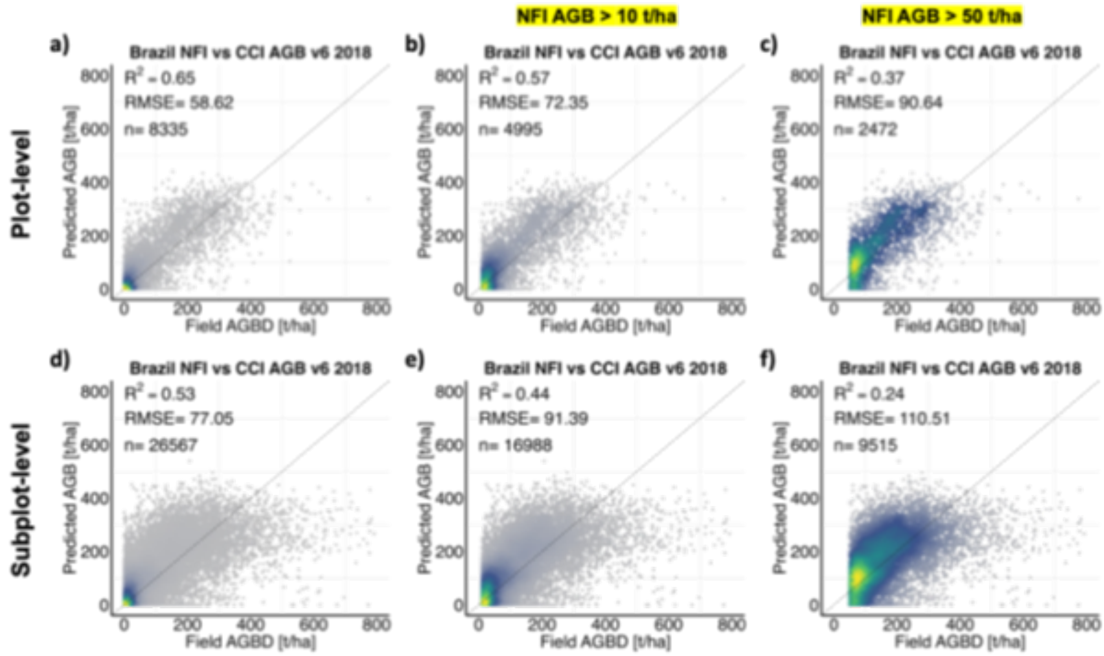

Figure 15, middle column) and to NFI AGB > 50 t/ha (

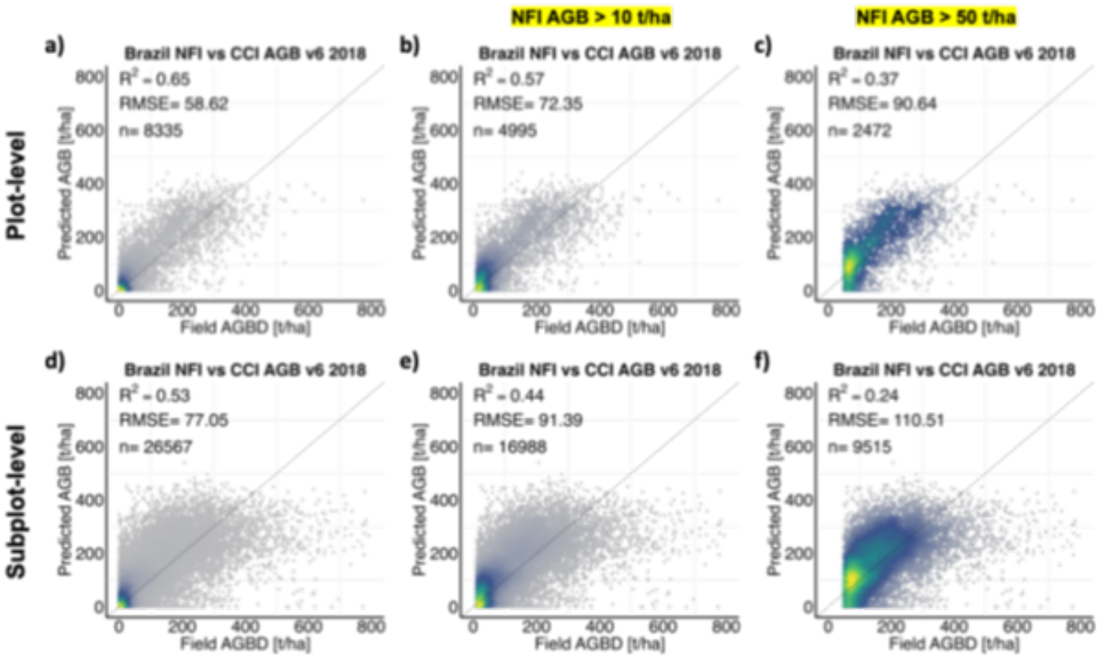

Figure 15, right column). The relatively high correlation observed when using the full dataset is likely driven by the large number of plots with low biomass (<50 t/ha). When these low biomass plots are excluded, the correlation between NFI and ESA CCI estimates decreases, and show a general overestimation of the ESA CCI product at higher biomass levels (>

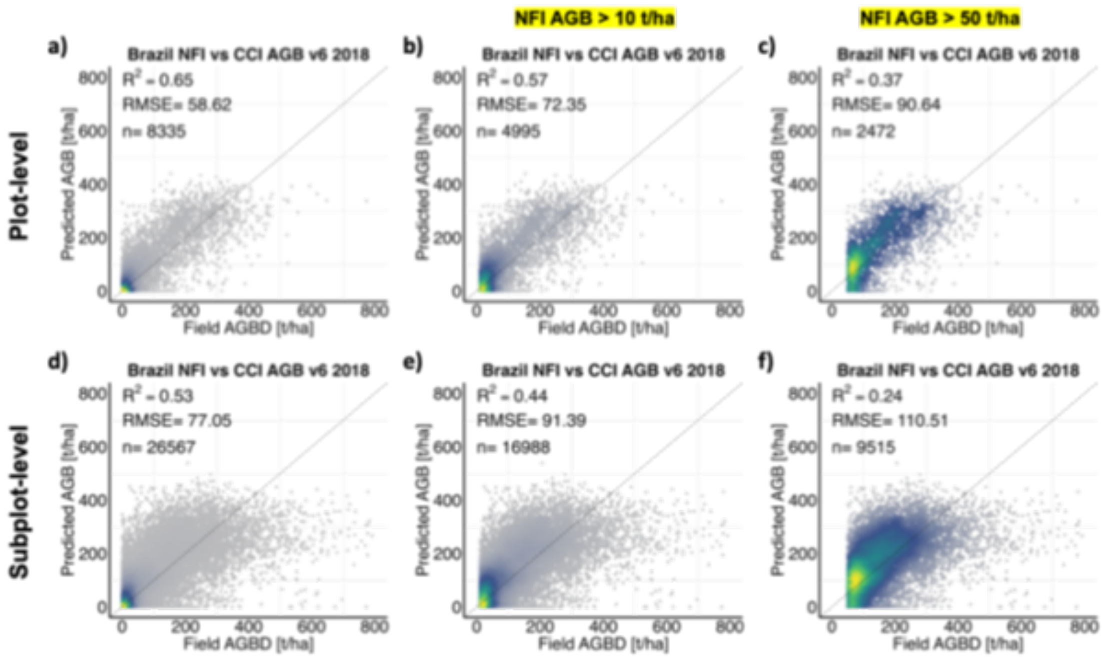

100 t/ha) (
Figure 15).

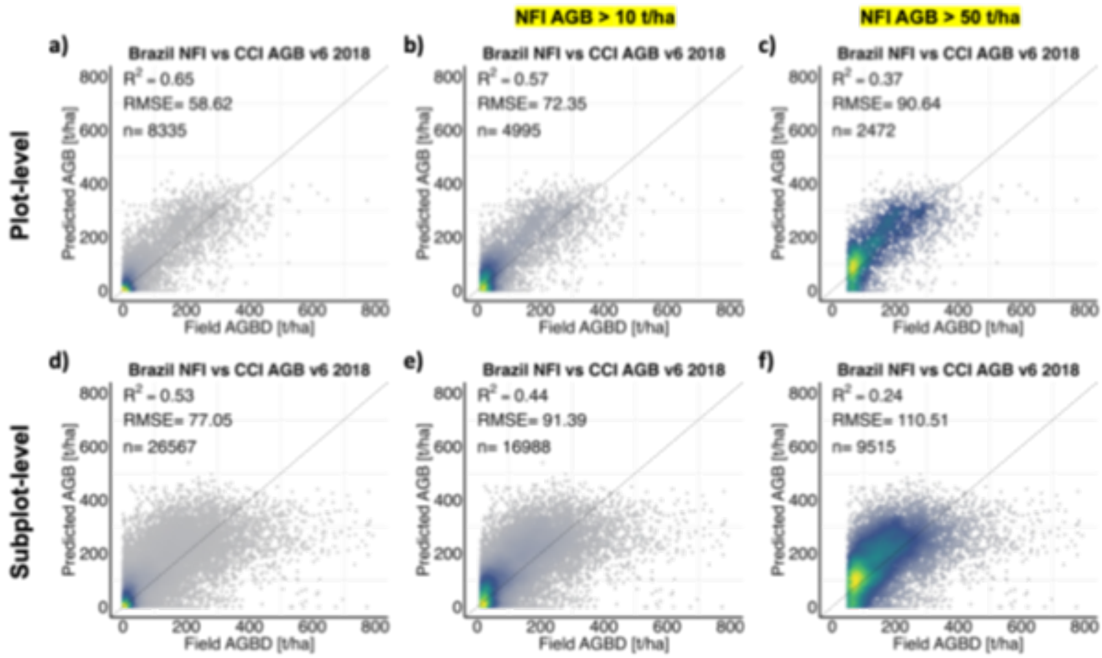

Figure 15. Comparison between Brazilian NFI and the ESA CCI Biomass v6 2018 product at the plot level (top row) and subplot level (bottom row). To address the high frequency of low AGB values in the NFI data (<10 t/ha), comparisons are also shown for subsets where NFI AGB exceeds 10 t/ha (middle column) and 50 t/ha (right column).

Finally, we evaluated the ESA CCI-Biomass product on an aggregated, binned scale. For this, we first divided the NFI values into 100 equal-sized percentile bins. For each bin, we then calculated the median NFI value, the median CCI estimate, and the standard deviation of the CCI values (displayed as error bars) (Figure 16). As in the full-data scatterplot

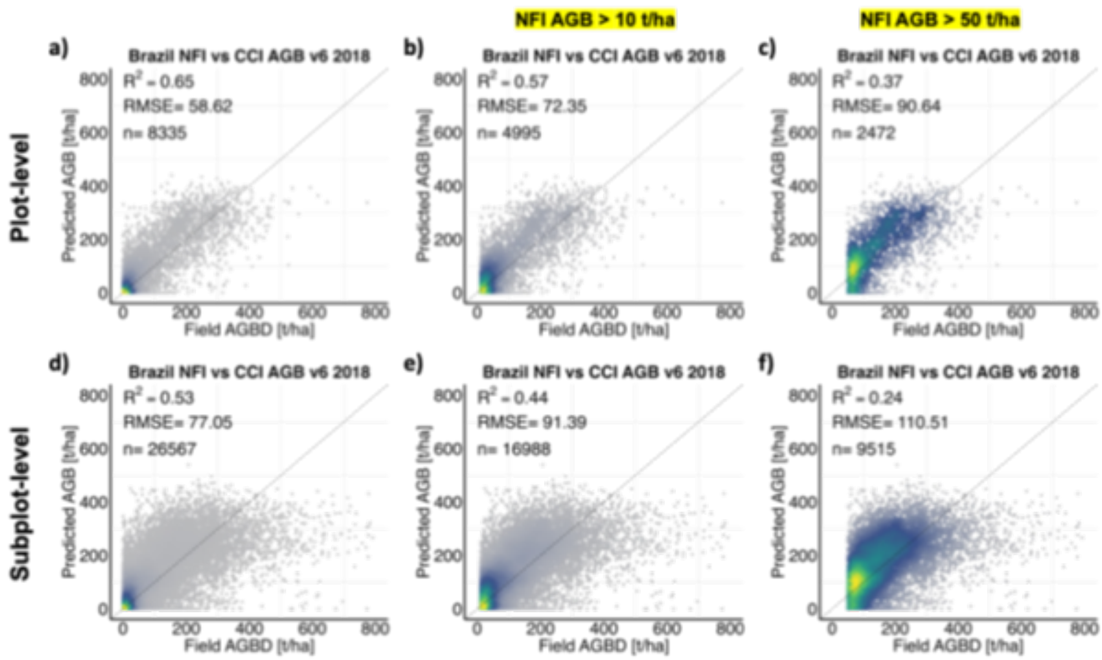

(

Figure 15), the ESA CCI product slightly overestimates AGB in the low-to-mid range (<200 t/ha). In contrast, it underestimates biomass at very high values (>250 t/ha), although those estimates are based on relatively few samples.

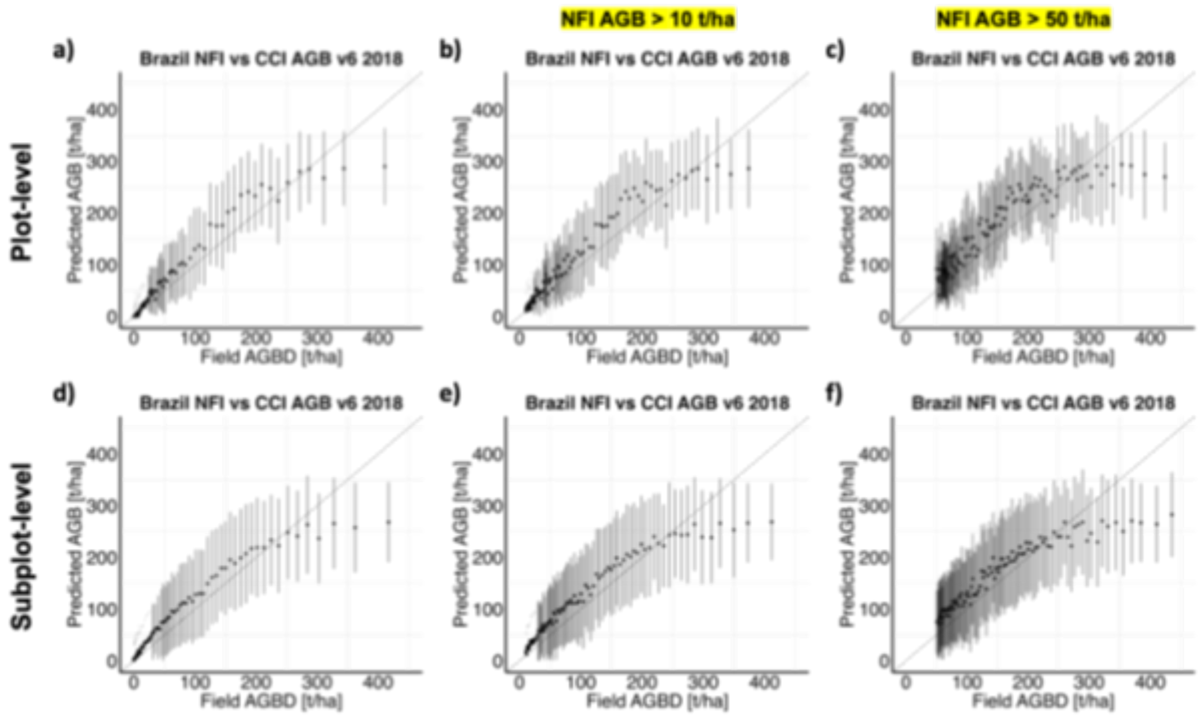

Figure 16. Binned comparison of AGB between the Brazilian NFI and the ESA CCI Biomass v6 2018 product at the plot level (top row) and subplot level (bottom row). NFI values were divided into 100 equal-sized percentile bins; for each bin, median NFI and CCI AGB are plotted, with CCI standard deviations shown as error bars. Panels show (left) all data, (middle) NFI AGB > 10 t/ha, and (right) NFI AGB > 50 t/ha.

Bearing in mind that the Brazilian NFI represents a fully independent reference dataset, the ESA CCI biomass product shows a strong agreement in the low-to-mid biomass range (0-200 t/ha), with only a very slight positive bias. As expected, at very high biomass range (250-300 t/ha), it is challenging to resolve the full biomass distribution. Currently, only a limited number of field plots exist in undisturbed Amazonian forests; as more plots are collected and made available over time, sampling density will increase and our understanding of the limitations of global remote-sensing biomass maps will improve.

3.6. Summary tables of the assessments by ecoregion

To facilitate interpretation of the AGB maps, we here summarise the bias and RMSD estimates for different AGB_{ref} bins by biome. Given the similarity in the results of the 2015-2020 maps, only the 2010 and the 2021 comparisons are shown, see Tables 58-61.

The tables re-emphasize our overall finding that in the lower and higher AGB ranges the bias and RMSD are larger than in the mid-ranges. The bias for the mid-ranges for most biomes is around or below 20%, while the RMSD is above 20%.

The quantity of available reference information differs for different regions and there is lower confidence for some with limited reference data, including the (sub-)tropical dry forests and grasslands, mangroves, temperate grasslands and tundra.

Table 58. AGB bias [Mg/ha] per biome and per AGB bin for the 2010 map. Colour shading is as in Figure 8.

AGB_{ref} [Mg/ha]	Boreal	Mangrove	Mediterranean	Temperate broadleaf/mixed	Temperate grasslands, savannas and shrublands	Tropical/ subtropical dry broadleaf	Tropical and subtropical grasslands	Tropical and subtropical moist broadleaf forest	Tundra
0-50	35	14	7	34	3	73	0	46	3
50-100	16	-18	14	22	-20	30	-23	31	-17
100-150	-30		11	60	-35	13	-16	11	-59
150-200	-102		-47	109	-27	-42	-48	-6	-152
200-250	-212		-38	58		-89	-58	55	-200
250-300		88	-89	-6	-118	-53	-77	64	
300-400	-328	81	-154	-62	-218		-159	22	-279
>400				-369	-226			-85	
Total	26	5	7	29	-24	22	42	43	-5

Table 59. Root mean square difference (RMSD) per biome and per AGB bin for the 2010 map. Colour shading is based on the legend shown in Figure 8; column headings are as above.

AGB_{ref} [Mg/ha]	Boreal	Mangrove	Mediterranean	Temperate broadleaf/mixed	Temperate grasslands, savannas and shrublands	Tropical/ subtropical dry broadleaf	Tropical and subtropical grasslands	Tropical and subtropical moist broadleaf forest	Tundra
0-50	39	41	13	49	20	101	20	67	15
50-100	23	47	27	44	43	85	38	68	30
100-150	38		83	123	55	70	48	68	72
150-200	114		86	173	59	78	79	94	152
200-250	212		88	151		99	80	124	200
250-300		88	117	117	118	55	92	101	
300-400	328	81	160	115	220		191	75	279
>400				451	226			139	
Total	36	44	24	98	66	87	43	88	34

Table 60. AGB bias [Mg/ha] per biome and per AGB bin for the 2021 map. Colour shading is as in Figure 8.

AGB_{ref} [Mg/ha]	Boreal	Mangrove	Mediterranean	Temperate broadleaf/mixed	Temperate grasslands, savannas and shrublands	Tropical/ subtropical dry broadleaf	Tropical and subtropical grasslands	Tropical and subtropical moist broadleaf forest	Tundra
0-50	28	11	10	31	2	68	3	48	4
50-100	8	-14	21	19	-23	49	-21	25	-12
100-150	-35		13	58	-38	25	-23	25	-46
150-200	-103		-28	85	-10	-16	-49	-3	
200-250	-216		-21	33		-48	-66	47	-237
250-300		85	-84	-15	-128	-40	-83	62	-294
300-400	-330	77	-164	-51	-227		-172	19	-384
>400				-371	-232			-85	-531
Total	19	8	10	25	-24	44	41	43	-10

Table 61. Root mean square difference (RMSD) per biome and per AGB bin for the 2021 map. Colour shading is is as in Figure 8; column headings are as above.

AGB_{ref} [Mg/ha]	Boreal	Mangrove	Mediterranean	Temperate broadleaf/mixed	Temperate grasslands, savannas and shrublands	Tropical/ subtropical dry broadleaf	Tropical and subtropical grasslands	Tropical and subtropical moist broadleaf forest	Tundra
0-50	32	31	16	46	18	103	19	74	16
50-100	18	32	36	48	42	96	40	61	27
100-150	42		87	62	59	62	56	71	57
150-200	115		81	64	50	77	82	82	
200-250	216		91	85		52	89	119	237
250-300		85	118	149	128	45	98	100	294
300-400	330	77	165	181	229		200	75	384
>400				581	232			139	531
Total	31	32	26	98	64	92	42	87	62

3.7. AGB map intercomparison

In this section, we assess the stability of map error among the current (Version 6) seven CCI-Biomass AGB products, compare Version 6 with the Version 5 products, and compare the CCI maps with other AGB map products.

3.7.1 Stability of AGB_{map} – AGB_{ref} differences among the 2007, 2010 and 2015-2022 AGB products

According to the World Meteorological Organization (2011), the user requirement for stability is in general a requirement on the extent to which the error of a product remains constant over a longer period. To assess stability of plot-map differences over the map years, Figure 17 illustrates the residuals between plot-based and mapped AGB aggregated to 0.1° for all combinations of map years. Most pairs, particularly 2007 and 2010 and 2015 to 2018 and 2019 to 2022, show strong agreement with R^2 values above 0.90, indicating high temporal consistency. In contrast, the 2020 map shows lower correlation with other years, including adjacent ones like 2021 and 2022. This suggests a disruption in stability specific to 2020, possibly due to changes in input data or processing methods. Outside of this anomaly, the remaining maps show a generally stable behavior over time.

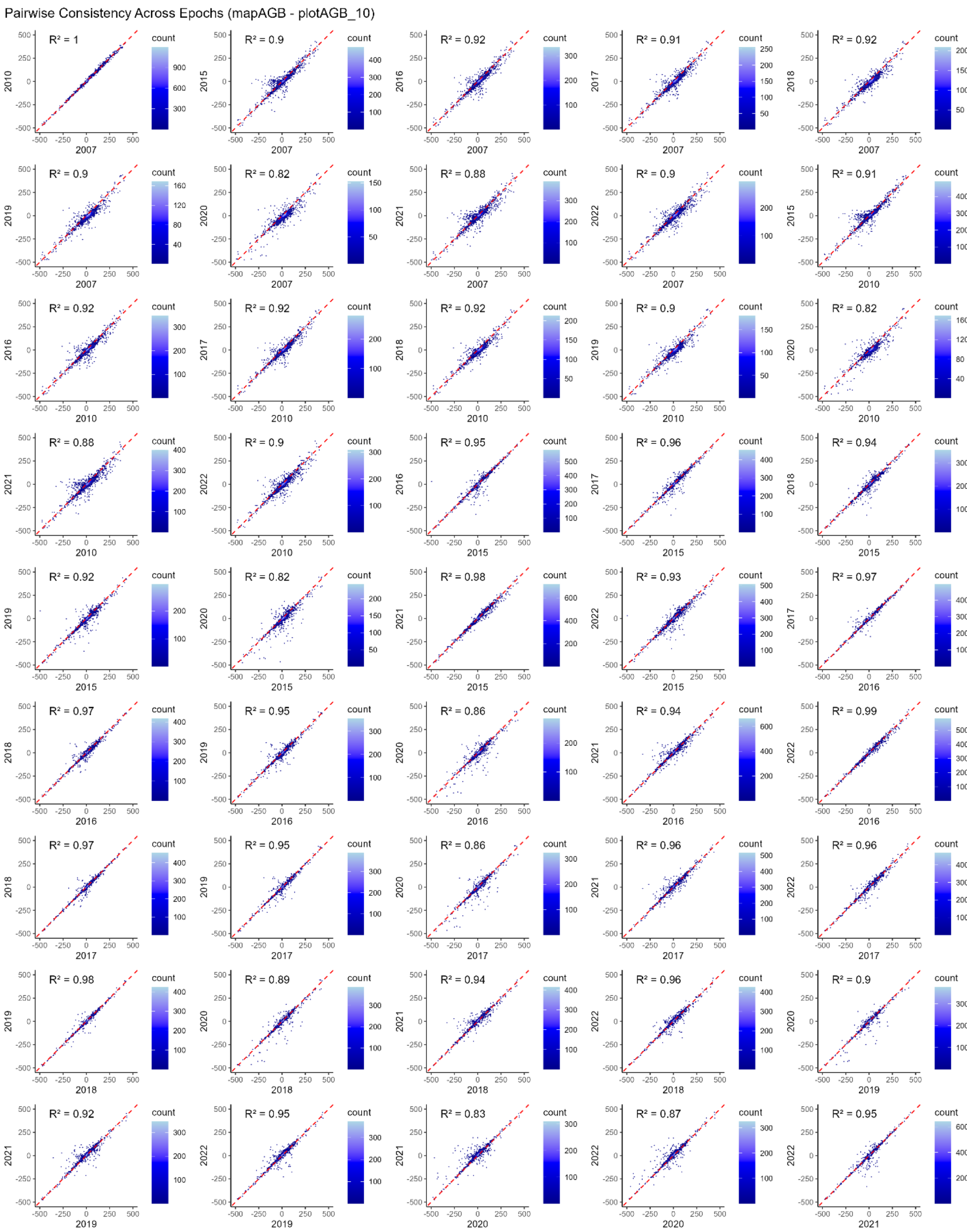

Figure 17. AGB residuals between harmonized Tier 1-3 plot data and mapped AGB at 0.1° cell level for each pair of map reference years. The red dashed line is the 1:1 line.

The map producer may want to know where the largest instabilities in the residuals occur. Such information is provided in Figure 17 where the locations of the 5% most negative differences between the 2010 and 2017 products (2010 – 2017;

i.e., points above the 1:1 diagonal in Figure 17) are plotted as red circles whilst the 5% largest positive differences (i.e., points below the 1:1 diagonal) are shown by blue crosses. Several sites have entirely either large positive or large negative differences but in other places, such as east Australia, Madagascar, the northern Balkans and Mexico (Yucatán), both extremes occur close to one another. Figure 19 is a virtually identical figure showing the locations of cells with the most extreme differences between 2010 and 2018 residuals while Figure 20 does so for the 2017 and 2018 residuals. This analysis is part of the previous PVIR.

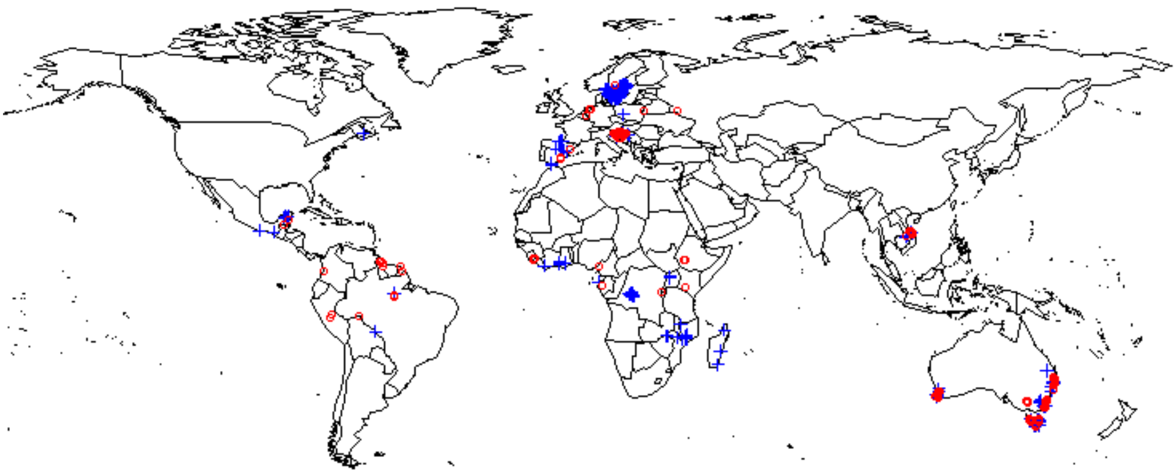

Figure 18. Locations of 0.1° cells with the most extreme differences between residuals in the 2010 and 2017 AGB products (2010 – 2017). The 5% cells with the most negative differences (i.e., 2017 > 2010) are indicated in red whilst the 5% largest positive differences (i.e., 2017 < 2010) are shown in blue.

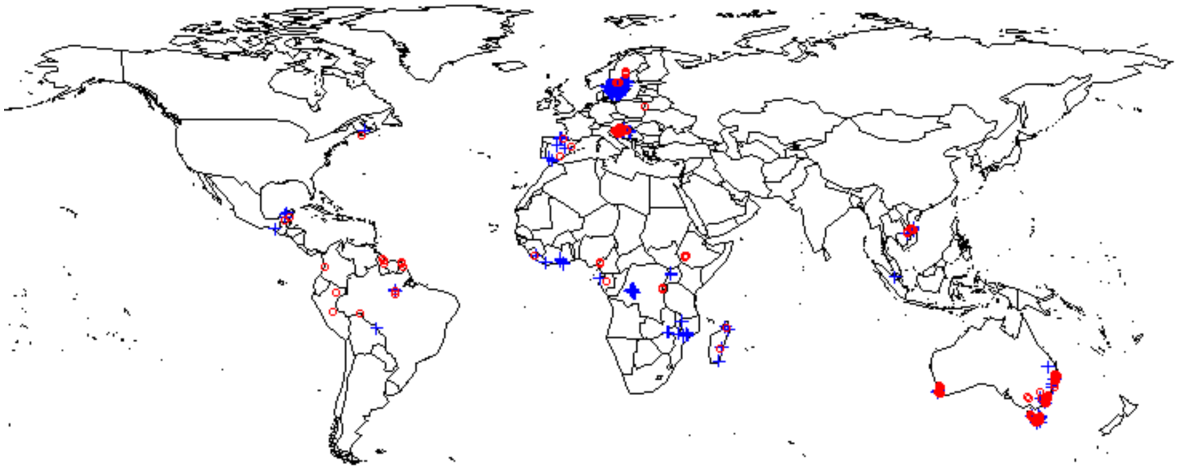

Figure 19. Locations of 0.1° cells with the most extreme differences between residuals in the 2010 and 2018 AGB products (2010 – 2018). The 5% cells with the most negative differences (i.e., 2018 > 2010) are indicated in red whilst the 5% largest positive differences (i.e., 2018 < 2010) are shown in blue.

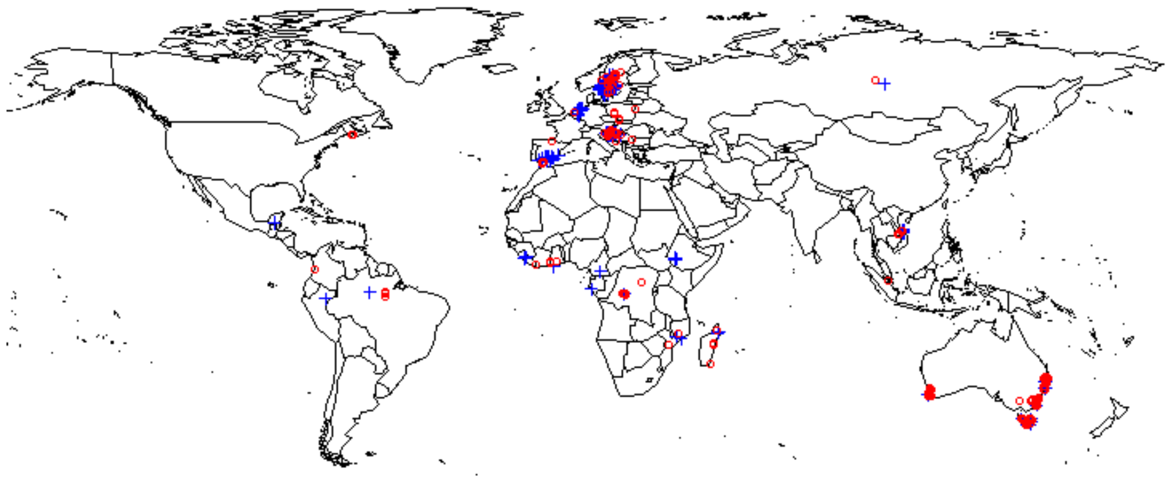

Figure 20. Locations of 0.1° cells with the most extreme differences between residuals in the 2017 and 2018 AGB products (2017 – 2018). The 5% cells with the most negative differences (i.e., 2018 > 2017) are indicated in red whilst the 5% largest positive differences (i.e., 2018 < 2017) are shown in blue.

3.7.2. Comparison of current maps with previous 2010, 2017 and 2018 AGB products

Figure 21 shows the global AGB_{map} - AGB_{ref} comparisons spatially aggregated to 0.1° and binned over 25 Mg/ha wide AGB ranges for CCI Biomass Versions 5 and 6 in two epochs. The new map version exhibits less underestimation in the highest AGB bins and a very slight overestimation from 110 to 310 Mg/ha bins.

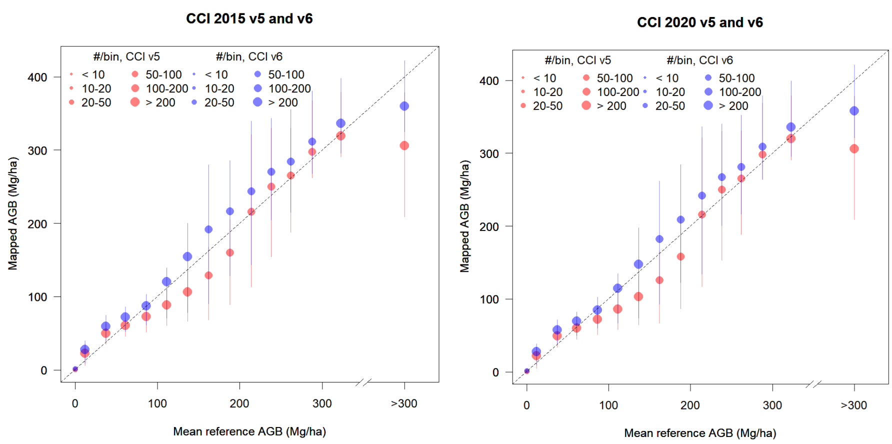

Figure 21. Global AGB_{map} - AGB_{ref} comparisons for 2015 and 2020 based on inverse variance weighted Tier 0-3 plot data spatially aggregated to 0.1° cells.

Figure 22 presents a visual intercomparison of AGB estimates from versions 4, 5, and 6 of the CCI Biomass product. Colors represent spatial agreement or divergence among the versions: white indicates strong agreement in high biomass areas, while dark tones indicate agreement in low biomass regions. Regions with reddish hues suggest that Version 6 differs from Versions 4 and 5, while green and blue highlight where Versions 5 and 4, respectively, deviate. Purple and brownish zones show closer alignment between specific version pairs, notably v6 with v4 or v5.

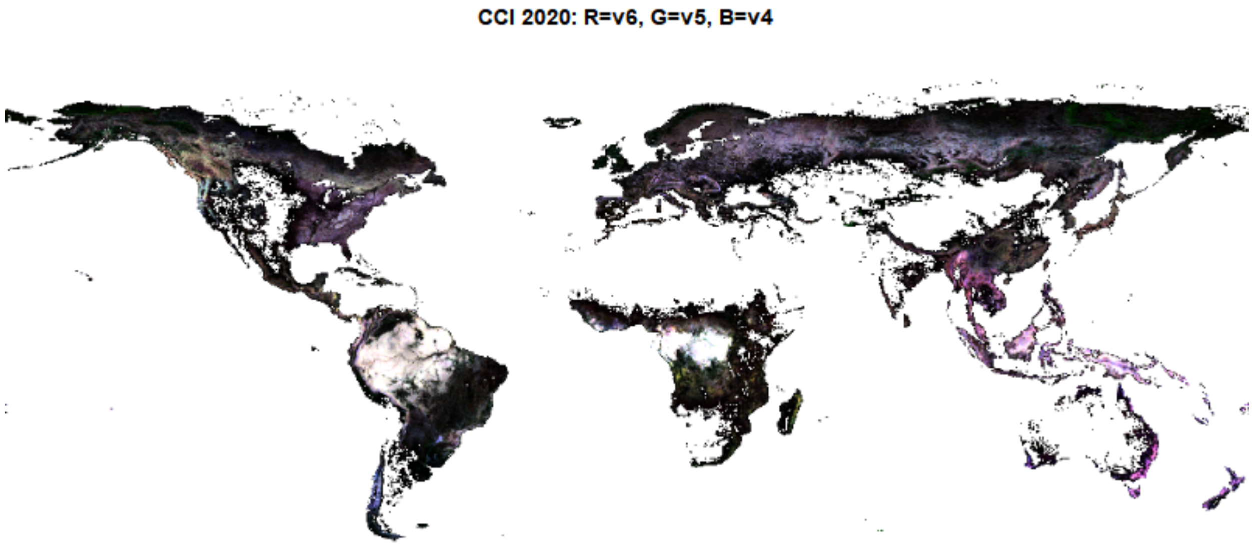

Figure 22. Spatial Agreement and Divergence Among CCI Biomass Product Versions (v4, v5, v6)

3.7.3. Comparison of the CCI maps with other AGB products

Figure 23 shows the global AGB_{map} - AGB_{ref} comparisons spatially aggregated to 0.1° using Tier 1-3 data and binned over 25 Mg/ha wide AGB ranges for CCI 2020 map and other AGB products. Comparison with the 2020 JPL AGB map (Xu et al. 2021) is in the left plot and with the 2020 AGB GEDI map on the right (Duncanson et al. 2022). Both show the non-CCI maps have higher overestimation at the lower biomass ranges and slightly lesser underestimation >300 Mg/ha. The GEDI map needed reprojection into WGS 84 and resamping from 0.001° to 0.1° using the average of all pixels. The JPL map by default has a spatial resolution of 0.1° so no pre-processing was needed.

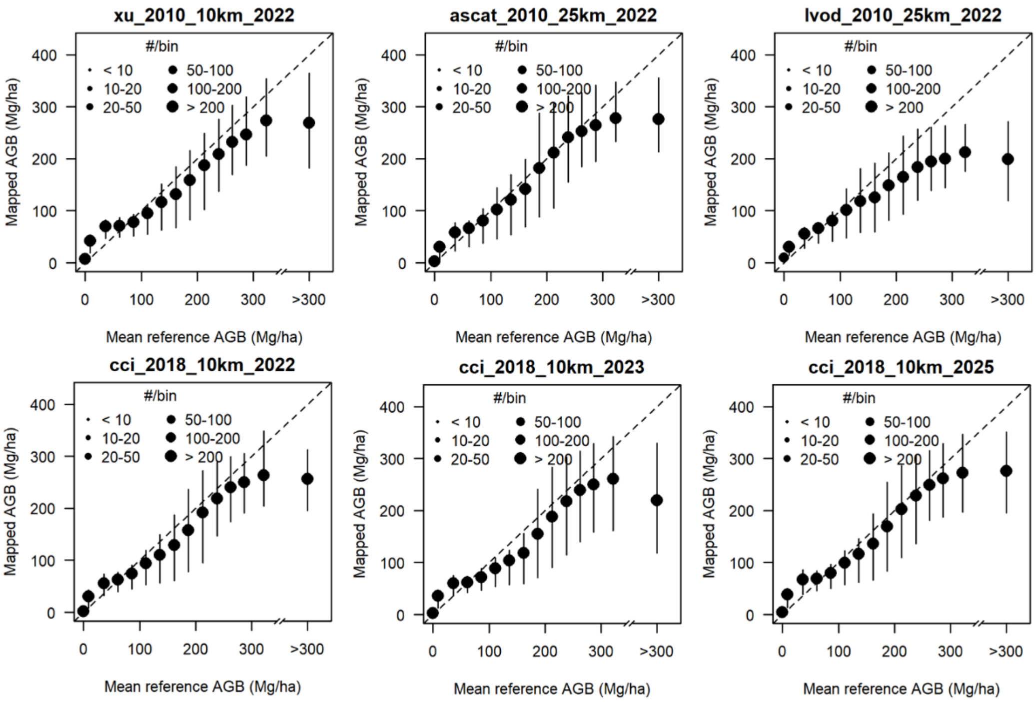

Figure 23. Compaisons among versions and other global AGB map products.

3.8. Within-pixel sampling error

Using the forest-only LiDAR-derived AGB data from forest sites in Remningstorp, Sweden (Ulander et al., 2011), and Lope, Gabon (Hajnsek et al., 2017), the variograms shown in Figure 24 were estimated. The Remningstorp variogram was modelled by two exponential structures with partial sills of 3579 and 1899 Mg^2 ha^{-2} and range parameters of 95 and 531 m, respectively. The Lope variogram was modelled by a 4053 Mg^2 ha^{-2} nugget and a single exponential structure with partial sill of 10553 Mg^2 ha^{-2} and a range parameter of 85 m. Note that the effective range of an exponential variogram is approximately three times the range parameter.

Not surprisingly, the tropical high biomass Lope site has much larger short-range spatial variation than the boreal Remningstorp site (note the different scales on the y-axes).

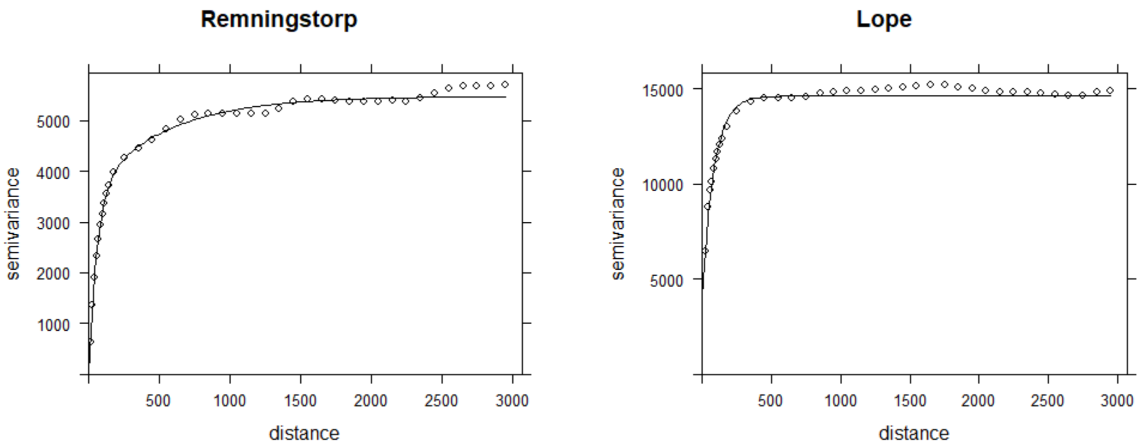

Figure 24. Variograms for the Remningstorp and Lope forest sites. Open dots indicate the experimental variogram and the solid lines represent the fitted models.

Based on the variograms, and assuming single plots with the size of the LiDAR footprints (i.e., 0.01 ha for Remningstorp and 0.04 ha for Lope) centred in 1 ha AGB map pixels, the variance of the plots was found to be 1421 and 6714 Mg^2 ha^{-2} for the two sites. Hence, the standard deviations amount to 38 and 82 Mg/ha, respectively, which is not negligible.

As demonstrated in the PUG (Santoro, 2020), within-pixel sampling error may suggest map bias even if the map provides a perfect representation of mean AGB at 1 ha spatial support. To replicate this issue using a geostatistical approach, Figure 25 shows a scatterplot of 0.04 ha plot AGB values on the x-axis centred and conditioned on 1 ha pixels that are plotted on the y-axis. The pixel values are in the range 10 to 400 Mg/ha and the plot values are drawn from Gaussian populations with mean given by the pixel value and variance and spatial correlation given by the Lope variogram. Any negative value drawn from a Gaussian population was set to zero.

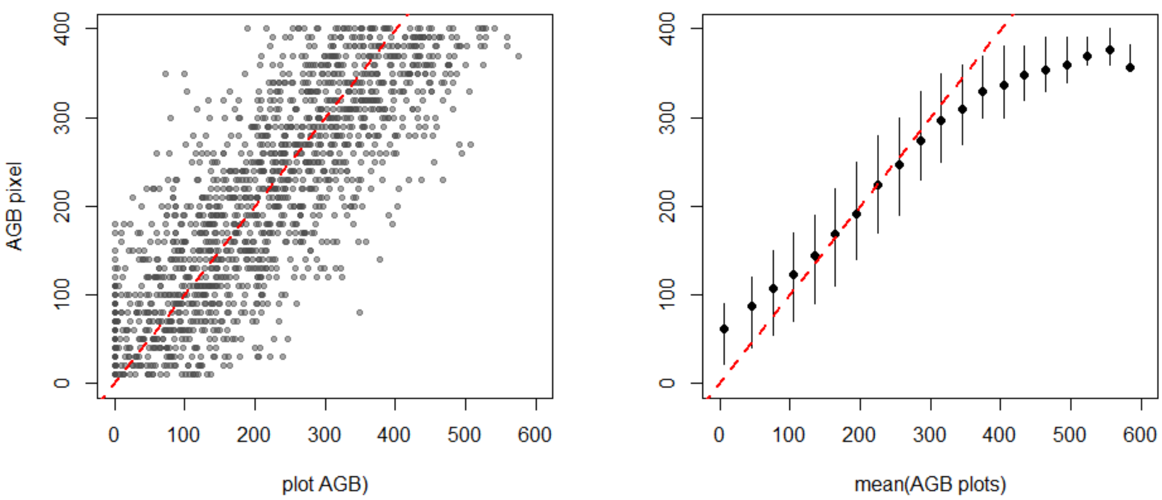

Figure 25. Scatterplot of 0.04 ha plot values conditioned on 1 ha pixel values (left) and binned over 30 Mg/ha wide biomass ranges with dots representing mean AGB and whiskers representing the interquartile range of pixel biomass values for plots inside the bins (right). The dashed red lines are 1:1 lines.

The scatterplot and the interquartile whisker plot in Figure 25 suggest the pixel overestimates low AGB and underestimates high AGB at plot level. However, the plot data were conditioned on the pixel data. Therefore, the observed effect is entirely due to the within-pixel sampling error.

The above effect reduces substantially if multiple plots are used to represent a pixel. To demonstrate this, the above experiment was repeated with five plots regularly spread over the pixel. In Figure 26, the means of the AGB from five plots are on the x-axis, while the conditioning pixel values are on the y-axis. In this figure, the bias observed in Figure 25 is mostly absent, except for the far ends of the AGB range.

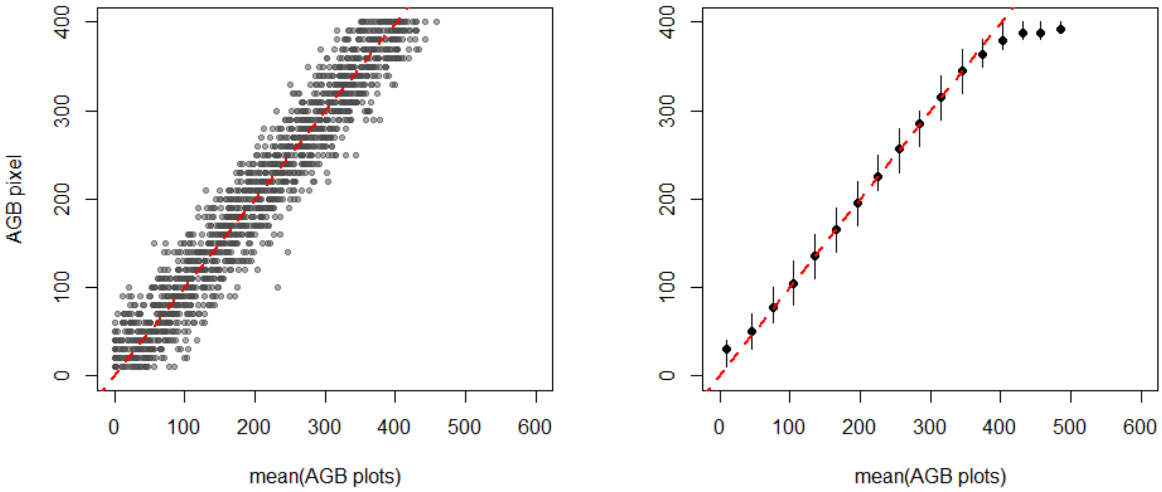

Figure 26. Scatterplot of the mean of 0.04 ha plot values conditioned on 1 ha pixel values (left) and binned over 30 Mg/ha wide biomass ranges with dots representing mean AGB and whiskers representing the interquartile range of pixel AGB values (right). The dashed red lines are 1:1 lines.

The reasons for including this section in the PVIR are: (1) to corroborate the experiment shown in the PUG (Santoro, 2020) and (2) to demonstrate a method for diagnosing the within-pixel sampling error and show the importance of taking it into account when validating map pixels with data from small plots. For the latter, we need variography for the different environmental circumstances (e.g., biomes), which can be obtained from small footprint (0.01-0.04 ha) LiDAR-derived AGB data, such as the data used in this section. Currently, we have such data only for a single boreal forest site and one site in a tropical forest. More data in these biomes as well as other biomes are needed to routinely account for the within-pixel sampling variance in AGB_{map} – AGB_{ref} comparisons.

3.9. Next steps

For the upcoming map validation exercises the following can be prioritized:

- Continuous updating of the reference database to include additional years
- Scope a concept for collecting and comparing reference and map-based estimates for biomass change
- Use of country forest masks for user-led validation in Section 3.6 (i.e. detailed 10 m resolution maps of land cover and semi-natural habitats in Wales).
- Revisit of certain biomass allometric models used in Appendix A, e.g. for AUS1.

Conclusions

Fully reported and transparent validation is important for increasing the acceptance of satellite-derived products in the user community. To assess the accuracy of the AGB estimates of the new 2007, 2010, 2015-2022 CCI Biomass global AGB maps, AGB predictions were compared with independent plot data, LiDAR-based AGB estimates and recently released CoFor and EMAP data, which were used as reference data.

The plot data were adjusted for temporal discrepancies and partial forest fraction (see PVP). Three tiers of plot data were defined, ranging from a large set of data, depending on the reference year of the AGB map) from small plots (on average 0.15 ha and including small NFI plots), to a small set of data from large (> 6 ha) research plots (21 – 27 plots). The latter Tier 3 data mainly consist of plots in the tropics that, though of high quality, are so few that they barely allow conclusions to be drawn about the quality of the CCI Biomass maps. Tier 2 plots (413 – 655 plots), with an average size of 1 ha, revealed that globally the CCI Biomass maps at their original 1 ha resolution tend to over-predict AGB_{ref} up to 180 Mg/ha for <2016 maps. For the Tier 1 data, the map under-prediction starts at a reference AGB of approximately 200 Mg/ha. It should be noted that part of the observed underestimation of high AGB and overestimation of low AGB observed for small plots can be attributed to within-pixel sampling error.

Spatial aggregation of plot and map data to 0.1° cells (a level of aggregation suitable for most climate modellers) considerably improved the agreement between AGB_{ref} and AGB_{map}, though over-prediction was still observed in the low and mid AGB range and higher reference AGB was under-predicted. Similar results were obtained with LiDAR-based AGB estimates and 1-km pixel Congo basin Forests AGB (CoFor) which suggests their suitability to serve as reference data for assessing global AGB products. The spatial aggregation also allowed 2010 results to be more consistent with the 2015-2021 result unlike in the non-aggregated results.

In general, between 50 Mg/ha and 400 Mg/ha, mean differences between AGB_{map} and AGB_{ref} were found to be well within 20% of AGB_{ref} at 0.1° cell level. This does not hold for the RMSD, which over the entire AGB range exceeds 20% of AGB_{ref} for the three maps. Nevertheless, it is concluded that spatial aggregation reduces the effect of localized AGB fluctuations in the map and plot-map geolocation mismatches. The AGB_{map} - AGB_{ref} comparisons at 0.1° resolution differentiated by biome (Dinerstein et al., 2017) produced patterns similar to the global comparison for many biomes and particularly highlighted the confidence in the regional AGB estimations up to 300 Mg/ha for the different tropical forest regions. The correspondence between AGB_{ref} and AGB_{map} was lower for the tropical and subtropical dry broadleaf forest biome. Similarly, the AGB_{ref} and AGB_{map} comparisons for tropical and subtropical grassland showed map under-estimation > 35 Mg/ha. Lack of access to a larger set of reference data for these biomes may have affected this finding.

The overall analysis at 0.1° cell level revealed that Version 6 of the CCI Biomass AGB maps provides better estimates in the high AGB range than previous versions and other global AGB maps. The 2007 and 2010 maps were also less consistent with AGB_{ref} than the 2015-2022 maps, which can be attributed to the different number of reference data used and also differences in the remote sensing input data of the CCI maps. Comparison with AGB_{ref} data revealed that all maps exhibit underestimation in the high biomass bins.

This PVIR demonstrated a geostatistical method for assessing the variance of within-pixel sampling error using variography derived from small-footprint LiDAR-based AGB estimates from forest sites in Sweden and Gabon. Additional datasets are needed to extend this analysis and use it for error budgeting when using (small) plot data for AGB map assessment.

Acknowledgments

We are grateful to all data contributors (see Appendix A) for providing forest plot data for the independent validation of the CCI Biomass maps. We are also thankful to Forest Research (in conjunction with the European Regional Development Fund/Welsh Government funded Ser Cymru Living Wales project) and the Russian Forest Federal Agency in conjunction with the team of Dmitry Schepaschenko for the user-led independent validation using country data.

References (including references from Appendix A)

Araza, A., De Bruin, S., Herold, M., Quegan, S., Labriere, N., Rodriguez-Veiga, P., ... & Lucas, R. (2022a). A comprehensive framework for assessing the accuracy and uncertainty of global above-ground biomass maps. Remote Sensing of Environment, 272, 112917.

Araza, A., De Bruin, S., & Herold, M. (2022b). Plot-to-map: an open-source r workflow for above-ground biomass independent validation. In IGARSS 2022-2022 IEEE International Geoscience and Remote Sensing Symposium (pp. 5575-5577). IEEE.

Avitabile, V., Baccini, A., Friedl, M. A., & Schmullius, C. (2012). Capabilities and limitations of Landsat and land cover data for aboveground woody biomass estimation of Uganda. Remote Sensing of Environment, 117, 366-380. https://doi.org/10.1016/j.rse.2011.10.012.

Avitabile, V., Schultz, M., Herold, N., de Bruin, S., Pratihast, A. K., Manh, C. P., . . . Herold, M. (2016). Carbon emissions from land cover change in Central Vietnam. Carbon Management, 7(5-6), 333-346. doi:10.1080/17583004.2016.1254009

Baccini, A. G. S. J., Goetz, S. J., Walker, W. S., Laporte, N. T., Sun, M., Sulla-Menashe, D., ... & Houghton, R. (2012). Estimated carbon dioxide emissions from tropical deforestation improved by carbon-density maps. Nature climate change, 2(3), 182-185.

Baccini, A., Walker, W., Carvalho, L., Farina, M., Sulla-Menashe, D., & Houghton, R. A. (2017). Tropical forests are a net carbon source based on aboveground measurements of gain and loss. Science, 358(6360), 230-234.

Bilolo, J. J., Dida, J. V., & Araza, A. (2024). COMPARISON OF THE USE OF SENTINEL-1 SAR AND ALOS-2 PALSAR-2 IN MANGROVE ABOVEGROUND BIOMASS ESTIMATION IN SAN JUAN, BATANGAS, PHILIPPINES. The International Archives of the Photogrammetry, Remote Sensing and Spatial Information Sciences, 48, 53-60.

Brown, S., Gillespie, A. J. R., & Lugo, A. E. (1989). Biomass Estimation Methods for Tropical Forests with Applications to Forest Inventory Data. Forest Science, 35(4), 881-902. https://doi.org/10.1093/forestscience/35.4.881.

Bai, Jiankun, Meng, Yuchen, Gou, Ruikun, Lyu, Jiacheng, Dai, Zheng, Diao, Xiaoping, Zhang, Hongsheng, Luo, Yiqi, Zhu, Xiaoshan, & Lin, Guanghui. (2021). Mangrove diversity enhances plant biomass production and carbon storage in Hainan Island, China [Data set]. https://doi.org/10.5061/dryad.c866t1g5s

Campbell, M. J., Eastburn, J. F., Mistick, K. A., Smith, A. M., & Stovall, A. E. (2023). Mapping individual tree and plot-level biomass using airborne and mobile lidar in piñon-juniper woodlands. International Journal of Applied Earth Observation and Geoinformation, 118, 103232.

Carreiras, J. M. B., Vasconcelos, M. J., & Lucas, R. M. (2012). Understanding the relationship between aboveground biomass and ALOS PALSAR data in the forests of Guinea-Bissau (West Africa). Remote Sensing of Environment, 121, 426-442. https://doi.org/10.1016/j.rse.2012.02.012.

Castillo, J. A. A., Apan, A. A., Maraseni, T. N., & Salmo III, S. G. (2017). Estimation and mapping of above-ground biomass of mangrove forests and their replacement land uses in the Philippines using Sentinel imagery. ISPRS Journal of Photogrammetry and Remote Sensing, 134, 70-85.CEOS (2021). Aboveground Woody Biomass Product Validation Good Practices Protocol, Version 1.0 (ed. Duncanson, L., Armston, J., Disney, M., Nickeson, J., Minor, D. & Camacho, F.)

Chave, J., Coomes, D., Jansen, S., Lewis, S. L., Swenson, N. G., & Zanne, A. E. (2009). Towards a worldwide wood economics spectrum. Ecology letters, 12(4), 351-366.

Chave, J., Réjou-Méchain, M., Búrquez, A., Chidumayo, E., Colgan, M. S., Delitti, W. B., ... & Vieilledent, G. (2014). Improved allometric models to estimate the aboveground biomass of tropical trees. Global change biology, 20(10), 3177-3190.

Clark, D. B., & Clark, D. A. (2000). Landscape-scale variation in forest structure and biomass in a tropical rain forest. Forest Ecology and Management, 137(1), 185-198. https://doi.org/10.1016/S0378-1127(99)00327-8.

de Bruin, S., Herold, M., & Araza, A. (2019a). CCI Biomass Product Validation Plan, Year 1, Version 1. Retrieved from http://cci.esa.int/sites/default/files/biomass%20D2.5%20Product%20Validation%20Plan%20%28PVP%29%20V1.0.pdf.

de Bruin, S., Herold, M., & Araza, A. (2019b). CCI Biomass Product Validation & Intercomparison Report Year 1 Version 1.0. https://climate.esa.int/sites/default/files/biomass_D4.1_Product_Validation_%26_Intercomparison_Report_V1.1.pdf.

de Bruin, S., Herold, M., & Araza, A., Lucas, R. (2020). CCI Biomass Product Validation Plan, Year 2, Version 2. https://climate.esa.int/sites/default/files/Biomass_D2.5_Product_Validation_Plan_V2.0.pdf.

de Bruin, S., Herold, M., & Araza, A., Lucas, R. (2021). CCI Biomass Product Validation Plan, Year 3, Version 3. https://climate.esa.int/sites/default/files/Biomass_D2.5_Product_Validation_Plan_V3.0.pdf.

DeVries, B., Avitabile, V., Kooistra, L., & Herold, M. (2012). Monitoring the impact of REDD+ implementation in the Unesco Kafa biosphere reserve, Ethiopia. Paper presented at the Sensing a Changing World, Wageningen. http://www.wageningenur.nl/upload_mm/9/d/c/f80b6db7-9c3c-4957-8717-6fdc6e46e60f_deVries.pdf.

Dinerstein, E., Olson, D., Joshi, A., Vynne, C., Burgess, N. D., Wikramanayake, E.,Saleem, M. (2017). An Ecoregion-Based Approach to Protecting Half the Terrestrial Realm. BioScience, 67(6), 534-545. https://doi.org/10.1093/biosci/bix014.

Duncanson, L., Kellner, J. R., Armston, J., Dubayah, R., Minor, D. M., Hancock, S., ... & Zgraggen, C. (2022). Aboveground biomass density models for NASA's Global Ecosystem Dynamics Investigation (GEDI) lidar mission. Remote Sensing of Environment, 270, 112845.

Fazakas, Z., Nilsson, M., & Olsson, H. (1999). Regional forest biomass and wood volume estimation using satellite data and ancillary data. Agricultural and Forest Meteorology, 98, 417-425.

GCOS (2015). Status of the Global Observing System for Climate, GCOS-195, WMO.

Hajnsek, I., Pardini, M., Jäger, M., Horn, R., Kim, J.S., Jörg, H., Papathanassiou, K., Dubois-Fernandez, P., Dupuis, X., Wasik, V. (2017). Technical Assistance for the Development of Airborne SAR and Geophysical Measurements During the AFRISAR Experiment. Final Report, Deliverable DD-4. pp. 152.

Hansen, M. C., Potapov, P. V., Moore, R., Hancher, M., Turubanova, S. A., Tyukavina, A., . . . Townshend, J. R. G. (2013). High-Resolution Global Maps of 21st-Century Forest Cover Change. Science, 342(6160), 850-853. https://doi.org/10.1126/science.1244693.

Hijmans, R. J. (2017). raster: Geographic Data Analysis and Modeling (Version 2.6). Retrieved from https://CRAN.R-project.org/package=raster.

Hirsh, F., Jourget, J. G., Feintrenie, L., Bayol, N., & Ebaá Atyi, R. (2013). Projet pilote REDD+ de la Lukénie. Retrieved from Bogor, Indonesia: https://agritrop.cirad.fr/572060/1/document_572060.pdf.

Horn, B. (1981). Hill shading and the reflectance map. Proceedings of the IEEE, 69, 14-47. doi:10.1109/PROC.1981.11918

IPPC. (2006). IPCC Guidelines for National Greenhouse Gas Inventories. https://www.ipcc.ch/report/2006-ipcc-guidelines-for-national-greenhouse-gas-inventories/

IPCC. (2019). 2019 Refinement to the 2006 IPCC Guidelines for National Greenhouse Gas Inventories. (table 4.9). https://www.ipcc.ch/report/2019-refinement-to-the-2006-ipcc-guidelines-for-national-greenhouse-gas-inventories/

Kamah Pascal Bumtu, Nkwatoh Athanasius Fuashi, & Longonje Simon Ngomba. (2020). Structure, Biomass Carbon Stock and Sequestration Rate of Mangroves in the Bakassi Peninsula, S W Cameroon. International Journal of Trend in Scientific Research and Development, 4(2), 843–854. https://doi.org/10.5281/zenodo.3843122

Khanal, S., Nolan, R. H., Medlyn, B. E., & Boer, M. M. (2023). Mapping soil organic carbon stocks in Nepal's forests. Scientific Reports, 13(1), 8090.

Kyriakidis, P.C. (2004). A Geostatistical Framework for Area-to-Point Spatial Interpolation. Geographical Analysis, 36: 259-289. https://doi.org/10.1111/j.1538-4632.2004.tb01135.x.

Labrière, N., Tao, S., Chave, J., Scipal, K., Toan, T. L., Abernethy, K., . . . Saatchi, S. (2018). In SituReference Datasets From the TropiSAR and AfriSAR Campaigns in Support of Upcoming Spaceborne Biomass Missions. IEEE Journal of Selected Topics in Applied Earth Observations and Remote Sensing, 11(10), 3617-3627. doi:10.1109/JSTARS.2018.2851606

Labrière, N., & Chave, J. (2020a) CCI Biomass project – In situ datasets: Processing and validation of Sustainable Landscape Brazil data (CCI Biomass internal report).

Labrière, N., & Chave, J. (2020b) CCI Biomass project – In situ datasets: Processing and validation of NEON data (USA) (CCI Biomass internal report).

Labrière, N., & Chave, J. (2020c) In situ datasets: Processing and validation of TERN data (CCI Biomass internal report).

Labrière, N., Davies, S. J., Disney, M. I., Duncanson, L. I., Herold, M., Lewis, S. L., ... & Chave, J. (2023). Toward a forest biomass reference measurement system for remote sensing applications. Global Change Biology, 29(3), 827-840.

Lewis, S. L., Sonké, B., Sunderland, T., Begne, S. K., Lopez-Gonzalez, G., van der Heijden, G. M. F., . . . Zemagho, L. (2013). Above-ground biomass and structure of 260 African tropical forests. Philosophical Transactions of the Royal Society B: Biological Sciences, 368(1625), 20120295. https://doi.org/10.1098/rstb.2012.0295.

Mello, L. N. C., Sales, M. H. R., & Rosa, L. P. (2016). Analysis of results of biomass forest inventory in northeastern Amazon for development of REDD+ carbon project. Anais da Academia Brasileira de Ciências, 88, 55-64.

Menlove, J., & Healey, S. P. (2020). A Comprehensive Forest Biomass Dataset for the USA Allows Customized Validation of Remotely Sensed Biomass Estimates. Remote Sensing, 12(24), 4141. https://doi.org/10.3390/rs12244141.

Mitchard, E. T. A., Saatchi, S. S., Lewis, S. L., Feldpausch, T. R., Gerard, F. F., Woodhouse, I. H., & Meir, P. (2011). Comment on 'A first map of tropical Africa's above-ground biomass derived from satellite imagery'. Environmental Research Letters, 6(4), 049001. https://doi.org/10.1088/1748-9326/6/4/049001.

Mitchard, E. T. A., Saatchi, S. S., Woodhouse, I. H., Nangendo, G., Ribeiro, N. S., Williams, M., . . . Meir, P. (2009). Using satellite radar backscatter to predict above-ground woody biomass: A consistent relationship across four different African landscapes. Geophysical Research Letters, 36(23). https://doi.org/10.1029/2009gl040692.

Morel, A. C., Saatchi, S. S., Malhi, Y., Berry, N. J., Banin, L., Burslem, D., . . . Ong, R. C. (2011). Estimating aboveground biomass in forest and oil palm plantation in Sabah, Malaysian Borneo using ALOS PALSAR data. Forest Ecology and Management, 262(9), 1786-1798. https://doi.org/10.1016/j.foreco.2011.07.008.

Paul, K. I., Roxburgh, S. H., Chave, J., England, J. R., Zerihun, A., Specht, A., . . . Sinclair, J. (2016). Testing the generality of above-ground biomass allometry across plant functional types at the continent scale. Global Change Biology, 22(6), 2106-2124. https://doi.org/10.1111/gcb.13201.

Pebesma, E.J. (2004). Multivariable geostatistics in S: the gstat package. Computers & Geosciences, 30: 683-691.

Planque, C, Punalekar, S, Lucas, R, Chognard, S, Owers, CJ, Clewley, D, Bunting, P, Sykes, H and Horton, C. (2020). Living Wales: Automatic and routine environmental monitoring using multi-source earth observation data. In K Schulz, U Michel and KG Nikolakopoulos (eds), Earth Resources and Environmental Remote Sensing/GIS Applications XI., 115340C, Proceedings of SPIE - The International Society for Optical Engineering, 11534, SPIE, Earth Resources and Environmental Remote Sensing/GIS Applications XI 2020. https://doi.org/10.1117/12.2573763

Ploton, P., MorTier, F., Barbier, N. et al. (2020). A map of African humid tropical forest aboveground biomass derived from management inventories. Sci Data 7, 221. https://doi.org/10.1038/s41597-020-0561-0.

Réjou-Méchain, M., Barbier, N., Couteron, P., Ploton, P., Vincent, G., Herold, M., . . . Pélissier, R. (2019). Upscaling Forest Biomass from Field to Satellite Measurements: Sources of Errors and Ways to Reduce Them. Surveys in Geophysics. https://doi.org/10.1007/s10712-019-09532-0.

Réjou-Méchain, M., Muller-Landau, H. C., Detto, M., Thomas, S. C., Le Toan, T., Saatchi, S. S., . . . Chave, J. (2014). Local spatial structure of forest biomass and its consequences for remote sensing of carbon stocks. Biogeosciences, 11(23), 6827-6840. https://doi.org/10.5194/bg-11-6827-2014.

Réjou-Méchain, M., Tanguy, A., Piponiot, C., Chave, J., & Hérault, B. (2017). biomass: an r package for estimating above-ground biomass and its uncertainty in tropical forests. Methods in Ecology and Evolution, 8(9), 1163-1167. https://doi.org/10.1111/2041-210X.12753.

Requena Suarez, D., Rozendaal, D. M. A., De Sy, V., Phillips, O. L., Alvarez-Dávila, E., Anderson-Teixeira, K., . . . Herold, M. (2019). Estimating aboveground net biomass change for tropical and subtropical forests: Refinement of IPCC default rates using forest plot data. Global Change Biology, 25(11), 3609-3624. doi:10.1111/gcb.14767

Rodda, S. R., Fararoda, R., Gopalakrishnan, R., Jha, N., Réjou-Méchain, M., Couteron, P., ... & Ploton, P. (2024). LiDAR-based reference aboveground biomass maps for tropical forests of South Asia and Central Africa. Scientific Data, 11(1), 334.

Rodriguez-Veiga et al. (unpublished). NCEO Africa Aboveground Woody Biomass (AGB) map for the year 2017 at 100 m spatial resolution.

Rozendaal, D. M. A., M. Santoro, D. Schepaschenko, V. Avitabile and M. Herold (2017). DUE GlobBiomass D17 Validation Report, European Space Agency (ESA-ESRIN): 26.

Ryan, C. M., Berry, N. J., & Joshi, N. (2014). Quantifying the causes of deforestation and degradation and creating transparent REDD+ baselines: A method and case study from central Mozambique. Applied Geography, 53, 45-54. https://doi.org/10.1016/j.apgeog.2014.05.014.

Santoro, M., 2024. CCI Biomass Product User Guide, Version 5. (CCI Biomass internal report).

Santoro, M., 2023b. End-to-end Uncertainty Budget Version 4. (CCI Biomass internal report).

Schepaschenko, D., Chave, J., Phillips, O. L., Lewis, S. L., Davies, S. J., Réjou-Méchain, M., . . . Zo-Bi, I. C. (2019). The Forest Observation System, building a global reference dataset for remote sensing of forest biomass. Scientific Data, 6(1), 198. https://doi.org/10.1038/s41597-019-0196-1.

Schepaschenko, D., Moltchanova, E., Fedorov, S., Karminov, V., Ontikov, P., Santoro, M., ... & Kraxner, F. (2021). Russian forest sequesters substantially more carbon than previously reported. Scientific reports, 11(1), 1-7. https://doi.rog/10.1038/s41598-021-92152-9.

Serviço Florestal Brasileiro. (n.d.). Sistema Nacional de Informações Florestais (SNIF). https://snif.florestal.gov.br/pt-br/

Serviço Florestal Brasileiro. (2021, November). Manual de campo: Procedimentos para coleta de dados biofísicos e socioambientais (Versão 7.4.1). Serviço Florestal Brasileiro. https://snif.florestal.gov.br/images/pdf/publicacoes/publicacoes_ifn/manual_de_campo/Manual_de_Campo_IFN__Versao_7_4_1.pdf

Ulander, L.M.H., Gustavsson, A., Flood, B., Murdin, D., Dubois-Fernandez, P., Dupuis, X., Sandberg, G., Soja, M.J., Eriksson, L.E.B., Fransson, J.E.S., Holmgren, J., Wallerman, J. (2011). BioSAR 2010 - Technical assistance for the development of airborne SAR and geophysical measurements during the BioSAR 2010 experiment.

Vaglio Laurin, G., Hawthorne, W., Chiti, T., Di Paola, A., Cazzolla Gatti, R., Marconi, S., . . . Valentini, R. (2016). Does degradation from selective logging and illegal activities differently impact forest resources? A case study in Ghana. [Does degradation from selective logging and illegal activities differently impact forest resources? A case study in Ghana]. iForest - Biogeosciences and Forestry, 9(3), 354-362. https://doi.org/10.3832/ifor1779-008.

Van Breugel, M., Bongers, F., & Martínez-Ramos, M. (2007). Species Dynamics During Early Secondary Forest Succession: Recruitment, Mortality and Species Turnover. Biotropica, 39(5), 610-619. https://doi.org/10.1111/j.1744-7429.2007.00316.x.

Vieilledent, G., Gardi, O., Grinand, C., Burren, C., Andriamanjato, M., Camara, C., . . . Rakotoarijaona, J.-R. (2016). Bioclimatic envelope models predict a decrease in tropical forest carbon stocks with climate change in Madagascar. Journal of Ecology, 104(3), 703-715. https://doi.org/10.1111/1365-2745.12548.

Xu, L., Saatchi, S. S., Yang, Y., Yu, Y., Pongratz, J., Bloom, A. A., ... & Schimel, D. (2021). Changes in global terrestrial live biomass over the 21st century. Science Advances, 7(27), eabe9829.

Willcock, S., Phillips, O. L., Platts, P. J., Balmford, A., Burgess, N. D., Lovett, J. C., . . . Lewis, S. L. (2014). Quantifying and understanding carbon storage and sequestration within the Eastern Arc Mountains of Tanzania, a tropical biodiversity hotspot. Carbon Balance and Management, 9(1), 2. https://doi.org/10.1186/1750-0680-9-2.

World Meteorological Organization (2011). Systematic observation requirements for satellite-based data products for climate: Supplemental details to the satellite-based component of the Implementation Plan for the Global Observing System for Climate in Support of the UNFCCC (2010 Update). https://library.wmo.int/doc_num.php?explnum_id=3710.

Zhao, Y., Chen, R. H., Bakian-Dogaheh, K., Whitcomb, J., Yi, Y., Kimball, J. S., & Moghaddam, M. (2022, July). Mapping Boreal Forest Species and Canopy Height using Airborne SAR and Lidar Data in Interior Alaska. In IGARSS 2022-2022 IEEE International Geoscience and Remote Sensing Symposium (pp. 4955-4958). IEEE.

Appendix A - Details on the used forest plot data

ID	Tier	Average year	Average size (ha)	Count	Biome	URL	Paper/ source	Data access
AFR_L	3	2011	25.00	1	Tropical rainforest	https://dspace.stir.ac.uk/retrieve/74d3b352-fa46-418f-ba95-728bb33f4cfc/08417912.pdf	(Labrière et al., 2018)	open
EU_FOS	3	2014	16.25	1	Tropical rainforest	https://www.-ture.com/articles/s41597-019-0196-1?fbclid=IwAR08vLoOm4xEQo4EUdLtoKsnP6nsNIY5CYnfcoqGcS5Z0_UcyaNIr-jcdDg	(Schepaschenko et al., 2019)	open
SAM_L	3	2010	7.65	20	Tropical rainforest	https://dspace.stir.ac.uk/retrieve/74d3b352-fa46-418f-ba95-728bb33f4cfc/08417912.pdf	(Labrière et al., 2018)	open
AUS1	3	2009	25.00	1	Tropical dry forest	http://data.auscover.org.au/xwiki/bin/view/Product+pages/Biomass+Plot+Library	(Paul et al., 2016)	source-WUR agreement
SAM_RF	3	2008	5.3	10	Tropical rainforest	http://www.rainfor.org/en/project/about-rainfor	Lopez-Gonzales et al., 2011	Open
AFR_FOS	2	2013	1.00	44	Tropical rainforest	https://www.-ture.com/articles/s41597-019-0196-1?fbclid=IwAR08vLoOm4xEQo4EUdLtoKsnP6nsNIY5CYnfcoqGcS5Z0_UcyaNIr-jcdDg	(Schepaschenko et al., 2019)	open
AFR_L	2	2016	1.00	56	Tropical rainforest	https://dspace.stir.ac.uk/retrieve/74d3b352-fa46-418f-ba95-728bb33f4cfc/08417912.pdf	(Labrière et al., 2018)	open
AUS_FOS	2	2008	1.00	2	Tropical dry forest	https://www.-ture.com/articles/s41597-019-0196-1?fbclid=IwAR08vLoOm4xEQo4EUdLtoKsnP6nsNIY5CYnfcoqGcS5Z0_UcyaNIr-jcdDg	(Schepaschenko et al., 2019)	open
CAM_FOS	2	2012	1.01	18	Tropical rainforest	https://www.-ture.com/articles/s41597-019-0196-1?fbclid=IwAR08vLoOm4xEQo4EUdLtoKsnP6nsNIY5CYnfcoqGcS5Z0_UcyaNIr-jcdDg	(Schepaschenko et al., 2019)	open
EU_FOS	2	2010	2.23	2	Boreal coniferous forest	https://www.-ture.com/articles/s41597-019-0196-1?fbclid=IwAR08vLoOm4xEQo4EUdLtoKsnP6nsNIY5CYnfcoqGcS5Z0_UcyaNIr-jcdDg	(Schepaschenko et al., 2019)	open

SAM_FOS	2	2011	1.00	23	Tropical rainforest	https://www.-ture.com/articles/s41597-019-0196-1?fbclid=IwAR08vLoOm4xEQo4EUdLtoKsnP6nsNIY5CYnfcoqGcS5Z0_UcyaNIr-jcdDg	(Schepaschenko et al., 2019)	open
SAM_L	2	2013	1.04	28	Tropical rainforest	https://dspace.stir.ac.uk/retrieve/74d3b352-fa46-418f-ba95-728bb33f4cfc/08417912.pdf	(Labrière et al., 2018)	open
SAM_BAJ	2	2017	1	3	Tropical rainforest	https://ieeexplore.ieee.org/abstract/document/8518871	Pacheco-Pasccagaza et al., 2020	source-WUR agreement
SAM_RF	2	2008	1	374	Tropical rainforest	http://www.rainfor.org/en/project/about-rainfor	Lopez-Gonzales et al., 2011	Open
UK_FOS	2	2015	1.20	1	Tropical rainforest	https://www.-ture.com/articles/s41597-019-0196-1?fbclid=IwAR08vLoOm4xEQo4EUdLtoKsnP6nsNIY5CYnfcoqGcS5Z0_UcyaNIr-jcdDg	(Schepaschenko et al., 2019)	open
AFR10	2	2007	1.00	7	Tropical rainforest	https://iopscience.iop.org/article/10.1088/1748-9326/6/4/049001/meta	(Mitchard et al., 2011)	source-WUR agreement
AFR13	2	2008	1.00	2	Tropical rainforest	https://agupubs.onlinelibrary.wiley.com/doi/full/10.1029/2009GL040692	(Mitchard et al., 2009)	source-WUR agreement
AFR14	2	2009	1.63	4	Tropical rainforest	https://www.sciencedirect.com/science/article/abs/pii/S014362281400109X	(Ryan, Berry, & Joshi, 2014)	source-WUR agreement
AFR6	2	2009	1.00	12	Tropical rainforest	https://cbmjour-l.biomedcentral.com/articles/10.1186/1750-0680-9-2	(Willcock et al., 2014)	source-WUR agreement
AFR7	2	2012	1.00	19	Tropical rainforest	https://royalsocietypublishing.org/doi/full/10.1098/rstb.2012.0295	(Lewis et al., 2013)	source-WUR agreement
ASI3	2	2007	1.00	92	Tropical rainforest	https://www.sciencedirect.com/science/article/abs/pii/S0378112711004361	(Morel et al., 2011)	source-WUR agreement
AUS1	2	2012	1.01	63	Subtropical steppe	http://data.auscover.org.au/xwiki/bin/view/Product+pages/Biomass+Plot+Library	(Paul et al., 2016)	source-WUR agreement

SAM2	2	2012	1.00	40	Tropical rainforest	http://geoinfo.cnpm.embrapa.br/geonetwork/srv/ eng/main.home		source-WUR agreement
SAM_FOS	1	2011	0.25	142	Tropical rainforest	https://www.-ture.com/articles/s41597-019-0196-1?fbclid=IwAR08vLoOm4xEQo4EUdLtoKsnP6nsNIY5CYnfcoqGcS5Z0_UcyaNIr-jcdDg	(Schepaschenko et al., 2019)	open
AFR15	1	2013	0.25	136	Tropical rainforest	https://besjour-ls.onlinelibrary.wiley.com/doi/full/10.1111/1365-2745.12548%4010.1111/%28ISSN%291365-2745.FORESTRY	(Vieilledent et al., 2016)	source-WUR agreement
AFR1	1	2008	0.50	1152	Tropical rainforest	https://agritrop.cirad.fr/572060/1/document_572060.pdf	(Hirsh, Jourget, Feintrenie, Bayol, & Ebaá Atyi, 2013)	source-WUR agreement
AFR10	1	2007	0.50	11	Tropical rainforest	https://iopscience.iop.org/article/10.1088/1748-9326/6/4/049001/meta	(Mitchard et al., 2011)	source-WUR agreement
AFR12	1	2008	0.16	108	Tropical rainforest	https://www.sciencedirect.com/science/article/abs/pii/S0034425711003609	(Avitabile, Baccini, Friedl, & Schmullius, 2012)	source-WUR agreement
AFR13	1	2008	0.50	23	Tropical rainforest	https://agupubs.onlinelibrary.wiley.com/doi/full/10.1029/2009GL040692	(Mitchard et al., 2009)	source-WUR agreement
AFR14	1	2009	0.51	70	Tropical dry forest	https://www.sciencedirect.com/science/article/abs/pii/S014362281400109X	(Ryan et al., 2014)	source-WUR agreement
AFR4	1	2012	0.13	110	Tropical mountain system	http://www.geo-informatie.nl/workshops/scw2/papers/deVries.pdf	(DeVries, Avitabile, Kooistra, & Herold, 2012)	source-WUR agreement
AFR5	1	2012	0.08	71	Tropical rainforest	https://pure.mpg.de/pubman/faces/ViewItemOverviewPage.jsp?itemId=item_2281402	(Vaglio Laurin et al., 2016)	source-WUR agreement
AFR6	1	2009	0.33	12	Tropical dry forest	https://cbmjour-l.biomedcentral.com/articles/10.1186/1750-0680-9-2	(Willcock et al., 2014)	source-WUR agreement
AFR8	1	2008	0.13	105	Tropical moist forest	https://www.sciencedirect.com/science/article/abs/pii/S0034425712001058	(Carreiras, Vasconcelos, &	source-WUR agreement

							Lucas, 2012)	
AFR9	1	2016	0.13	9642	Tropical dry forest	https://www.mdpi.com/2072-4292/5/4/1524 https://fndsmoz.maps.arcgis.com/apps/MapSeries/index.html?appid=6602939f39ad4626a10f87bf6253af1e	(Carreiras et al., 2012)	open, source-WUR agreement
AFR_KEN	1	2011	0.09	362	Tropical and subtropical grasslands, savannas and shrublands			source-WUR agreement
ASI1	1	2008	0.05	2903	Tropical mountain system and rainforest	https://www.tandfonline.com/doi/full/10.1080/17583004.2016.1254009	(Avitabile et al., 2016)	source-WUR agreement
ASI10	1	2008	0.10	1268	Subtropical mountain system	https://www.sciencedirect.com/science/article/abs/pii/S0034425719303608	Zhang et al. 2019	source-WUR agreement
ASI2	1	2011	0.11	119	Tropical dry forest	http://www.leafasia.org/sites/default/files/public/resources/WWF-REDD-pres-July-2013-v3.pdf	WWF and OBf, 2013	source-WUR agreement
ASI4	1	2010	0.02	70	Tropical dry forest	http://citeseerx.ist.psu.edu/viewdoc/download?doi=10.1.1.972.708&rep=rep1&type=pdf	Wijaya et al., 2015	source-WUR agreement
ASI9	1	2012	0.13	74	Tropical rainforest	http://leutra.geogr.uni-je-.de/vgtbRBIS/metadata/start.php	Avitabile et al., 2014	source-WUR agreement
ASI_FOS	1	2014	0.25	2	Tropical rainforest	https://www.-ture.com/articles/s41597-019-0196-1?fbclid=IwAR08vLoOm4xEQo4EUdLtoKsnP6nsNIY5CYnfcoqGcS5Z0_UcyaNIr-jcdDg	(Schepaschenko et al., 2019)	open
AUS1	1	2011	0.12	5611	Tropical dry forest	http://data.auscover.org.au/xwiki/bin/view/Product+pages/Biomass+Plot+Library	Paul et al. 2016	source-WUR agreement
EU1	1	2011	0.01	16819	Temperate broadleaf and mixed forests and Boreal forests	https://www.slu.se/en/collaborative-centres-and-projects/swedish--tio-l-forest-inventory/	Sweden NFI	source-WUR agreement

EU2	1	2007	0.20	7177	Mediterranean forests	http://www.magrama.gob.es/es/desarrollo-rural/temas/politica-forestal/inventario-cartografia/inventario-forestal--cio-l/	Spain NFI	source-WUR agreement
EU3	1	2013	0.06	3021	Temperate oceanic forest	https://library.wur.nl/WebQuery/wurpubs/454875	Netherlands NFI	source-WUR agreement
EU4	1	2007	0.06	5967	Temperate broadleaf and mixed forests and Mediterranean forests	https://www.agriculturejour-ls.cz/publicFiles/01003.pdf	Cienciela et al. 2008	source-WUR agreement
EU_FOS	1	2015	0.28	514	Boreal forests	https://www.-ture.com/articles/s41597-019-0196-1?fbclid=IwAR08vLoOm4xEQo4EUdLtoKsnP6nsNIY5CYnfcoqGcS5Z0_UcyaNIr-jcdDg	(Schepaschenko et al., 2019)	open, source-WUR agreement
NAM1	1	2010	0.04	586	Boreal coniferous forest	https://www.p-s.org/content/112/18/5738.short	Liang et al., 2015	source-WUR agreement
NAM2	1	2004	0.04	75	Temperate mountain system	https://www.nature.com/articles/nature07276	Luyssaert et al., 2008	source-WUR agreement
NAM3	1	2010	0.03	588	Temperate continental forest			source-WUR agreement
NAM4	1	2010	0.04	2794	Temperate mountain system		Alaska NFI	source-WUR agreement
SAM2	1	2013	0.23	241	Tropical rainforest	https://www.paisagenslidar.cnptia.embrapa.br/webgis/	Embrapa, undated	source-WUR agreement
SAM3	1	2011	0.13	111	Tropical rainforest		CIFOR, undated	source-WUR agreement
SAM4	1	2014	0.15	7	Tropical rainforest		CIFOR, undated	source-WUR agreement
SAM5	1	2014	0.60	23	Tropical rainforest		CIFOR, undated	source-WUR agreement

SAM_BAJ	1	2017	0.25	363	Tropical rainforest	https://ieeexplore.ieee.org/abstract/document/8518871	Pacheco-Pasccagaza et al., 2020	source-WUR agreement
SAM_RF	1	2008	1	125	Tropical rainforest	http://www.rainfor.org/en/project/about-rainfor	Lopez-Gonzales et al., 2011	Open
SAM_TAPA	1	2009	0.5	138	Tropical rainforest	https://www.tandfonline.com/doi/full/10.1080/07038992.2014.913477?casa_token=EZxeZoegekkAAAAA%3AZHCN98XtpZRrsS9KoGTBhPy1_yzhAkkLZHfck3fomwSnvSaO7YDiuPV_hne6Mj1Wdn-7ME_sPChP	(Bispo et al., 2014)	source-WUR agreement
AFR_COF	0	2009	100	35029	Tropical moist forest,	https://www.nature.com/articles/s41597-020-0561-0	(Ploton et al., 2020)	open
LIDAR	0	2014	1	744397	Tropical rainforest		SLB, TERN, NEON	Open
LIDAR_SP	0	2017	1	54058	Temperate broadleaf and mixed forests and Mediterranean forests		(Gonzales et al., under preparation)	source-WUR agreement
EU_BEL	1	2013	0.1	688	Temperate broadleaf and mixed forests		Belgium TreeMort	source-WUR agreement
EU_BUL	1	2019	0.1	22	Temperate broadleaf and mixed forests		Dmitrov et al., under preparation	source-WUR agreement
EU_CZR	1	2014	0.1	25	Temperate conifer forests	https://www.sciencedirect.com/science/article/pii/S0925857416307182 https://www.mdpi.com/1999-4907/11/3/268	Brovkina et al., 2017; Novotny et al., 2020	source-WUR agreement
AFR_GHA	1	2010	0.1	94	Tropical rainforest	https://www.sciencedirect.com/science/article/pii/S0378112720310057	Brown et al., 2020	source-WUR agreement
EU_WLS	1	2016	0.5	134	Temperate broadleaf	https://www.forestresearch.gov.uk/tools-and-resources/national-forest-inventory/	Wales NFI	source-WUR

					and mixed forests			agreement
ASI_ind	2	2015	0.5	420	Tropical rainforest		Kumar et al. 2023	source-WUR agreement
ASI_nep	2	2015	0.5	2004	Tropical mountainous forest		Khanal et al. 2023	open
LIDAR_JUNI	0	2016	1	132405	Temperate woodlands		Campbell et al. 2023	source-WUR agreement
LIDAR_LVIS	0	2016	1	148051	Boreal forest	https://lvis.gsfc.nasa.gov/Data/Maps/ABoVE2017Map.html	Zhao et al. 2022	Open
EU_FOS	1	2016	0.2	264	Different biomes		(Schepaschenko et al., 2019)	source-WUR agreement
SAM_guy	1	2019	0.1	473	Tropical rainforest		Sukhadeo et l. / Guyana NFI	source-WUR agreement
NAM_TUND	0	2012	0.3	222	Tundra		Open	
ASI_IND	1	2018	0.5	412	Tropical and subtropical dry broadleaf forest		source-WUR agreement	
ASI_NEP1	1	2022	0.1	2009	Temperate broadleaf and mixed forests		source-WUR agreement	
ASI_NEP2	1	2022	0.1	1010	Temperate broadleaf and mixed forests		Open	Khanal et al. 2023

NAM_JUNI	0	2022	1	132405	Woodlands		source-WUR agreement	Campbell et al. 2024
SAM_KEL	0	2019	1	10000	Tropical rainforest		source-WUR agreement	Ometto et al. 2023
ASI_PAK	1	2022	0.1	268	Temperate broadleaf and mixed forests		source-WUR agreement	
ASI_MANG	1	2022	0.1	100	Mangroves		source-WUR agreement	Bilolo et al. 2024